Order Number 9207093

Applications of thermal analytic techniques in materials engineering

Ledesma, Ramona, Ph.D.

City University of New York, 1991

U·M·I
300 N. Zeeb Rd.
Ann Arbor, MI 48106

A

APPLICATIONS OF THERMAL ANALYTIC TECHNIQUES IN MATERIALS ENGINEERING

BY

RAMONA LEDESMA

A dissertation submitted to the Graduate Faculty in Engineering in partial fulfillment of the requirements for the degree of Doctor in Philosophy, The City University of New York.

1991

This manuscript has been read and accepted for the Graduate Faculty in Engineering in satisfaction of the dissertation requirement for the degree of Doctor of Philosophy.

May 16 1991
Date

Leslie Isaacs
Chair of Examining Committee

5/22/1991
Date

Gerard J. Gleason
Executive Officer

Professor Charles Maldarelli

Professor Carol Steiner

Professor Gabriel Tardos

Dr. Dominick Mazzone, Mobil Research and Development Corporation

The City University of New York

ABSTRACT

APPLICATION OF THERMAL ANALYTIC TECHNIQUES

IN MATERIALS ENGINEERING

by

Ramona Ledesma

Advisor: Professor Leslie Isaacs

This thesis studies the applicability of thermal analysis techniques to the task of determining thermal characteristics of various materials. An extensive investigation was conducted through an experimental program which featured the use of differential scanning calorimetry (DSC), differential thermal analysis (DTA), dilatometry, and thermomechanical analysis (TMA).

Differential scanning calorimetry (DSC) was employed to measure heat capacities of coal ashes in the temperature range from 150°K to 900°K. Some of the determined heat capacities were correlated with ash constitution. Ash samples were obtained from finely ground coal ranking from lignite to low volatile bituminous.

The minimum sintering temperature of coal ash powder was measured using a high temperature, push-rod dilatometer over

the range from ambient to 1250°K.

The applicability of differential thermal analysis (DTA) to determine the fusibility behavior of coal ashes was investigated between 300°K and 1900°K. This technique proved useful to obtain four specific temperature points which describe the fusion characteristics of coal ash. These points are: minimum sintering temperature, the softening point, the point of complete fluidity, and the reaction temperature which is tentatively identified as the eutectic temperature.

Thermomechanical analysis (TMA) and differential scanning calorimetry (DSC) was employed to study the effect of polyethylene terephthalate (PET) additives obtained from used soda bottles on the thermal properties of pure asphalt. This technique was used to determined the expansion coefficient, the glass transition temperature, the melting point, and the flow properties of asphalt, PET, and PET/asphalt mixtures samples. The temperature range used for these measurements was between 100°K to 600°K.

This thesis features a variety of useful applications of analytic thermal techniques and is intended to enhance our knowledge of existing methods and explore new techniques to determine thermal properties of different materials in materials engineering applications.

To my beloved mother Mercedes,

without whose encouragement, love and support

this dissertation could never have been possible

ACKNOWLEDGEMENTS

One of the most difficult task in writing a dissertation is to put in words what your heart is saying. The technical chapters were by no means easy to write as they required thorough knowledge of the material being discussed, which is only obtained after years of research, learning and investigating. But this is a function of the brain and sentimentalism is not a factor as far as the writing is concerned. However, in writing the acknowledgements, it is the heart that speaks and sends signals through the nervous system to the brain that upon receiving them puts them in words. This process is unlikely to be 100% efficient and sometimes words can not be found to express one's appreciation to all those special people who deserve to be recognized as instrumental in the successful completion of such an endeavor. It is with great pleasure that I welcome the opportunity to acknowledge all those people who were and still are contributing to my education and professional career.

First of all, I would like to thank God, for it was his/her allowance that made this dissertation possible. Thanks be to God for letting me successfully undertake such an endeavor, for showing me the way, and for giving me a helping hand when I needed it the most. It has been said many times that God works in mysterious ways, and I can certify this, for

I am a witness as well as a recipient of his/her love.

Looking back, names of so many special people come to mind. Unfortunately, it is not possible to acknowledge individually all their contribution. Therefore, I will mention faculty members first and my family and friends last, but certainly not least.

My most sincere thanks go to Dr Leslie Isaacs my mentor and Professor, and the Assistant Dean of the School of Engineering, whose knowledge, understanding, and professionalism provided me with the tools necessary to tackle such an endeavor. His encouragement, guidance, and support throughout these years made it all possible, and I am greatly indebted to him.

Many thanks are due to Professors Gabriel Tardos, Carol Steiner, and Charles Maldarelli from the Chemical Engineering Department. They generously supplied information and suggestions which resulted in many improvements in my research and thesis. Also many thanks to Dr. Dominick Mazzone from Mobil Research and Developmental Corporation who served on the examining committee during my defense and who provided me with many useful recommendations.

I wish to express my appreciation to my colleagues and

friends Dr. Abdulkadir Dualeh, Dr. Kathleen Stebe, and Dr. Charalambos Varelas for their invaluable help and encouragement. I also would like to acknowledge the support of the Chemical Engineering Department over the years. Faculty as well as staff members, especially Mr William Hall and Ms. Charmaine Frances, have contributed in many ways that are greatly appreciated.

I thank W.R. Grace Co. for their financial support during the past three years, and the Plastic Institute of America for the supplemental stipend they provided.

The Center of Analysis for Structures and Interfaces (CASI) deserves to be acknowledged as instrumental in the completion of this dissertation. Their financial and moral support during the last year of my doctoral studies are invaluable to me. I am deeply grateful to all the members of the program, especially Dr. Ronald Brown and Dr. Daniel Akins, individuals who would go beyond the call of duty in an effort to help a student in need.

I would like to acknowledge the support of Professor Mirian Sarachick from the physics department, and of Dr. Gerard G. Lowen, the Executive Officer of my examination committee, and Associate Dean of the School of Engineering for his support and understanding.

I wish to gratefully acknowledge the support, encouragement, and assistance of my family. Words can not be found to express my gratitude to them; especially to my mother Mercedes, whose perseverance, courage, and love for her family have served as an example that inspires all of us to persuade our dreams.

My brothers and sister deserved my deepest appreciation. I thank my brothers Miguel Angel and Andres for their understanding and for their confidence in me, Hector for encouraging me to come back to school at a time when I though it was not possible, Raphael and Brandon for their generous support. Thanks are due to my sister Fabiola, my sister-in-law Ovetta, and my uncle Pedro for their love.

My most special thanks go to Alexander and his faithful companion Hephaistion for being there for me in such a unique way when I needed them the most.

This dissertation is a result of the contributions of so many wonderful people. It is not possible to name them all here, but I thank all of them; for I could never have done it without their support.

TABLE OF CONTENTS

LIST OF FIGURES

LIST OF TABLES

Introduction

Thermal analysis, as defined by Mackenzie [1,2] and the International Confederation for Thermal Analysis [3], is: "A group of techniques in which a physical property of a substance and/or its reaction is measured as a function of temperature while the substance is subjected to a controlled temperature program." DuPont Instruments gives the following definition: "Thermal analysis measure changes in physical or reactive properties of materials as a function of temperature and time."

Examination of both definitions shows that there are three necessary and sufficient conditions to be satisfied by a thermal technique before it can be regarded as thermoanalytical:

1. A physical property must be measured.
2. The results must be expressed as functions of temperature or time.
3. The measurement has to be made using a temperature program.

There are numerous physical and/or chemical parameters that can be measured thermoanalytically; thus, thermal analysis provides information which characterizes: polymers,

organic and inorganic substances, metals, glasses, ceramics, and most other materials.

During the past 25 years, modern thermal analytical instrumentation has progressed from home made laboratory devices designed by individual researchers to highly sophisticated commercial systems which are used as analytical tools for material's research, product design, process optimization, and quality control.

From among the most widely used thermal analysis techniques, we employed differential scanning calorimetry (DSC), differential thermal analysis (DTA), dilatometry, and thermomechanical analysis (TMA) in our studies on the thermal behavior of coal ashes, asphalt, polyethylene terephthalate (PET), and PET/asphalt mixtures samples.

The thermal characteristics of coal ashes are of great interest. Most coal in the United States is used for power generation or as raw material for chemical processes. The so called fluidized bed is the type of reactor proposed for the conversion of coal to synthetic fuels. This and other processes involve at least a partial combustion of the coal. The generation of large amounts of ash usually accompanies coal combustion. Stack gases carry a portion of the ash, the "fly ash," into the atmosphere, contaminating the environment.

The portion of the ash that remains in the reactor, the "bottom ash," can agglomerate there, causing operational problems. It is of great interest to find uses for the voluminous amounts of ash produced, or to find safe and economic means for its disposal. In either case, even to design a system to remove the ash from the reactor, one requires information on the thermal characteristics of various kinds of ashes. The important thermal properties include the ash heat capacities, fusion characteristics, and thermal conductivities. In this thesis, the fusion behavior of coal ashes was determined using differential thermal analysis (DTA), the ash heat capacities were evaluated by differential scanning calorimetry (DSC) technique, and dilatometry was employed in measuring the minimum sintering point of the ashes.

Another facet of our research involved the investigation of the thermal properties of asphalt cement, PET, and mixtures of PET and asphalt samples. Asphalt occurs naturally, but is most often obtained as a byproduct of petroleum refining. It is a mixture of high molecular weight compounds which behaves like a viscoelastic (plastic) material. This type of material undergoes a phenomenon called "the glass transition"; this transition from flexible to rigid, glass- like, state occurs at a given temperature, Tg, which is characteristic of the material. Crossing this temperature causes microscopic cracks

to form which may lead to the actual breakdown of the material. Research was aimed to see if filler material obtained from used plastic bottles made of PET can be used to reinforced asphalt cement. The thermal behavior of asphalt, waste plastic (PET), and asphalt-PET mixtures samples was investigated using differential scanning calorimetry (DSC) and thermomechanical analysis (TMA). These techniques were used to measure melting points, glass transition temperatures (Tg), expansion coefficients, and flow properties of these materials.

This thesis is divided into six chapters. The first is a literature review of previous work related to this investigation; Chapter 2 describes the experimental techniques employed in our studies; in Chapters 3, 4, and 5 each facet of the experimental program is discussed together with the presentation of the results; and in Chapter 6 recommendations for future studies are presented. Some of the work presented in this thesis has been published.

CHAPTER 1

Literature Review

In this chapter we review previous investigations related to the thermal behavior of coal ash, asphalt, and asphalt-polyethylenes mixtures. For convenience, it is divided into two sections according to the material studied. Section 1.1 refers to the thermal properties of coal ashes, and section 1.2 deals with the thermal behavior of asphalt and asphalt-polyethylenes mixtures.

1.1 Thermal Properties of Coal Ashes.

Interest in the thermodynamic properties, such as the specific heat and fusion temperatures, of coal and related substances (e.g. ash, coke, char, tar, etc.) at various temperatures arises from the need to have reliable data available for calculations related to their utilization, storage, and processing.

Precise thermal information for coal and coal products, specifically coal ashes, is scarce. Furthermore, a study of the earlier literature revealed many discrepancies in the data for the specific heat of such materials, and a lack of

experimental results in the temperature range used in practical applications.

In an effort to alleviate this situation, a joint study of the thermal behavior of coal and related products was undertaken by the Bureau of Mines and the Tuscaloosa Metallurgy Research Center. The project was headed by Manuel Gomez, John B. Gayle, and Arthur R Taylor, Jr. The report [4] was published in 1965 and contained heat content data at various temperatures of coals, chars, ashes, and other related substances.

In that investigation, the heat content of coal ashes prepared from lignite, lignitic char, high volatile A bituminous coal, and spent shale was measured at various temperatures between 105°C and 945°C using a Bunsen ice calorimeter. The obtained data were correlated by algebraic equations expressing heat content as function of temperature. The general form of the equation used was:

$$H_t - H_o = a + bt + ct^2 + dt^3 + et^4 \qquad (1.1)$$

where $(H_t - H_o)$ is the heat content of the sample in calories per gram, and the temperature, t, is in degree centigrade.

The corresponding specific heat relationship is:

$$C_p = b + 2ct + 3dt^2 + 4et^3 \qquad (1.2)$$

where C_p is the specific heat of the sample in calories per

gram per degree centigrade.

The heat content data for ash correlated well with temperature according to the equation:

$$H_t - H_o = 0.189t + 1.042x10^{-4}t^2 - 2.309x10^{-8}t^3 - 2.396x10^{-11}t^4 \quad (1.3)$$

The corresponding ash specific heat equation was found to be:

$$C_p = 0.189 + 2.084x10^{-4}t - 6.927x10^{-8}t^2 - 9.584x10^{-11}t^3 \quad (1.4)$$

Heat content values for ash are shown in Fig. 1. Estimates of the reproducibility of the results were not available, and, in addition, the ash specific heat study was limited to the determination of equation (1.4). However, upon examination of the results it was noted that all ash samples showed essentially the same heat content at corresponding temperature; thus, it appeared that the heat content, as well as the specific heat, is largely independent of the type and origin of the parent substance from which it was prepared.

In that same year, Kirov [5] presented a set of correlations for the approximate computation of the specific heat of coal and its solid products. These correlations were obtained by assuming that specific heats of such materials can be represented by the summation of the component specific heats, weighted by the respective weight fractions.

Using the principle of additive contribution from each

component and taking into account the average mineral composition of ashes from coal, Kirov concluded that the specific heat of coal ash may be expressed with sufficient accuracy by the equation:

$$C_a = 0.18 + 7x10^{-5}t \qquad (1.5)$$

where C_a is the mean specific heat, in calories per gram of ash per degree centigrade, of the sample at temperature t.

Data considered by Kirov in obtaining the above expression together with experimental values from literature and a variety of products with similar composition are shown in Fig. 2. These results are found to fall within 5% of those given by equation 1.5.

Kirov's correlation has been widely used to determine the specific heat of coal ashes for more than two decades. However, it should be noted that the resulting curve fails to reveal any thermal effects, such as glass transition and phase transformation, occurring upon heating the ash sample. Furthermore, in its derivation Kirov assumed that the individual and collective properties of the mineral components of coal remained unchanged throughout the ashing process, which may or may not be the case. These observations suggest that a more reliable method to determine the specific heat of coal ash is needed in order to fully understand its thermal behavior.

Subsequent work on the thermal properties of coal ashes were generally based on either Kirov's correlation [5] or on Gomez et al [4] investigations, or on both. In 1976, The Energy Research and Development Administration [6] reported that Kirov's expression for the specific heat , equation 2.5, appeared to be adequate for ash; and in 1979, Eiserman et al [7] published a paper containing values of specific heat of coal ash obtained using Kirov's correlation in SI units. These values were compared to the ash specific heat results of Gomez et al [4] and found to be in excellent agreement.

There are very few specific heat data available for coal ashes. Most of the literature work concentrated on the thermodynamic properties of coal and its other derivatives (e.g. char, tar, coke, etc.) with little attention given to ashes. The
above investigations do not provide satisfactory results as they were based on indirect measurements of ash heat capacity, or on empirical studies of the limited ash data in literature. From the above discussion, it is clear that thermal analysis can play an important role in the determination of the thermal behavior of coal ash since it provides reliable means to directly measure its thermal properties. Data on the heat capacity of chars by Isaacs and Wang [8] indicates that there is an interaction between the organic matter and the ash in the char.

Thermal analysis techniques have been employed to measure thermodynamic properties of pyrite [9], quartz [10], illite [11,12], calcite [12], and other materials that are present in coal ashes, as well as to determine the thermal behavior of coal [13,14,15], oil shales and sands [15], and related substances. For example, Mraw and Naas [9] measured the heat capacity of pyrite samples by differential scanning calorimetry as a test for the accuracy of the apparatus . The heat capacity of the pyrite samples had been previously determined using precision adiabatic calorimetry; thus, excellent data was available for comparison. The apparatus used was the Perkin-Elmer DSC-2. When the DSC results were compared to those previously determined, it showed that the accuracy of the heat capacity measurements of pyrite was approximately 1% over most of the temperature range, and within 2% at the very lowest and higher temperatures. Therefore, the DSC technique was proven to be a reliable and suitable method for accurate measurements of heat capacity.

Another facet of the thermodynamic studies of coal and related substances involves investigations of the fusibility behavior of coal ashes. One key characteristic of these studies is the temperature range at which ash softens and melts. When heated at a specified rate, coal ashes pass through certain defined stages of fusing and melting. Because ashes are heterogeneous mixtures of kaolinite, illite, quartz, and other minerals, some of their particles melt at lower

temperatures than others; thus, giving a single ash sample a range of fusion temperatures.

The standard method to determine the fusibility of coal ashes is the ASTM D-1857 "Fusibility of Coal Ash" [16]. It defines a preparation and measuring scheme which yields four "call points" that presumably characterize ash fusion behavior. In this method, ashed coal moistened with a dextrin solution is molded to form equilateral triangle based pyramids of 3/4 inch in height and 1/4 inch in width at each side of the base. After drying, the ash pyramids are mounted on refractory plates composed of a mixture of equal parts of kaolin and alumina, and then placed inside a furnace which provides means of observing the ash pyramids during heating. Thermocouples in contact with the samples are used to measure the temperature.

Upon heating the sample, the critical temperature points to be observed are as follows:

(a) Initial Deformation Temperature - The temperature at which the first rounding of the apex or the edges of the ash cone occurs.

(b) Softening Temperature, Spherical -

Temperature at which the cone has fused down to a spherical lump in which the height is equal to the width of the base.

(c) Softening Temperature, Hemispherical - The temperature at which the cone has fused down to a hemispherical lump whose height is one half the width of the base.

(d) Fluid Temperature - The temperature at which the fused ash mass has spread out in a nearly flat layer with a maximum height of 1/16 inch.

The measurements should be carried out under either a reducing or oxidizing atmosphere. This method is empirical and strict observance of the requirements is necessary to obtain reproducible results.

Numerous investigators have used the standard ASTM method to obtain ash fusion data. O'Gorman and Walker in their paper "Thermal behavior of mineral fractions separated from selected American coals" [17] published in 1972 devoted a section to the fusion behavior of coal ashes. The fusion temperatures were determined using the ASTM test for four ash samples obtained from an Illinois high-volatile bituminous coal, a

Pennsylvania anthracite, a West Virginia low-volatile coal, and a medium volatile bituminous coal.

Their results showed significant differences between ash fusion data obtained under reducing conditions and those under oxidizing atmosphere. These differences were attributed to variations in the mineralogical composition of the coal ashes. For example, the softening temperature for the ash sample obtained from the Illinois coal showed a difference of about 155°C when examined under reducing and oxidizing conditions. This appears to be due to the high iron content of this sample. Under reducing conditions, ferrous oxide is formed which has more influence on the melting point than higher oxides. In contrast, the ash sample from the Pennsylvania anthracite, which is high in kaolinite content, exhibited extremely high fusion temperatures. For the ash obtained from the low-volatile bituminous coal, the softening point under reduced conditions was 139°C lower than when an oxidizing atmosphere was used. This can again be associated with the high iron content, but also with the low clay-mineral content of this sample which makes it highly refractory. Both of these effects produced a comparatively low ash melting point. For the medium- volatile coal ash sample, the difference in the softening point under a different atmosphere was only 50°C.

O'Gorman and Walker [17] noted during the experiments

that the ashes did not melt sharply and completely at a given temperature and that, in most cases, a wide interval of temperatures was observed between the onset of sintering and completion.

It has been argued that the Initial Deformation Temperature, IDT, from the ASTM method corresponds to the minimum sintering temperature at which the onset of agglomeration occurs. This has been shown not to be the case.

In 1984, Conn and Austing [18] determined the onset of sintering of coal ashes using the Raask shrinkage and electrical method [19,20]. A plot of log resistance versus the inverse temperature (1/T) gives a straight line. The slope of this line changes as sintering commences. The temperature at which this occurs is called the electrical sintering temperature.

The reasons for the change in the slope of the log resistance Vs 1/T characteristic temperature line are not yet clear. The actual resistance measured depends on sample size, geometry, packing density and, most of all, on the particle size distribution and the number of contact points; thus, the resistance varies between different compacts. The theory of electrical resistance (in solid materials) predicts that the logarithm of the resistance decreases as the temperature is

increased. When sintering commences, there is a growth of necks between particles that causes a change in the slope of the temperature curve. This variation of the electrical resistance is attributed to solid state conduction, contact resistance, liquid ionic conduction, and the change in geometry of electrical paths. The precise mechanism and chemistry of sintering can not be derived using the Raask technique because of the many factors affecting the results.

A comparison of the Conn and Austin data [18] with the results obtained by O'Gorman et al [17] showed the former sinter point to be 460°C less than that of the latter for the Illinois coal ash. Bearing in mind the difference in methods, it should be safe to conclude that the electrical sintering point does not correspond to the Initial Deformation Temperature resulting from the ASTM test.

Another method to determine the minimum sintering temperature of powdery materials is to use the elongation-contraction curve obtained using a push-rod dilatometer. This technique was employed by Basu and Sarka [21] to examine the relations between the IDT of Indian coal ashes and defluidization velocity in fluidized-bed rectors. Sintering temperatures for ash in several ranges of particle size were measured with a dilatometer. It has been observed that agglomeration of bed materials, generally ashes, may occur at

temperatures well below the ash softening point. For best combustion efficiency, the reactors should operate at the maximum possible temperature, and agglomeration is a limiting factor in selecting fluidized-bed combustion operating parameters.

In their experiments, Basu and Sarka [21] packed ash powder into a dilatometer tube . An electric furnace was used to heat the dilatometer tube and changes in the length of the ash column were measured. Under constant load the length of the ash column increases linearly with temperature until a point is reached where a decreasing effect occurs due to sintering. The temperature at which these two opposing effects become equal is called the initial sintering point.

Basu and Sarka observed that the initial sintering temperature increased with ash particle size. This may be explained by the fact that the surface of contact between small particles is greater per unit volume than that of larger particles. As a result, it may be expected that smaller ash particles will become defluidized at lowered temperatures. It should be noted that their measured sintering temperatures falls well below the ash IDT obtained from ASTM method [17].

Several empirical methods have been developed to approximate ash fusion temperature. Rhinehart and Attar [22] proposed a model that predicts the ash fusion points from the

ash composition. Using the thermodynamic equation that relates mole fraction of a solute in an ideal solution to the melting point,

$$\ln(1-X_i) = \frac{\Delta H}{R}\left[\frac{1}{T} - \frac{1}{T_o}\right] \qquad (1.6)$$

where X_i is the mole fraction of the solute at temperature T, ΔH is the heat of fusion of the pure solvent at absolute temperatures, R is the gas constant, and T_o is the absolute melting point of the mixture, and the following assumptions:

1. An average coal ash composition exists that can be used as a pseudo-pure component.
2. From ash to ash, the composition changes are small enough so that they can be treated as perturbations about the average composition.
3. The small composition changes do not result in new phases.
4. The solutions behave as ideal ones.
5. Each component is considered as a perturbing component.

they were able to obtain the following mathematical formulation of the model:

$$\frac{1}{T} = \frac{1}{T_o} + \sum_{i=1}^{N} \frac{R}{\Delta H} \ln(1 - \Delta X_i) \qquad (1.7)$$

where ΔH and To refer to the average ash properties, ΔXi is the deviation of the mole fraction of the ith component from that of the average mole fraction of the ith component, and N is the total number of components. Equation 1.7 was greatly improved when ΔH was allowed to be an adjustable parameter; thus,

$$\frac{1}{T} = \frac{1}{T_o} + \sum_{i=1}^{N} \frac{R}{A_i} \ln(1 - \Delta X_i) \qquad (1.8)$$

where A_i is used to replaced ΔH.

The theory requires use of the mole fractions of the components as they exist in the ash, but these values are not recorded in the literature as such. Therefore, in a very elementary way the ash was reconstructed as being composed of SiO_2 , Al_2O_3, FeO, CaO, MgO, and the "others," where the "others" refers to the combination of TiO, Na_2O, and K_2O. As a result, equation 1.8 is a seven-parameter correlation, six A_i's from each of the elementary components and T_o, that approximates ash fusion temperature.

Rhinehard and Attar [22] used a wide range of data from the literature in order to determine the seven parameters needed to approximate each of the three fusion temperatures, i.e. initial deformation temperature (IDT), softening

temperature (ST), and fluid temperature (FT). Two hundred and sixty three data sets were accepted from which the Ai's were determined.

The standard error ranged from 63°C to 69°C in the predicted temperatures. The ASTM test allows 56°C to 83°C interlaboratory differences. Considering the variety of data source used and the time span for the data, the standard error of this correlation appears to be comparable to the expected laboratory differences. However, the thermodynamic approach used was based on the freezing depression point equation (1.6) which is valid only for dilute ideal solutions; since coal ashes are neither ideal mixtures nor pure components, the activity coefficient can not be assumed equal to unity as it has been done here. Further, it was assumed that the coal ash consists of several pure oxides; the fact is that ashes are heterogeneous mixtures of silicates, oxides, sulfates, phosphates, and other substances whose thermal behaviors may be far different from those of pure oxides.

In general, most of the literature found concerning ash fusion temperatures was based on the methods described above. To our knowledge, thermal analysis (TA) has never been employed to determine the fusion behavior of ashes. A TA technique such as differential thermal analysis (DTA) could be essential in the elucidation of fusion effects studies.

1.2 Asphalt and Polyethylene Additives

Bituminous materials rank among the world's oldest and most common construction materials. A fundamental and widely used material in highway construction and maintenance is asphalt which is a byproduct of crude oil refining. Like tar, asphalt is a bitumen or residue containing the higher melting components that remain after distillation removes gaseous and fluid fractions. It does not have a specific composition; rather, asphalt is a mixture of many molecular species in which hydrocarbons predominate [23].

The asphalt composition can be divided into three general categories: asphaltenes, resins, and oils. The asphaltenes are high molecular weight hydrocarbons which precipitate from asphalt, making up the body of the mixture. Resins are hydrocarbons that play a role in the adhesiveness and the ductility of asphalt, while the oils influence its viscosity [24].

In effect, asphalts are viscoelastic materials that soften upon heating, as a thermoplastic, in the approximate range of 71°C to 99°C; thus, asphalt is applied hot and made to fall into place with the aid of rollers [24]. In addition, asphalt undergoes a change in behavior which may vary from

flexible to glass like rigid behavior. The temperature at which this phenomenon occurs is called the "glass transition temperature," Tg. Typically, the Tg of asphalt is near -20°C, which is in the temperature range of asphalt use.

When appropriate amounts of fine and coarse aggregates are mixed with asphalt, a composite paving material , referred to as asphalt concrete, is produced. Asphalt concrete mixes are designed to possess certain properties depending on the specific application. However, the thermoplastic characteristics of asphalt cause difficulty with roads. For example, in the high summer temperatures asphalt roads undergo viscous flow or creep; in winter and under heavy load, these roads become brittle (below the glass transition temperature) and this leads to fracture causing the familiar pothole [25].

Various attempts have been made to use fillers that would enhance the properties of asphalt. For example, ground glass has been added to increase traction, and rubber to obtain better resiliency at low temperatures. The serviceability of asphalt pavements depends on a number of material properties [26]. Asphalt research is aimed to improve pavement performance through increased understanding of the chemical and physical properties of asphalt and asphalt cement [27].

Methods to determine the thermal properties of asphalt

have been the subject of numerous investigations. Because viscosity and the glass transition temperature, Tg, are usually considered to be the fundamental measures of asphalt properties, they are the primary properties included in asphalt specifications.

In 1966, Smith and Santucci [28] published a paper in which they described a convenient method for determining the Tg of asphalt and presented new constants for the use of the William-Landel-Ferry (WLF) equation [29] for calculating asphalt viscosity at low temperature. Fifty two asphalts, representative of commercial production in the United States, were examined by this method. The Tg of asphalt was measured using a modified dilatometry method that employed dilatometry cells with expansion measuring capillary tubes attached to them.

In this method, the sample is immersed in an expanding liquid inside the dilatometry cell. Volumetric changes in the content of the cell are measured as the fluid surrounding the sample moves up or down in the measuring tube in response to temperatures changes. Tg values were obtained by a mode in which the temperature was either decreasing from room temperature or increasing from below the Tg of the sample. The bath temperature was measured by thermocouples and methyl alcohol was used as the expanding fluid. A plot of the height

of this liquid versus temperature was used to determine the Tg values. In general, the capillary tube height is a linear function of temperature that experiences a change of slope at the point at which the state of the sample changes from glass-like to fluid. The temperature at which this occurs is the Tg of the sample.

The repeatability of the Tg measurements was reported by the authors to be 4.4°F. This value was attributed to the extreme variety of types and grades of the fifty-two asphalts tested. The obtained Tg data was then used to determine new constants for the WLF equation [29] of the form:

$$\log \frac{\eta(T)}{\eta(Tg)} = \frac{-C_1(T-Tg)}{C_2+(T-Tg)} \qquad (1.9)$$

where η is the viscosity at T and Tg, C_1 and C_2 are constant depending on the substance used. By substituting T_1 and T_2 for T in equation 1.9 and combining to eliminate η(Tg), the following equation was obtained:

$$\log \frac{\eta_1}{\eta_2} = \frac{C_1(T_2-Tg)}{C_2+T_2-Tg} - \frac{C_1(T_1-Tg)}{C_2+T_1-Tg} \qquad (1.10)$$

By substituting experimentally determined values for Tg and η_2 (the viscosity at T_2), the viscosity η_1 at the temperature T_1 can be calculated. C_1 and C_2 were determined using the Tg values of the fifty-two asphalts and their corresponding viscosities at selected temperatures.

Schmidt and Santucci [28] found that the obtained viscosities were not of high degree of accuracy because the application of the WLF equation is limited to steady state viscosity of low molecular weight (not a crosslinked) polymers or of high molecular weight substances stressed for long periods of time, so that internal structure is uniform. The viscoelastic properties of asphalt are not expected to follow the same temperature dependency displayed by steady state viscous materials, except where the viscosity is Newtonian. However, it has been observed that most alphalts behave as non-Newtonian materials [30].

The Schmidt and Santucci data [28] was the basis of an investigation carried out by Breen and Stephen [31] in which the interrelationship between the glass transition temperature and the molecular distribution was studied. Breen and Stephens determined the molecular distribution of the asphalts used by Schmidt and Santucci in the hope that these values together with the reported Tg data [28] and the physical properties reported by others [32] would give insight into the nature of asphalt.

It had been suggested by Wood [33] that for a polymer system, such as styrene-butadiene system, the Tg can be described by the following equation:

$$\frac{1}{Tg} = \frac{W_1}{Tg_1} + \frac{W_2}{Tg_2} + \ldots + \frac{W_n}{Tg_n} \qquad (1.11)$$

where Tg_1, Tg_2,..., Tg_n are the glass transition temperatures for pure homopolymers, and W_1, W_2,..., W_n are the corresponding weight fractions. If as previously suggested [34] that asphalt consists of asphaltenes, resins, and oils, then asphalt may be considered as a pseudo-polymer or copolymer, where the asphaltenes and resins act as pseudo-polymers of the oil fraction. This would permit the development of a model which would predict the glass transition temperature of the asphalt. The molecular distribution of the group of asphalt used was determined by Gel Permeation Chromatography (GPC). This technique involves column chromatography in which a stationary phase is a solvent-swollen polymer network varying over many orders of magnitude. The column effluent was continuously monitored by a differential refractometer, and from the various fractional readings, it was possible to determine the actual molecular weight of the samples.

For the most part, the resulting correlations of the average Tg with the molecular weight distribution were very poor. This may be due to the variability of the gel chromatograph test. Any further evaluation requires determination of the reliability of the distribution chromagrams. It should be noted that the basic idea of this work appears to be worthy of further investigations and may

prove to bring useful information towards the understanding of the nature of asphalts once reliable correlations between Tg and the molecular distribution are found.

Another aspect of asphalt studies involves investigations directed to the modification of asphalt cement with different fillers that would improve asphalt paving surface performance. Previous investigations show that most bitumens exhibit an apparent glass transition temperature near zero degree centigrade. As a result, most asphalt paving surfaces are susceptible to low temperature cracking. In order to find an acceptable solution to this problem, various attempts have been made to produce improved paving materials by adding rubber [35], glass [25], coal ashes [26], and other types of fillers to asphalt cement.

Prior studies [35] suggested that the most effective additives for asphalt improvement are those polymers which possess the lowest Tg. In this way of thinking, Jew and Woodhahms [36] conducted an investigation designed to evaluate the laboratory performance of polyethylene-modified asphalt material and to develop specification for a hot mix which would be useful for conventional road laying practices. Polyethylene scrap as filler in asphalt cement is an attractive candidate for two basic reasons. First, the glass transition temperature of polyethylene has been reported to be

between -80oC and -120°C, which is considerably lower than that of asphalt. Second, the vast production of polyethylene plastics manufactured in North America generates a considerable amount of waste plastic material which can be recovered for a relatively low price.

Asphalt obtained as a residual from western Canada crude was selected by Jew and Woodhams together with ten different grades of polymer supplied by various sources. The mixtures were prepared by slowly adding a weighted amount of polyethylene pellets to heated asphalt maintained at 140°C while been stirred with a high speed laboratory mixer. After several minutes, the smooth mixture was cast into rectangular molds, and then placed in a freezer at -20°C until required for testing.

The flexural stress, the flexural module, and the elongation to break at each temperature (down to -50°C) were obtained using an Instron tester attached to an environmental chamber that was cooled with liquid nitrogen. Testing was performed after the samples reached thermal equilibrium. Resilient modulus measurements were made according to the method of Emery [37], and the viscosity of polyethylene dispersion in heated asphalt was measured with a Brookfield viscometer.

Considerable difficulty was encountered in the

preparation of the polyethylene dispersions greater that 5% concentration by weight due to the extreme viscosity of polyethylene and the tendency for the mixture to creep up the shaft of the mixer. In addition, the viscosity measurements were complicated by the tendency of the dispersion to slowly separate into layers, with the molten polymer rising up to the surface forming a viscous rubber -like layer. Thus, the resulting viscosities may not be typical due to poor dispersion and/or partial separation of the polyethylene from the asphalt during the measurements. However, when the logarithm of the viscosities were plotted versus the reciprocal of temperature (Arrhenius plot), the familiar linear relationship was observed. Furthermore, it was found that the viscosity of the mixture noticeably increased in comparison to that of the unmodified asphalt. This is an undesirable characteristic which increases the time and energy require to mix the polyethylene modified asphalt with a mineral aggregate. In addition, it was noted that there appears to be a dependency of the viscosity on the molecular weight of the dispersed polymer, which suggests that composition may influence solubility and the resulting viscosity.

Low temperature flexural properties were obtained by observing the complete force-displacement response of asphalt mixtures specimens as they were subjected to a bending stress

a low temperature (about -20°C). In most cases, the unmodified asphalt samples are brittle and fail in a catastrophic mode at low temperatures. From the plots of flexural force versus bending displacement for unmodified asphalt samples and for polymer-asphalt mixtures, it was apparent that a small addition, 5 to 10%, of polyethylene greatly increases the maximum yield stress, the flexural modulus, the ultimate elongation, and the energy to fracture at -20°C of asphalt. Further, from the plots of flexural strength versus polyethylene content percent, it was evident that the addition of polyethylene produces a gradual increase in the flexural strength which becomes more pronounced at concentrations greater the 5 percent. It should be here that while it is interesting to consider the possible benefits of asphalt binder containing polyethylene dispersions, mixtures with concentrations greater than 5 percent exhibit large viscosities which are formidable obstacles in their use as conventional paving materials. Nevertheless, Jew and Woodhams' results clearly showed polyethylene as a potential useful modifier for increasing the low temperature fractural toughness of asphalt concrete, and it may also contribute to additional pavement stability at elevated temperature to minimize rutting and distortion caused by creep.

In general, the investigations of types of bitumens, including asphalt, consists basically of the analysis of their

thermal behavior and of their physico-chemical properties. A significant portion of the information needed for the investigation of bitumen results from analytical studies using complex and expensive laboratory methods. Consequently, the search for new methods that are less laborious and that offer reliable information on the properties of bitumens is of great theoretical and practical value.

In an attempt to determine the usefulness of thermal analysis for diagnosing solid forms of bitumen and asphaltites, Krasavina and Onosko [38] carried out a thermographic investigation using the method of differential thermal analysis (DTA) on well-studied standard specimens of bitumens from various regions of Europe, Asia, and America. In this investigation, thermograms from microsamples weighing 0.02 to 0.03 grams were obtained by the DTA method using a heating rate of 30-35 °C/min.

Examination of the recorded thermograms revealed that each class of bitumen is characterized by specific heating curves. For example, all thermograms obtained for asphalts showed a small endothermic peak in the 120°C to 200°C range which corresponds to the melting of asphalt. This small peak is then followed by an intense exothermic effect in the region of 450°C to 650°C that may be due to the oxidation-combustion of organic matter. For asphaltites, the thermograms are, for

the most part, similar to those of asphalt , except that the first endothermic effect occurs between 200°C and 300°C, and that this peak is preceded by a small exothermic effect beginning at about 150°C.

The results indicated that definite thermographic characteristics are inherent to each genetic type of solid bitumen, and that thermal analysis for very small samples can be a promising tool in the study of their properties.

Thermal analysis was also used by Razo and Asomoza [39] in their investigation of the thermal characterization of polyethylene and asphalt. Razo and Asomoza employed the methods of differential scanning calorimetry (DSC) and thermomechanical analysis (TMA). They measured linear expansion coefficients, the softening points, and the penetration temperatures of various polyethylene and asphalt samples using the TMA method over the range of -180°C to 500°C. The heating rate range used was from 0.5°C to 30 °C/min, and the instrument was calibrated using an aluminum cylinder. On the other hand, the DSC technique was employed to determine fusion temperatures, heat of fusion, % crytallinity, and the heat capacity of the polyethylene samples. Specifications on the experimental procedures of these two methods, DSC and TMA, are given in detail in chapter 2 of this thesis. In their conclusions, the authors found these thermoanalytic techniques to yield rapid and reliable data for the thermal properties of

polyethylene and asphalt that are most relevant to the processing of these materials. However, their result are presented in a very vague form and no effort was made to determine the glass transition temperature which is one of the most important properties needed in the characterization of polyethylene and asphalt.

Investigations of asphalt-polymer systems were conducted by Liszynska and Bukowski [40]. The aim of their studies was to examine the possibility of applying thermal analysis techniques to investigate systems composed of petroleum asphalt and poly(methyl methacrylate), PMM. The practical aspect was to evaluate the chance of utilizing waste products for asphalt modification. The samples used were obtained by the polymerization of methyl methacrylate initiated by ultraviolet radiation in the presence of petroleum asphalt and its component groups, i.e. asphalt oils, asphalt resins, and asphaltenes.

In order to learn more about their composition and structure, Liszynska and Bukowski [40] subjected the products to fractionation. One of the methods employed was asphalt elution with carbon disulfide, CS_2, and another was polymer precipitation by cyclohexane from benzene solution. The fractions obtained were named by their coloring: a "dark" fraction, with asphalt predominance, and the "light" fraction,

with PMM as the predominant substance. The residue obtained after elution were subjected to thermal analysis using differential thermal analysis (DTA) with thermogravimetry to determine transition temperatures and mass losses over the temperature range from 0°C to 1273°C. For the sake of comparison, PMM thermal curves were also recorded. The heating rate applied was 10 °C/min, and aluminum oxide, Al_2O_3 , was used as the reference material.

It was found that the thermocurves of the dark and light fraction samples did not differ significantly from those of pure PMM. The heating curves of PMM and of the light fraction samples indicated the presence of three endothermic transitions, one about 200°C, another around 300°C, and the last one close to 400°C. On the other hand, the heating curves for the dark fraction sample exhibited these three changes plus one additional transition at 460°C. The authors made no attempt to explain the origin of these transitions, but concluded that thermal analysis is of great value in the determination of the structure of asphalt-polymer system.

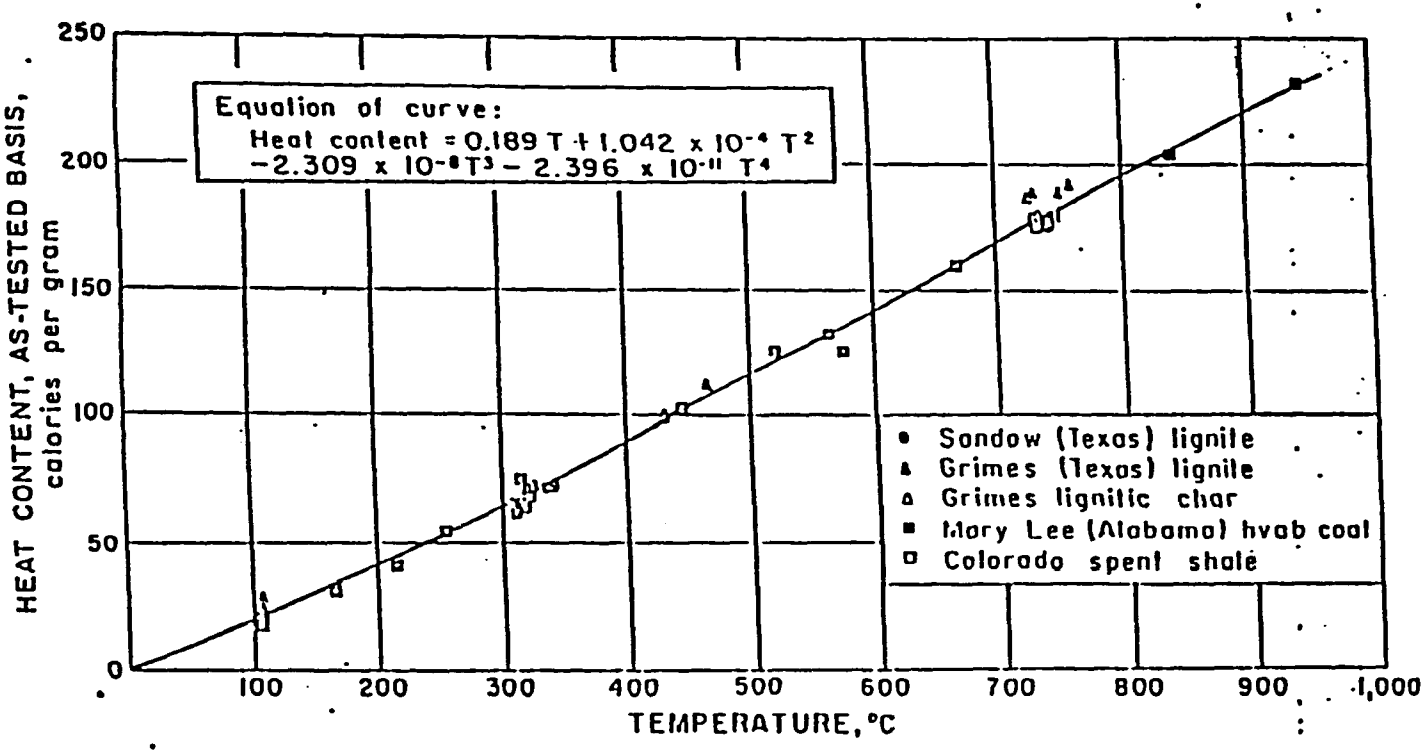

FIGURE 1. - Heat Content of Ash From Coal, Char, and Spent Shale.

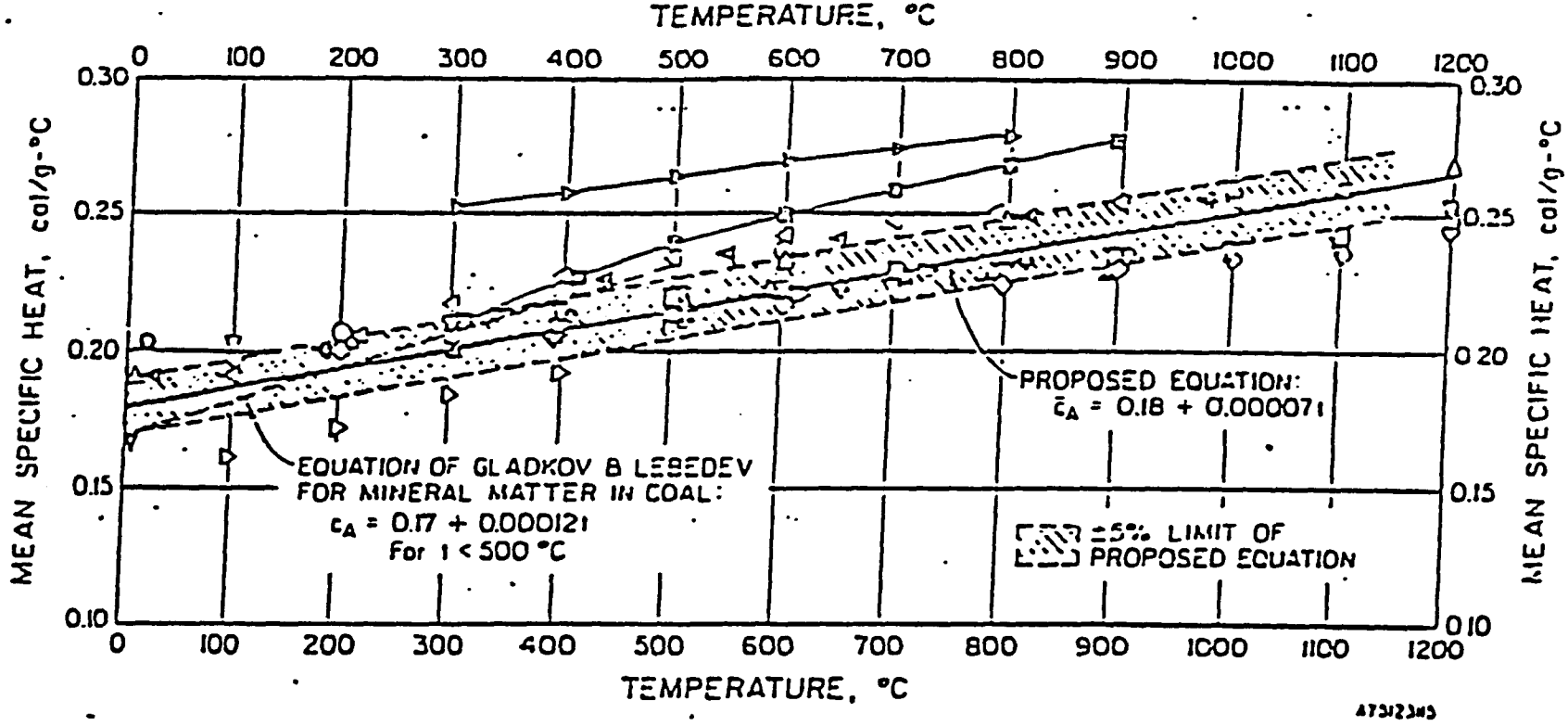

- O SILICA BRICK
- Δ FIREBRICK
- □ PORTLAND CEMENT CLINKER
- ▽ BLAST FURNACE SLAG
- ◇ OPEN HEARTH SLAG
- ◁ QUARTZ (SiO_2)
- ▷ 50% Fe_2O_3 + 50% Fe_3O_4
- ○ CALCIUM CARBONATE ($CaCO_3$)
- ▲ CALCIUM OXIDE (CaO)
- ▫ ALUMINA (Al_2O_3)
- ▼ COAL ASH (COLES)
- ◆ ASH FROM A GERMAN BROWN COAL (TERRES)
- ◀ ASH IN COKE (DEBRUNNER)
- ▶ MgO

FIGURE 2. - Mean Specific Heats of Ash, Slag, Clinker, and of their main constituents.

CHAPTER 2

Experimental Techniques

In this chapter we describe the experimental techniques used in this investigation. The chapter is divided into four sections according to the thermal analytic technique presented, so that section 2.1 is dedicated to the DSC method; section 2.2 refers to the DTA technique; section 2.3 examines the TMA technique; and section 2.4 to dilatometry.

2.1 DSC Technique.

In a generic sense [41], differential scanning calorimetry (DSC) is a technique in which the difference in energy inputs into a substance and a reference material is measured as a function of temperature or time while the substance and the reference material are subjected to a controlled temperature program. All DSC instruments feature similar characteristics:

1. In all cases the recorded output is the

heat flow derived from the temperature difference between the sample and the reference taken using temperature sensors as the primary transducers.

2. The temperature sensors are located external to the sample in order to make calorimetric measurements [42].
3. All DSC devices display the heat flow as their primary output.

An example of the differential temperature type DSC is the DuPont 910 DSC System. A cross sectional diagram of the module is shown in Fig. 1. In the DuPont module, pans containing sample and reference materials are placed on raised portions of a constantan disk which serves as the primary heat source and as one element of the temperature measuring thermoelectric junctions. The chromel wafers attached to the underside of the constantan platform form a chromel-constantan differential thermocouple system which allows the differential temperature, ΔT, to be monitored. The actual temperature of the sample is determined by a chromel-alumel thermocouple formed by chromel and alumel wires connected underneath the chromel disks. The temperature output is fed to a variable gain amplifier which amplifies and electronically scales the signal to be displayed in heat flow units. This differential power output can be plotted either versus sample temperature

or versus time.

At a constant rate, the heat capacity of a sample through its melting point theoretically increases to infinity while the sample temperature becomes invariant; thus, a ΔT develops between the sample and the constantly rising reference temperature. The ΔT signal is proportional to the heat flowing into the sample.

The theoretical interpretation of the DSC and other differential analytical curves have been the subject of numerous theories. Gray [43] developed a general theory describing DSC and DTA curves which was later improved by Baxter [44]. The essential components of a thermal analysis cell are shown schematically in Fig. 2. They consist of a sample at temperature T_s, its container at temperature T_{sh}, and a temperature programmed source at temperature T_b. Heat will flow between sample and reference sites at a constant rate of di/dt depending on the temperatures involved and the thermal resistances connecting these positions. The sample and its container have a heat capacity C_s. Similar descriptions can be developed for the reference side.

Assuming that the calorimeter is symmetrical, that the thermal resistances are identical on the reference and sample sides at any given temperature, that the temperatures of the

sample and reference and their containers are uniform, and that the heat flow between the sample and the reference can be neglected, then the response of the calorimeter can be described using heat balances and thermal ohm's law relationships.

According to Newton's Law, all heat flow in the system is proportional to temperature difference,

$$\frac{dq}{dt} = A\Delta T$$

where dq/dt is the heat flow, di/dt, between two stages separated in temperature (ΔT) by a barrier with a heat transfer coefficient "A". The thermal resistance (R_d and R_c) is the inverse of the heat transfer coefficient (A_d and A_c). Assuming that the sample is generating heat at a rate dH/dt (exothermal transition) then the equations for heat flow on the sample and reference sides are:

$$\frac{di_s}{dt} = \frac{T_{sh} - T_b}{R_d} = \frac{T_s - T_b}{R_c + R_d} \qquad (2.1)$$

$$\frac{di_r}{dt} = \frac{T_{rh} - T_b}{R_d} = \frac{T_r - T_b}{R_c + R_d} \qquad (2.2)$$

Heat evolved by the sample can either increase the sample temperature or be lost to the surroundings. Since energy must be conserved, the sum of these two effects must be equal to

Dh/dt; thus,

$$\frac{dH}{dt} = C_s \frac{dT_s}{dt} + \frac{di_s}{dt} \tag{2.3}$$

$$0 = C_r \frac{dT_r}{dt} + \frac{di_r}{dt} \tag{2.4}$$

Combination of equations (2.1) and (2.3), and (2.2) and (2.4) yields:

$$\frac{dH}{dt} = C_s \frac{dT_s}{dt} + \frac{T_s - T_b}{R_c + R_d} \tag{2.5}$$

$$0 = C_r \frac{dT_r}{dt} + \frac{T_r - T_b}{R_c + R_d} \tag{2.6}$$

Subtracting the equation for the reference (2.6) from that of the sample side, equation 2.5, gives:

$$\frac{dH}{dt} = C_s \frac{dT_s}{dt} - C_r \frac{dT_R}{dt} + \frac{T_S - T_r}{R_c + R_d} \tag{2.7}$$

$$\frac{dT_s}{dt} - \frac{dT_r}{dt} = \frac{d(T_s - T_r)}{dt} \tag{2.8}$$

Substituting equation (2.8) into (2.7) yields:

$$\frac{dH}{dt} = \frac{T_s - T_r}{R_c + R_d} + (C_s - C_r)\frac{dT_r}{dt} + C_s \frac{d(T_s - T_r)}{dt} \tag{2.9}$$

The quantity measured is the difference in temperature between the sample and reference holders, not the sample and

the reference temperatures themselves. Using equations (2.1) and (2.2), the following relationship is obtained:

$$\Delta T = T_{sh} - T_{rh} = \frac{R_d}{R_c + R_d}(T_s - T_r) \qquad (2.10)$$

The final expression is obtained by combining equations (2.9) and (2.10)

$$\frac{dH}{dt} = \frac{T_{sh} - T_{rh}}{R_d} + (C_s - C_r)\frac{dT_r}{dt} + C_s\frac{R_d + R_c}{R_d}\frac{d(T_{sh} - T_{rh})}{dt} \qquad (2.11)$$

From equation (2.11), at any time, the rate of heat evolution can be consider the sum of three terms (see Fig. 3):

I. The instrument response divided by a constant, $(T_{sh}-T_{rh})/R_d$, which is proportional to the difference between the sample and reference sides.

II. A term, $(C_s-C_r)Dt_r/dt$, depending on the heat capacity of the sample and on the heating rate, which is the displacement from the zero level.

III. A term, $[(R_d+R_c)/R_d]C_c d(T_{sh}-T_{rh})/dt$, involving the time constant, $[(R_d+R_c)/R_d]C_s$, and the rate of change of the recorded quantity.

For DSC, the measured quantity is the difference in heat

flow into or out of the sample and reference.

$$\Delta q = \frac{di_s}{dt} - \frac{di_r}{dt} \qquad (2.12)$$

Substituting the temperature values from equations (2.1) and (2.2) for the individual heat flow yields:

$$\Delta q = \frac{T_{sh} - T_{rh}}{R_d} = \frac{\Delta T}{R_d} \qquad (2.13)$$

Where the temperature difference sensed by the detectors is directly proportional to the heat flow into or out of the sample and reference.

Substituting equation (2.13) into equation (2.11) yields the DSC final equation:

$$\frac{dH}{dt} = \frac{dq}{dt} + (C_s - C_r)\frac{dT_r}{dt} + C_s(R_d + R_c)\frac{d^2q}{dt^2} \qquad (2.14)$$

This experimental program employed the DSC technique to determine the heat capacity of coal ashes and to investigate the thermal properties of asphalt, plastic and asphalt-plastic mixture samples.

By definition heat capacity (specific heat) is the amount of energy that must be absorbed by a material in order to raise its temperature one degree. In the past, heat capacity measurements have been accomplished using tedious and complex procedures. With the introduction of the differential scanning calorimetry (DSC) technique, many of the problems which made

these measurements difficult have been eliminated.

The basic method for heat capacity measurements using the DSC technique was originally described by O'Neil [45] and modified by Cassel [46]. Samples for heat capacity measurements are generally encapsulated in sample pans. Different versions of these pans are available and the physical and chemical characteristics of the samples determine the type of pan to be used. Once the sample pan has been selected, it should be weighed, then filled with the sample and weighed again. The mass of the sample can be determined from the difference between these weighings. Using an empty pan with lid in the reference side, the first run involves a scan with an empty pan and lid on the sample side. The empty pan should be similar to the one that will contain the sample. The second run, also with an empty pan on the reference side, is a scan of a sample pan containing a material whose heat capacity is well known, such as sapphire. From this run a calibration factor, F, can be determined using the equation:

$$F = \frac{C_p(sapphire, lit.)}{C_p(sapphire, obs.)} \qquad (2.15)$$

This factor, F, is actually the individual calibration constant of the calorimeter at each temperature, Cp is the heat capacity of the standard material.

Subsequent runs are for the samples themselves, each of

which should be encapsulated in pans similar to the one used on the reference side. The heat capacity of the sample, Cp, is determined by using the heat flow values obtained together with the equation:

$$C_p = F\frac{Y}{m} \qquad (2.16)$$

where Y is the difference in heat output between sample and empty pans curves at each temperature of interest, and m is the mass of the sample.

Measurements of phase transitions can usually be treated with the method for the heat capacity described above. The main concern is to assign the correct temperature in regions where the heat capacity is varying rapidly. Second order transitions, such as glass transition, are determined by observing that the slope of the DSC signal changes when the transition occurs at a temperature which is characteristic of the material. In general, other transitions, such as melting, are reflected as a peak on the DSC curve. The area under this peak is direct measurement of the enthalpy involved in the transition [47].

2.2 DTA Technique.

Differential thermal analysis (DTA) is a thermal

technique in which the difference in temperature between a substance and a reference material is recorded as a function of temperature as the two specimens are subjected to identical temperature regimes in an environment heated or cooled at constant rate [45,46].

The DTA curve shows a series of peaks, provided the substance is thermally active in the temperature range provided, which are directly related to temperature changes in the sample. These changes are due to endothermic or exothermic transitions or reactions such as those caused by phase changes, fusion, boiling, oxidation, destruction of crystalline lattice, and other chemical reactions.

The DTA method provides qualitative information and semiquantitative calorimetric measurements. This technique has been used throughout this century and is schematically shown in Fig. 4. A sample (s) and a reference material (r) are subjected to a single heat source (h) in a furnace. Assuming that the heat capacity of the sample is greater than that of the reference, then the temperature of the sample, T_s, will lag behind that of the reference, T_r. The difference in temperature, T_s-T_r, is monitored by the differential thermocouple, T_s, and is the function recorded. In particular, when the sample undergoes a significant change such as melting (endothermic transition) or decomposition (exo- or endothermic

transition), the output curve deviates from a horizontal position to form a peak in either the upward or the downward direction depending on the enthalpy change. In principle, small temperature changes can be detected and the peak area is proportional to the enthalpy change and the sample mass. However, the proportionality factor for the temperature difference depends on the thermal resistivity of the sample and reference materials and on how well the thermocouple junctions made contact with the materials. Boersma [41] realized that a significant improvement could be made by placing on top of the thermocouple junctions cups containing the sample and reference materials. Using this arrangement, the proportionality factor is independent of the heat transfer or other properties of the sample and reference materials.

In the DuPont DTA cell, sample and reference cups rest on top of two independent thermocouple pedestals (see Fig. 5). These cups are surrounded by a furnace capable of heating at a programmable rate. The presence of transitions and the temperature at which they occur are measured by thermocouple which can contact the samples directly or be isolated from them by using platinum or alumina cups.

The theory describing the DTA curves is very similar to that of the DSC described in the preceding section. The final expression representing DTA curves is given by equation (2.9).

In the DTA apparatus, the instrument response is the differential temperature, T_s-T_r, of the recorded curve; thus, knowing the time constant, $[(R_d+R_c)/R_d]C_s$, a DTA curve can be graphically constructed that reflects the thermal behavior of the sample (see Fig. 6).

A typical DTA curve is illustrated in Fig. 7. It shows four types of transitions: (I) A second-order transition, such as a glass transition temperature, that is represented by a change in the horizontal baseline; (II) an endothermic curve peak due to fusion or melting; (III) a broad endothermic curve peak caused by a decomposition or dissociation reaction; and (IV) an exothermic curve peak due to crystalline phase change. The number, position, and shape of these curve peaks may be used for qualitative identification of the substance under investigation.

In the presented research work, the DTA technique will be used to measured the minimum sintering temperature, the softening point, the point of complete fluidity, and the reaction temperatures of coal ashes. Sintering of a powder causes a reduction in volume and, thus, in surface energy; this is an exothermic effect which shows up as an increase in the slope of the DTA signal versus temperature plot. On the other hand, fusion is an endothermic phenomenon and is reflected as a decrease on the slope of the DTA curve.

Chemical reactions are either endo or exothermic events and show up as an increase, a decrease, or slope change in the DTA signal. Therefore, DTA measurements should yield the fusion temperatures of coal ashes.

2.3 TMA Technique.

Although the most widely used thermal analysis techniques are the DSC and the DTA methods, there are a number of other thermal techniques that are employed to supplement or complement the principal techniques in solving chemical and technological problems. Thermomechanical analysis (TMA) is one of these complementary techniques.

Thermomechanical methods constitute the broad area of thermal analysis that involve measurements of changes in volume, shape, length, and other properties relating the physical change of a substance. Three techniques are commonly associated with these methods; they are dilatometry, thermomechanical analysis (TMA), and dynamic mechanical analysis (DMA). The difference between these techniques lies on their methods of measurements.

For TMA, a non-oscillatory stress is applied to the sample as it is heated at a constant rate and the deformation

under the load is measured as a function of temperature. The measured linear and volumetric changes are directly related to crystal structure changes, and changes in the physical and/or chemical state of the sample under investigation.

A Change in the sample length can be expressed the equation:

$$L = L_o(1 + \alpha T) \qquad (2.17)$$

where L is the sample length at temperature T, Lo is the sample length at 0°C, and α is the linear coefficient of thermal expansion. In the TMA method, L is recorded as a function of temperature. Differentiation of equation (2.17) assuming that α is constant gives:

$$\frac{dL}{dT} = L_o \alpha \frac{dT}{dt} \qquad (2.18)$$

where dT/dt is the constant heating rate.

When compared to other techniques, the TMA instrumentation is quite simple. For the DuPont model 943 TMA module (see Fig. 8), linear displacements of the sample probe are sensed by a linear variable displacement transformer (LVDT). A thermocouple used to measure the sample temperature is in direct contact or in close proximity to the sample which is surrounded by a controlled cylindrical heater and Dewar assembly. The final output is a plot of the sample dimensional change, and/or its derivative, versus temperature or time.

Various types of probes allow the TMA apparatus to be used in expansion, compression, penetration, tension, stress relaxation, and other measurements. In our studies, TMA was used to determine the glass transition temperatures, and softening points, and to measure expansion coefficients and viscosity as functions of temperatures of asphalt, plastic, and asphalt-plastic mixtures samples.

2.4 Dilatometry.

The determination of the volume change of a substance as a function of temperature or time is called dilatometry. In this technique , the powder is placed into a small quartz tube inside a furnace assembly. The sample is then compressed by an adjustable load, a push rod, and heated at a known constant rate. Measurements of the change in length, contraction, or expansion of the sample are detected by a push-rod connected to a linear variable differential transducer (LVDT). The change in sample length is sensed by the transducer and recorded as a function of temperature.

Dilatometry is one of the method used to determine the minimum sintering temperature of coal ashes in the current research work. In general, a powder will dilate upon heating due to thermal expansion. Eventually, a point will be reached

where the surface of the sample starts to deform resulting in contraction of the sample. This point is considered the minimum sintering temperature, Ts, of the powder.

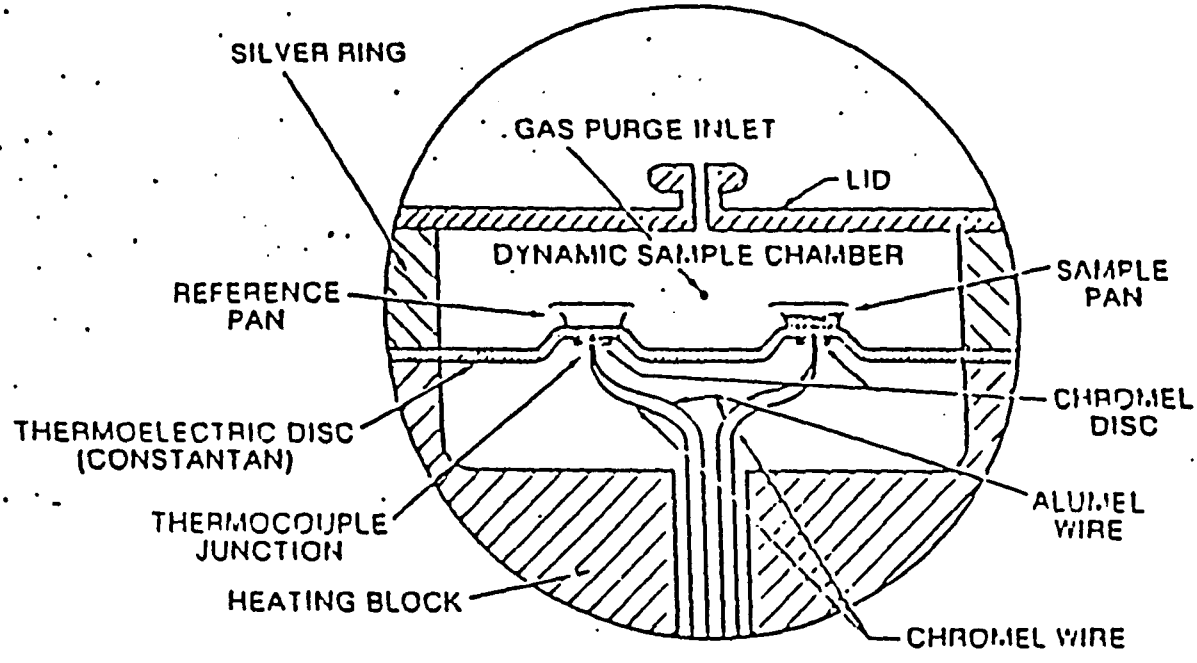

FIGURE 1 . - DSC Cell Cross-section

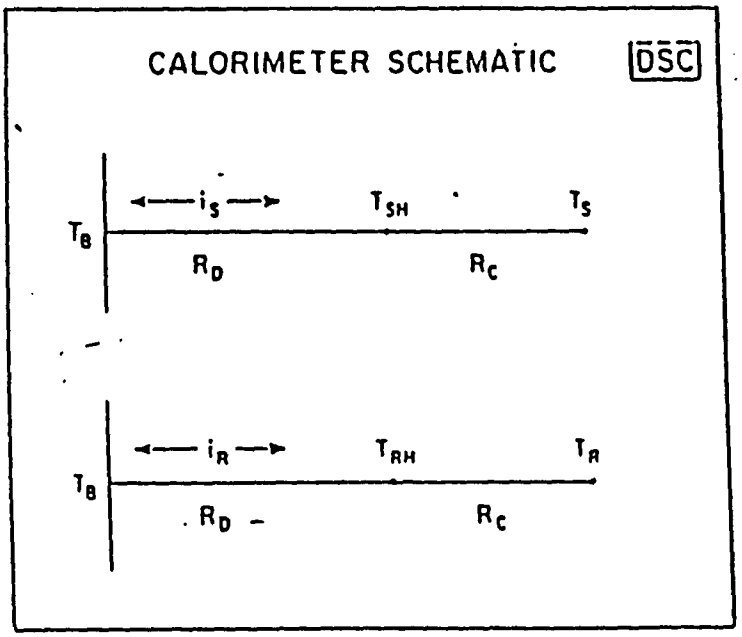

Figure 2

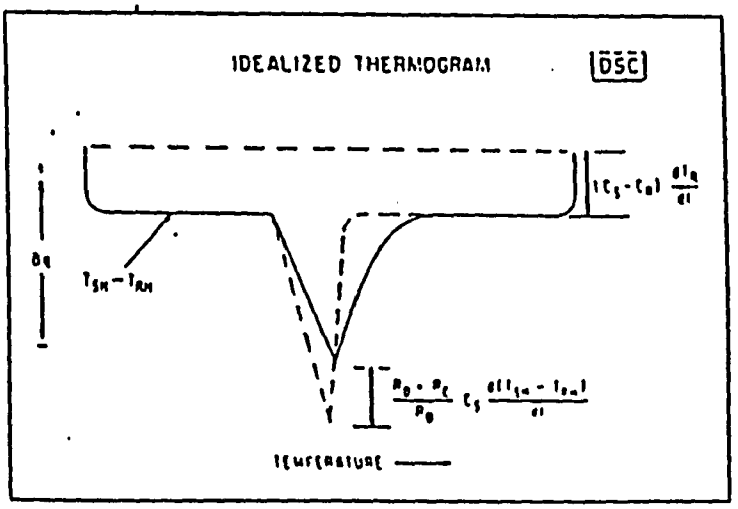

Figure 3

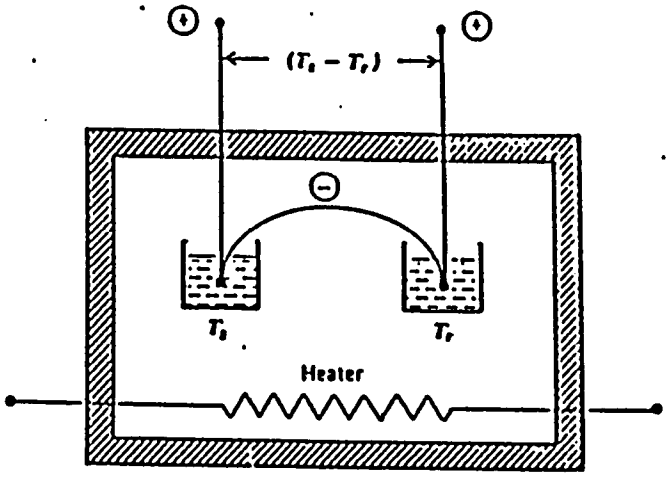

FIGURE 4 . — Basic DTA system.

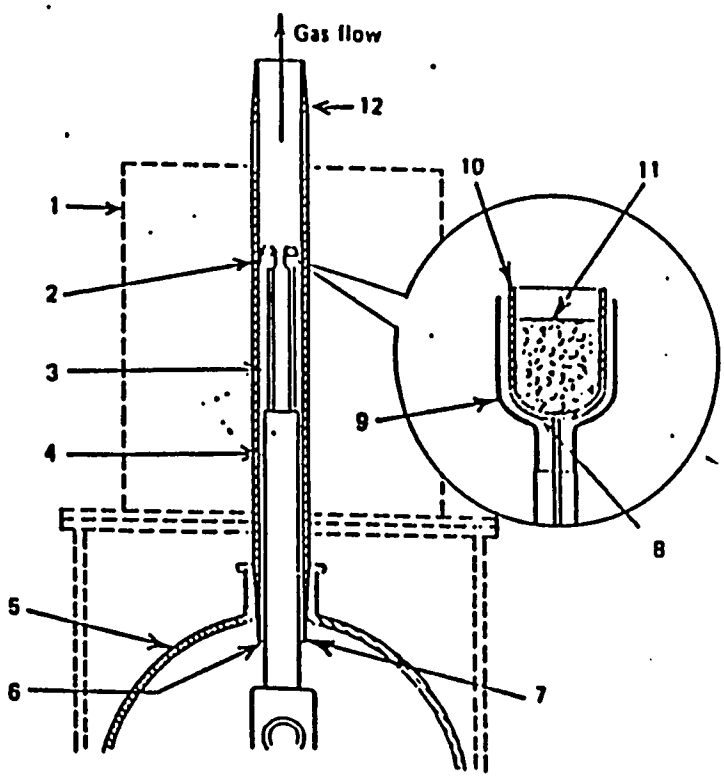

FIGURE 5 . — Du Pont 1200°C DTA cell according to Miller and Wood (92): 1, furnace 2, shoulder; 3, ceramic insulator; 4, ceramic support; 5, bell jar; 6, gas flow; 7, tapered joint; 8, thermocouple junction; 9, platinum cup; 10, liner; 11, sample; 12, alumina furnace tube.

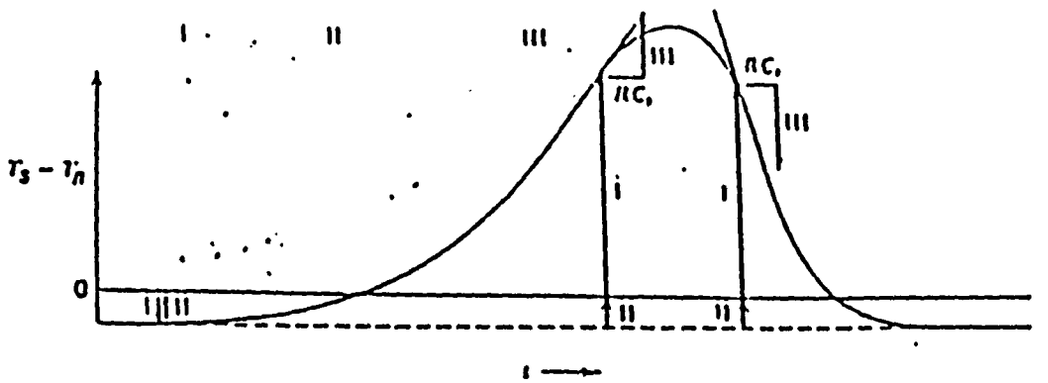

FIGURE 6. - Determination of R dH/dt from DTA

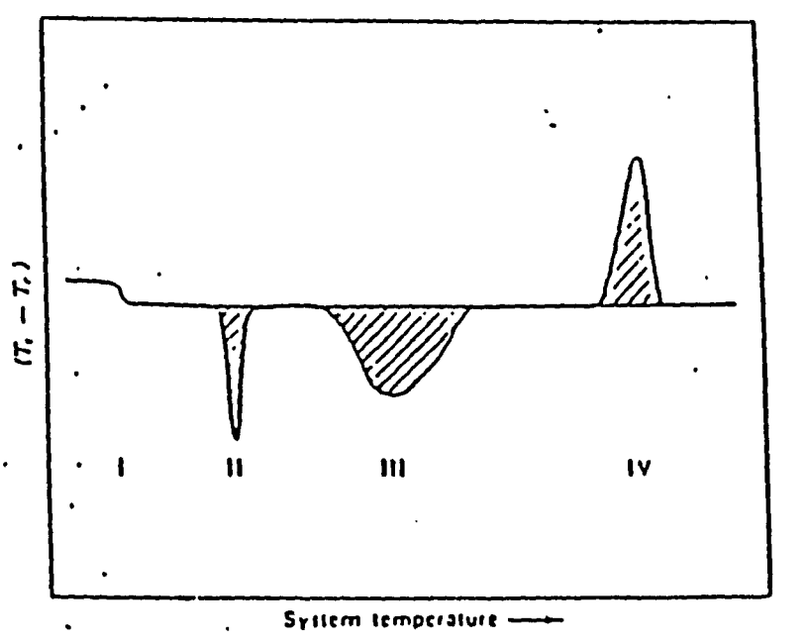

FIGURE 7. - Typical DTA Curve.

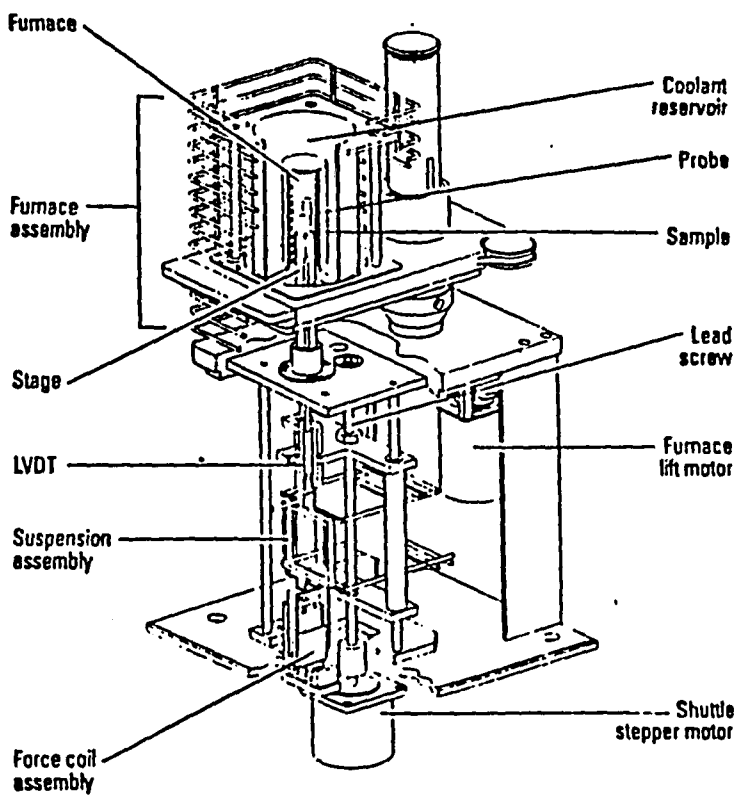

Figure 8 *TMA 2940 schematic.*

CHAPTER 3

Thermal Characterization of Coal Ash Powder: Heat Capacities and Minimum Sintering Temperatures

3.1 Abstract

Ash mineral matter from ground coals were prepared by combustion at 973°K. Five coal samples ranging in rank from lignitic to high-volatile bituminous coals were used as starting materials. The heat capacities of the coal ash materials were measured between 140°K and 900°K by differential scanning calorimetry. The minimum sintering temperatures of each of the ash powders were determined using a high temperature dilatometer.

3.2 Introduction

The use of coal either for power generation or as a raw material in chemical processes is usually accompanied by generation of ash. The ash comes from the mineral content of the coal and may amount to as much as 15% of the total weight for soft coal. The ash contribution to the heat load must be accounted for in an energy balance.

Most of the processes proposed for the conversion of coal

to synthetic fuels (and feedstocks) require the use of fluidized bed reactors. Since the agglomeration of ash particles in such reactors is an operational problem, the value of the minimum sintering temperature becomes an important operating parameter.

Because of the wide variation in the composition of coal mineral matter, it is necessary to ascertain how ash property vary with the composition and the type of coal. In this communication, the results of thermal characterization experiments on ashes derived from low temperature (973°K) combustion of five different coals, specifically the results of heat capacity and dilatometry measurements, are reported.

3.3 Experimental

3.3.1 Ash Preparation

A suite of five coals was obtained from the Pennsylvania State University Coal Bank. Their rank and other pertinent properties are listed in Table I. In Table II, the major mineral constituents of some similar type coals [1] are listed. The coals were ground with a ball mill and sized by sieving. The 250 mesh sieve fractions were used for the preparation of the ash powder. These were prepared by placing five gram portions of the coals into muffle furnaces which were preheated to 825°K, and then raising the temperature

slowly to 973°K. The ashes were kept at 973°K for two or three hours to ensure total combustion. No indication of particle size coarsening was observed. The chemical composition of the prepared ashes were not determined directly. Spectroscopic analysis of the ashes obtained from coal according to ASTM procedures, reported as oxides, for the coals whose mineral constitution breakdown is given in Table II, indicate that they contain: 33-55 wt% SiO_2, 10-25 wt% Al_2O_3, 5-15 wt% Fe_2O_3 and 2-20 wt% CaO as their mayor constituents [1].

3.3.2 Heat Capacity Measurements

Ash heat capacities were determined by differential scanning calorimetry (DSC) [2,3]. A DuPont 1090 thermal analyzer system was used for these measurements. The temperature range involved was between 140°K and 900°K. However, some of the measurements were done only between 300°K and 900°K. Sample sizes of the order of six to ten milligrams were used. Heat capacities were calculated by comparing the heat flow curves for the samples with heat flow curves for a sapphire standard. Each sample run was accompanied by a standard run. The data were reproducible (multiple runs) and the estimated precision was 2%.

3.3.3 Dilatometry measurements

One of the methods for finding the minimum sintering temperature, Ts, of a granular material is to use elongation-

contraction versus temperature data obtained by the use of push-rod dilatometry [4]. In these experiments the powder to be tested is placed into a quartz tube and piston assembly, and the sample is compressed by an adjustable load. The experimental assembly is then heated at some preselected rate and the expansion or contraction of the sample is detected by a linear variable differential transducer and recorded as a function of temperature. In general, the powder dilates upon heating due to thermal expansion. Eventually, a temperature is reached where the surface of the particle begins to deform due to viscous flattening and/or sintering at intergranular contact points resulting in the contraction of the sample. The temperature at which this phenomenon occurs is the minimum sintering temperature, Ts, which is characteristic of each powder and is the temperature at which particle agglomeration first occurs.

In this work, the minimum sintering temperature of the five coal ash powder listed in Table I were determined by dilatometry. the samples were tested in air without sieving. they were loaded into a six millimeter quartz tube and compressed by a 23 gram load. The assembly was heated at 12 K/min. rate from ambient temperature to approximately 1250°K. The heating rate was comparable to the heating rate (10 K/min.) used for the DSC measurements. The change in length of the sample is reported as L/Lo, where Lo is the initial length

of the sample.

It should be noted that the value of the piston weight use to compress the sample was chosen so that the intergranular force was kept small, thereby simulating a zero compressing sintering process. Some minimum load is necessary; if too small a load is used, frictional forces become important and the results become irreproducible. Intergranular forces resulting from sample compression loads of the order of 20-30 grams have shown to lower the minimum sintering temperatures of various materials by 2-4% [5].

3.4 Results and Discussion

3.4.1 Heat Capacity of Ashes

Figures 1-5 show the heat capacity of ashes prepared at 973°K, T_{ash}, as a function of temperature. Measured heat capacities at 300°K, 600°K, and 900°K are tabulated in Table I. The data are rather similar to each other irrespective to the source of the ash. The magnitude of the observed heat capacities is in good agreement with literature data [6] on ashes obtained from the combustion of tar sands and other ash like materials.

The non-monatomic behavior of the heat capacity as a function of temperature is real and reproducible. The

conversion of coal minerals to ash involves several processes; dehydration, thermal decomposition, dehydroxylation of clays, oxidation, and phase transformation. Certain features of the obtained heat capacity curves are explainable in terms of these processes.

In the ashing process the coal minerals were dehydrated and formed a material that is porous in character and rather hydroscopic. Water from the air was adsorbed on the ashes. It has been observed [3] that in high porosity material the adsorbed water behaves as two distinct entities, nonfreezable (molecular) water, adsorbed in the pores, and the freezable (bulk) water adsorbed in the surface. The onset of the molecular motion for the pore adsorbed water molecules is endothermic and an anomalous increase in the matrix heat capacity, between 150°K and 250°K is observed. The melting and vaporization phase transformations of the adsorbed bulk water, instead of occurring over the usual narrow temperatures ranges, now spread out over a wide temperature range. The broad maxima in the heat capacities of the ashes between 250°K and 450°K are associated with the desorption of water.

Iron pyrite (FeS_2) is one of the materials associated with the coals used in this study. The heating of iron pyrite in air leads to the formation of the oxide, Fe_3O_4, and of nitrite, Fe_4N, and may leave a range of compounds formulae

Fe_yS_x. A number of these compounds are magnetic. The curie temperature of the above mentioned compounds are respectively 858°K, 763°K and 573°K. When the ash was heated, a series of magnetic to non-magnetic phase transitions took place. Each of these transition was observed to be a lambda type discontinuity in the heat capacity.

Quart is a mayor constituent of the coals used in this study. While quartz remained unaffected by the low temperature ashing process, it underwent the inversion a 845°K. The inversion transformation is accompanied by a lambda type discontinuity in the heat capacity. In Figure I the expected discontinuities in the heat capacity are indicated.

The magnitude of the heat capacity at a given temperature depends on the actual composition of the ash. We do not have analyses of the ash compositions which could be used to correlated the heat capacity with the ash composition. In principle, since ash components do not interact chemically, simple additivity rule for heat capacity should hold. This conjecture is supported by comparing the data of the ashes derived from the two Illinois coals in figure 6. The difference between the mineral contents of these coals is small, But there is a significant difference in pyrite content. The two heat capacity curves differ significantly from each other only in the temperature region where the phase

transition for Fe_4N, Fe_3O_4 and quartz occur.

An important question with respect to the properties of coal ashes is the extent to which they are dependent on the method and condition of ash formation. In particular, the combustion temperature is an important variable. In Figure 7, The data for the heat capacity of the ash obtained from the Virginia HVA coal at 973°K and at 1373°K is shown. Exposing the ash to a higher temperature increases its heat capacity significantly over most of the temperature range covered. This reflects the sequence of reactions involved in the conversion of coal's mineral matter to ash as the temperature is increased. The original heating of coal to 973°K results in dehydration, dehydroxylation and pyrite conversion of the mineral components. The dehydroxylation and pyrite conversion are irreversible reactions. Above 1073°K additional irreversible reactions are possible, including decarbonation of calcite, dolomite and siderite and the high temperature phase transformation of clays. Therefore, it is not surprising that ashes heated to higher temperatures show changed heat capacities.

3.4.2 Sintering temperatures

The dilatation vs temperatures curves obtained for the five coal ashes are shown in Figure 8. The minimum sintering temperatures obtained are listed in Table I. Illinois #6,

Illinois #6 HVB and Wyoming subbituminous ashes behave similarly in the dilatometer. These samples dilates due to thermal expansion right up to the minimum sintering temperature at which point a large contraction occurs in the 1036°K to 1084°K range. The minimum sintering temperature is taken to be the temperature at which this contraction begins. In the cases of North Dakota Lignite and Virginia HVA ashes the large contraction occurring at 1035°K (North Dakota Lignite) and 1101°K (Virginia HVA) are preceded by a plateau regions beginning at 853°K and 927°K respectively during which the magnitude of the surface softening is just enough to counter-balance thermal expansion. Inspection of the cooled samples showed that weak agglomerates, which are easily broken, had formed in all cases.

These results correspond well with the findings of Raask [7] who developed a method of simultaneous shrinkage and electrical conductance measurement to determine the sintering temperatures of powders. This method was also later used by Conn and Austin [1]. These authors found that some non-bituminous coal ashes including certain lignites show weak sintering at temperatures as much as 200°K below the temperature at which major shrinkage of the samples begins. The low temperature sintering point could only be detected by a change in the electrical conductance of the sample. For example, Conn and Austin reported a weak electrical sintering

point at 873°K and large shrinkage begins at 1023°K for the North Dakota Lignite coal ash, whereas Illinois #6 HVB ash sintered only at 1123°K as indicated by large changes in both conductance and the length of the sample. Dilatometry has also been used by others to measure coal ash sintering temperatures [8,9]. Siegell [8] measured values for Ts ranging from 975°K to 1148°K for various ashes which were obtained from actual boilers.

Additional methods such as sieving agglomerates formed at various temperatures [10] and hot lens microscopic [11] have also been developed for Ts determination and give similar results, that is, minimum sintering temperatures in the 950°K to 1150°K range for a variety of coal ashes. It should be noted that the ASTM method for fusibility of coal and coke ashes [12] give minimum sintering temperatures which are too high. Apparently the ASTM method does not respond to surface softening and is sensitive only to gross particle deformation.

Table I. Properties of Ashes and Coals.

Sample Identification	PSU Number	Total Mineral Matter Content as % (dry)	Pyritic Sulfur as %(dry)	FeS_2 as %(dry)	C (KJ/Kg-^oK)			T_s (K)
					300^oK	600^oK	900^oK	
No. Dakota Lignite	PSOC-246	10.99	0.03	0.06	0.63	0.54	0.46	(853) 1035
Wyoming Subbit. B	PSOC-241	8.13	0.46	0.86	0.74	0.60	0.82	1036
Illinois #6	PSOC-022	11.88	0.89	1.67	0.63	0.72	0.93	1084
Illinois #6 HVB	PSOC-282	11.78	0.64	1.20	0.60	0.72	0.66	1066
Virginia HVA	PSOC-265	17.98	0.02	0.04	0.68	0.67	0.35	(927) 1101

Table II. Mineralogical Analysis of the Low Temperature Ash of Three Coals. (Taken from Conn and Austin [1].)

Mineral (wt%)	Keystone	Ill. #6 HVC	N. Dakota lig.
Quartz	25	20-25	25
Pyrite	10	10-15	10
Calcite	-	1-5	2-5
Gypsum	5	1-5	5-1
Kaolinite	30	20-25	5
Illite	20-40	10-20	-
Feldspar	-	1-5	-
Coquimbite	-	5-10	-

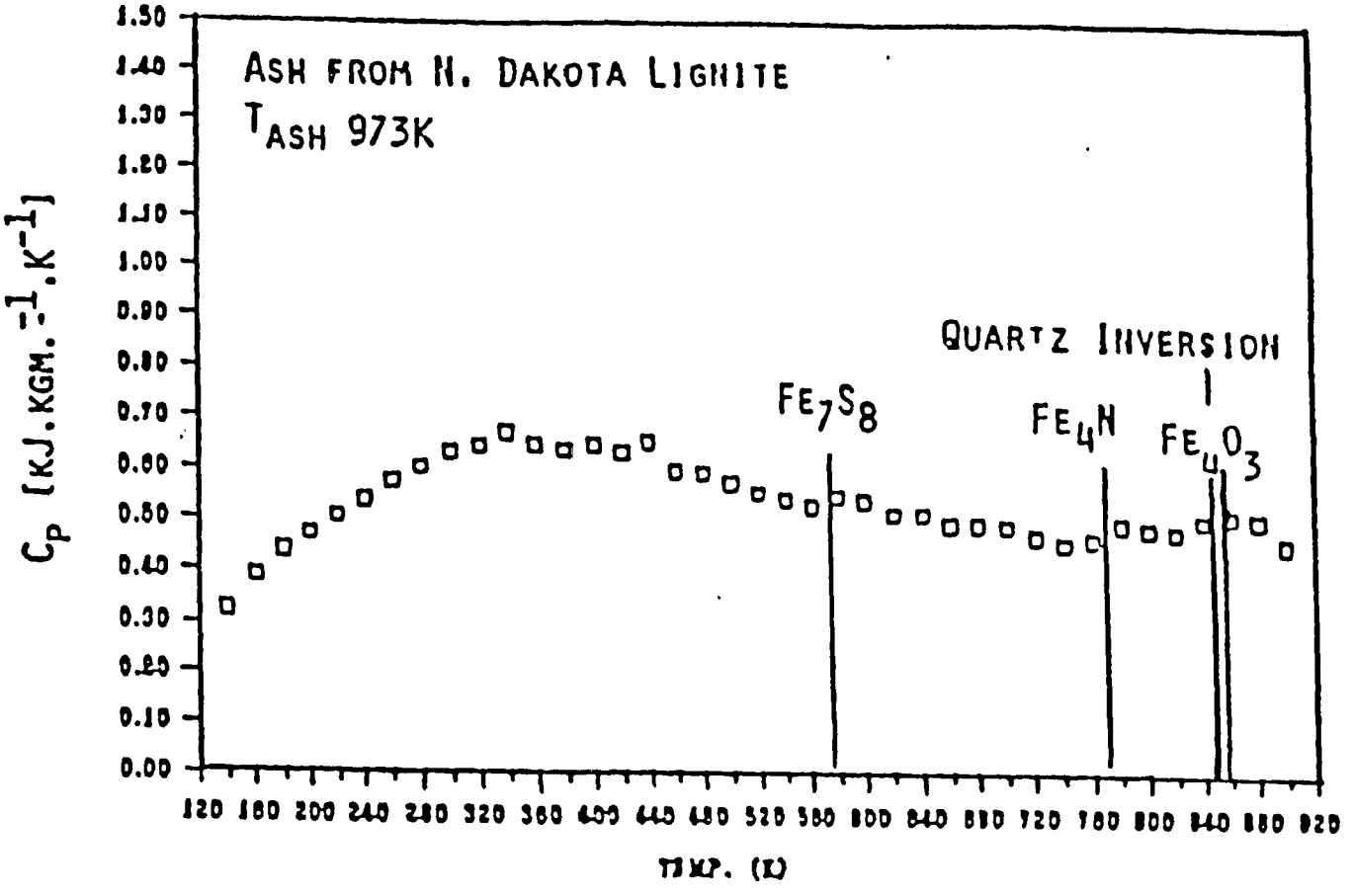

Figure 1. Ash Heat Capacity vs. Temperature

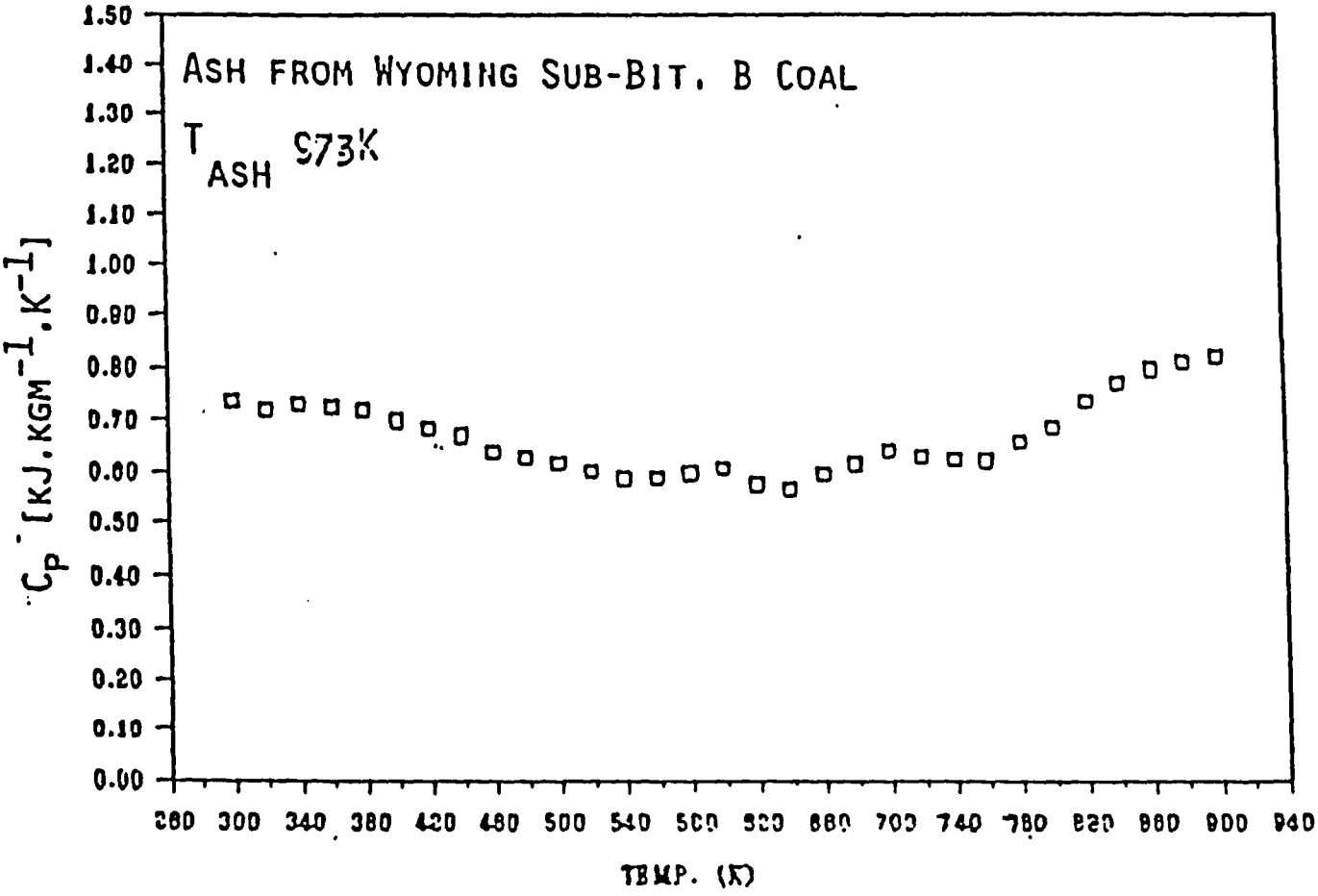

FIGURE 2. ASH HEAT CAPACITY VS. TEMPERATURE

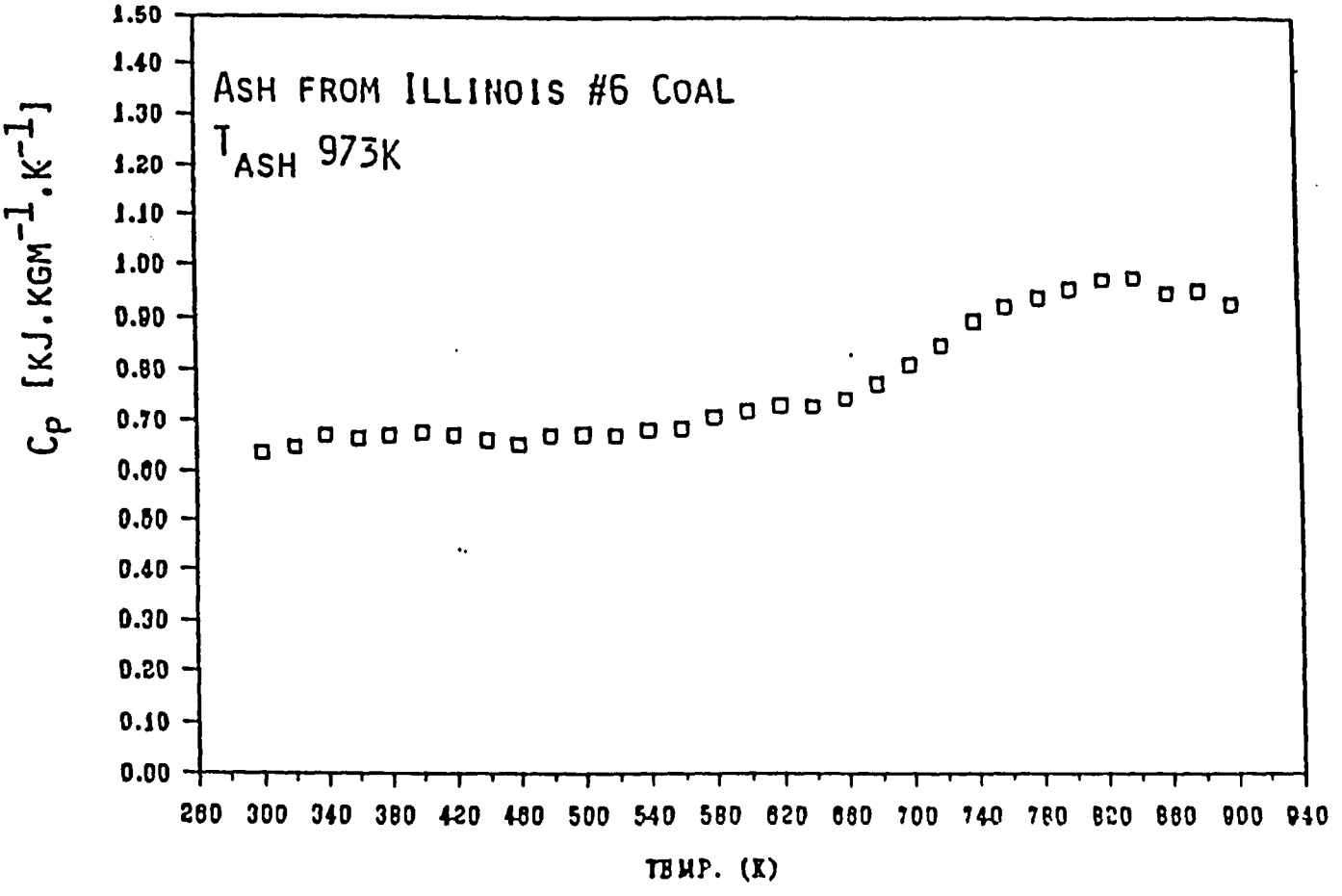

FIGURE 3. ASH HEAT CAPACITY VS. TEMPERATURE

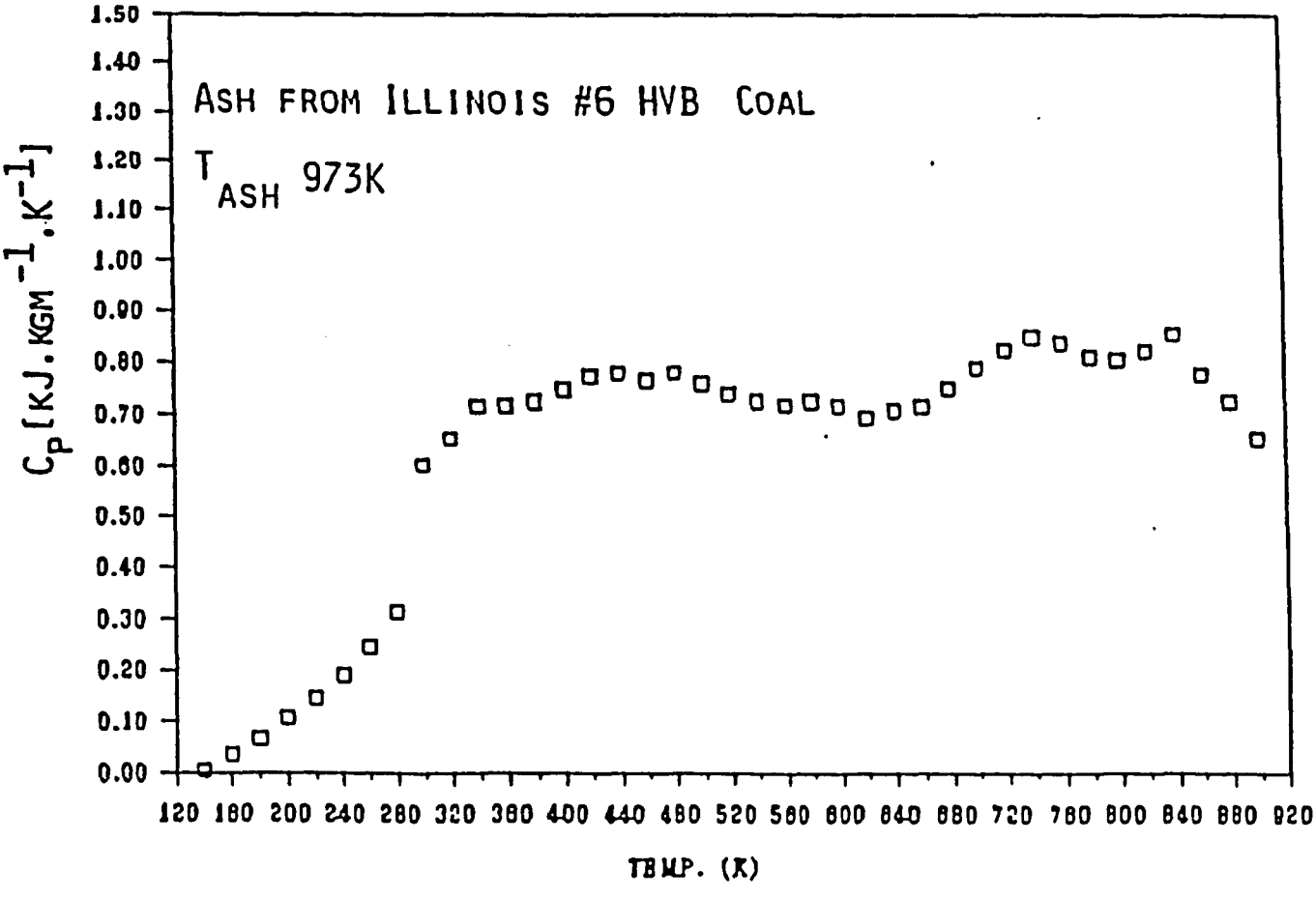

FIGURE 4. ASH HEAT CAPACITY VS. TEMPERATURE

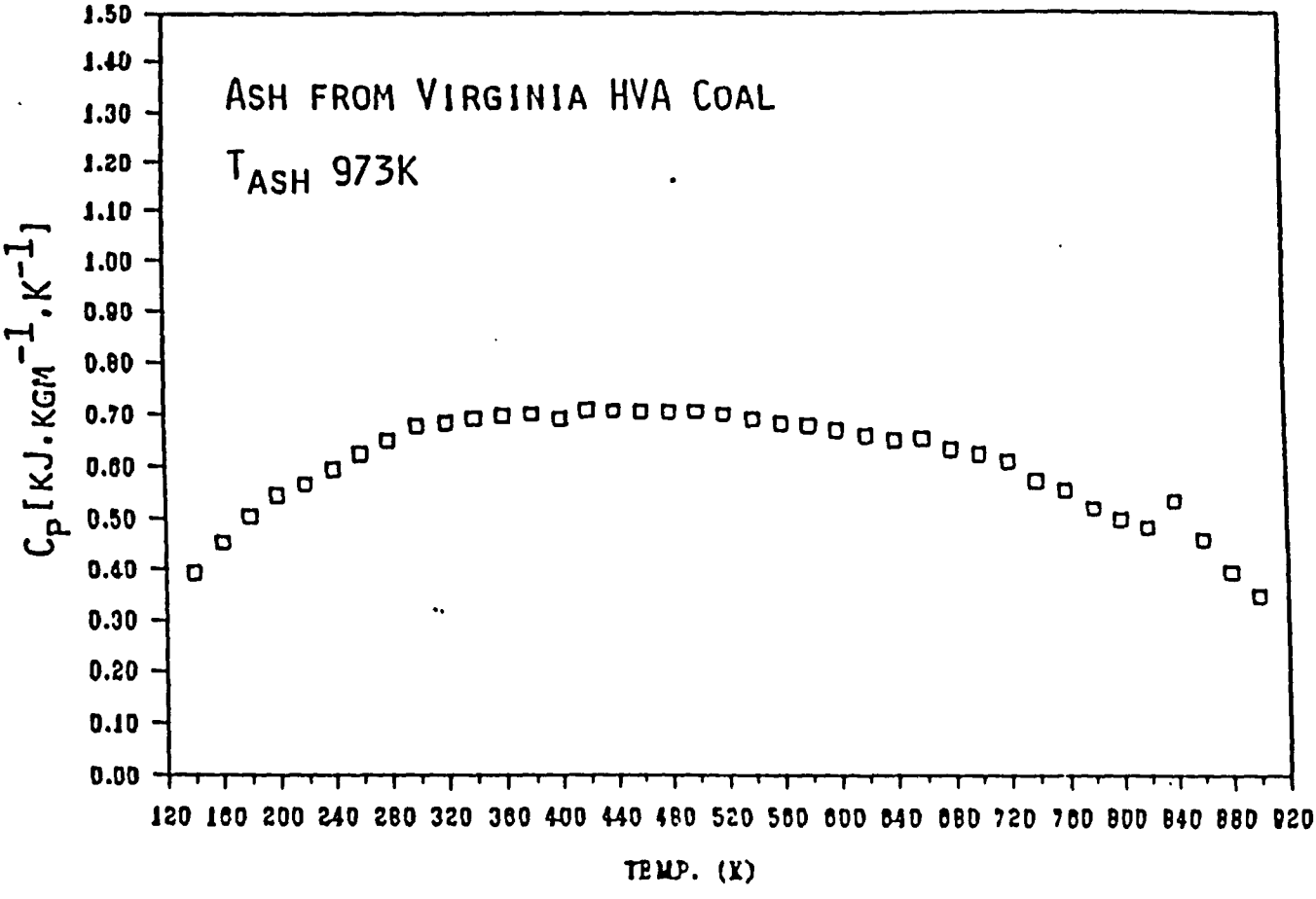

FIGURE 5. ASH HEAT CAPACITY VS. TEMPERATURE

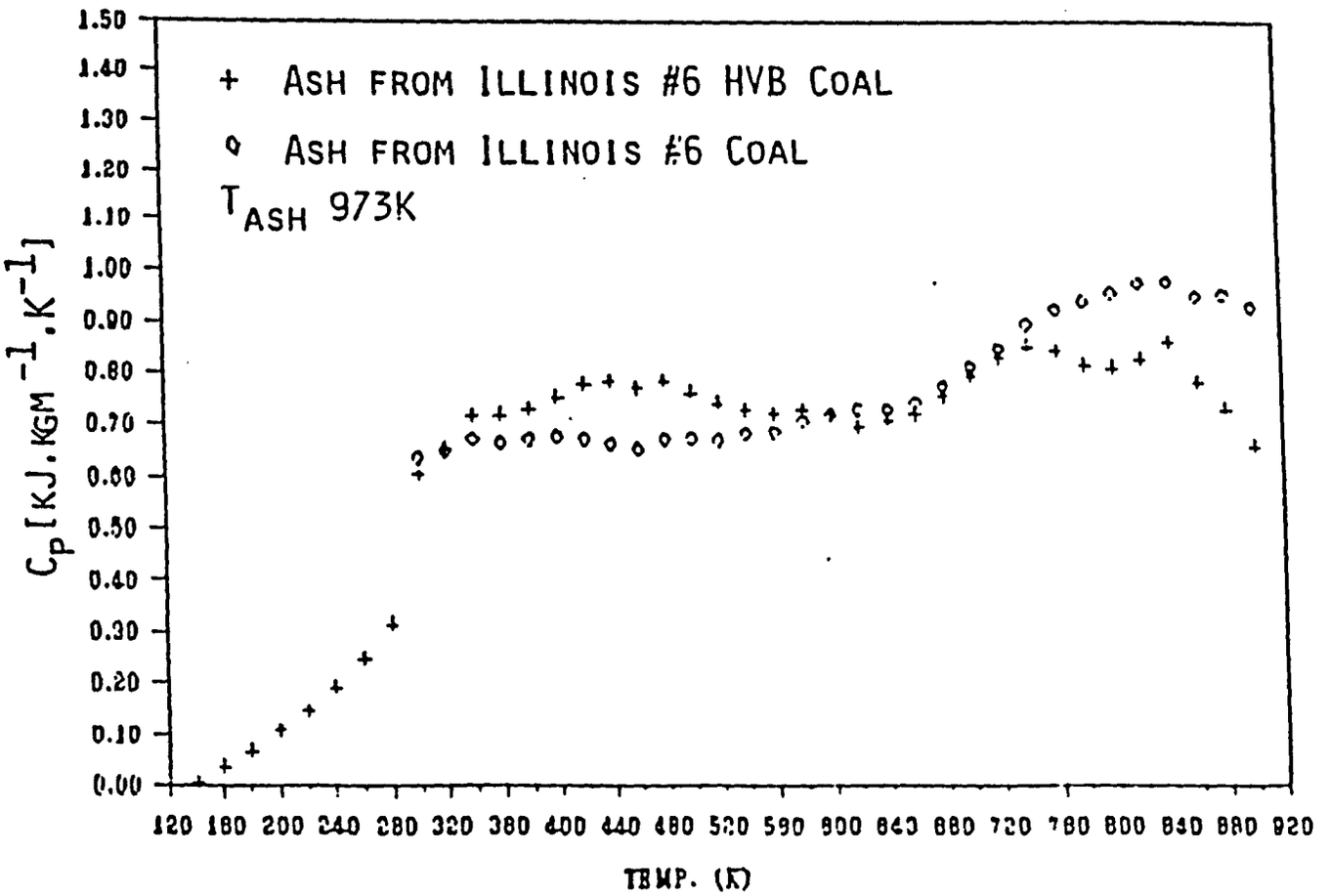

FIGURE 6. ASH HEAT CAPACITY DEPENDENCE ON COMPOSITION

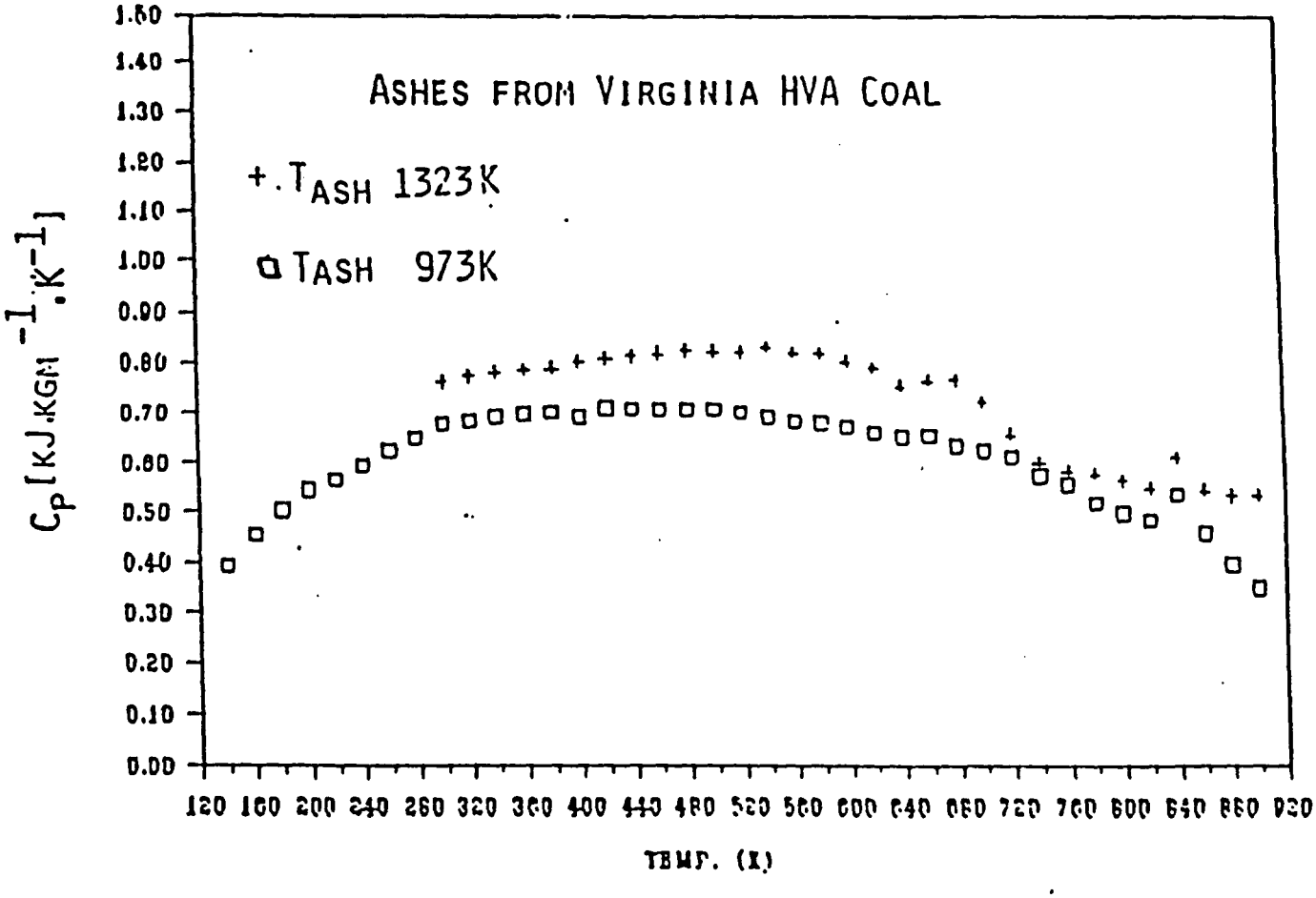

FIGURE 7. DEPENDENCE OF ASH HEAT CAPACITY ON ASHING TEMPERATURE

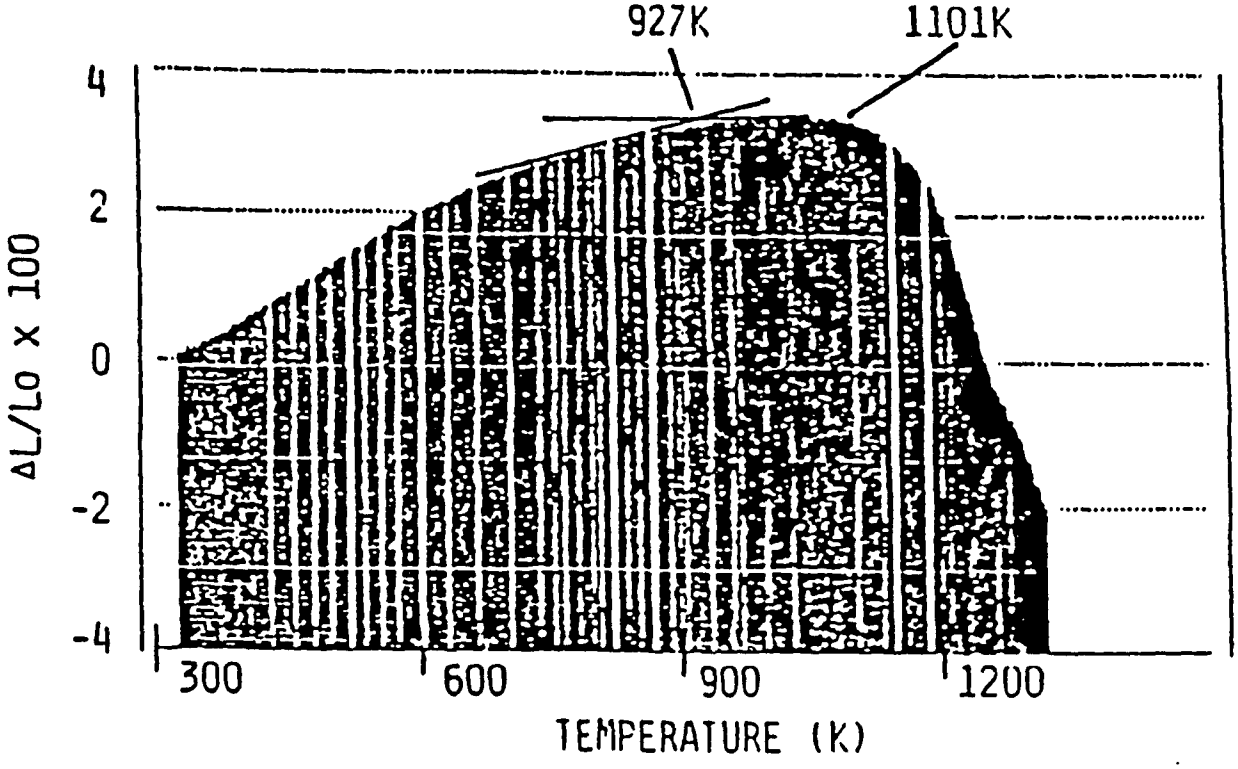

Figure 8. Elongation-Contraction for Virginia HVA.

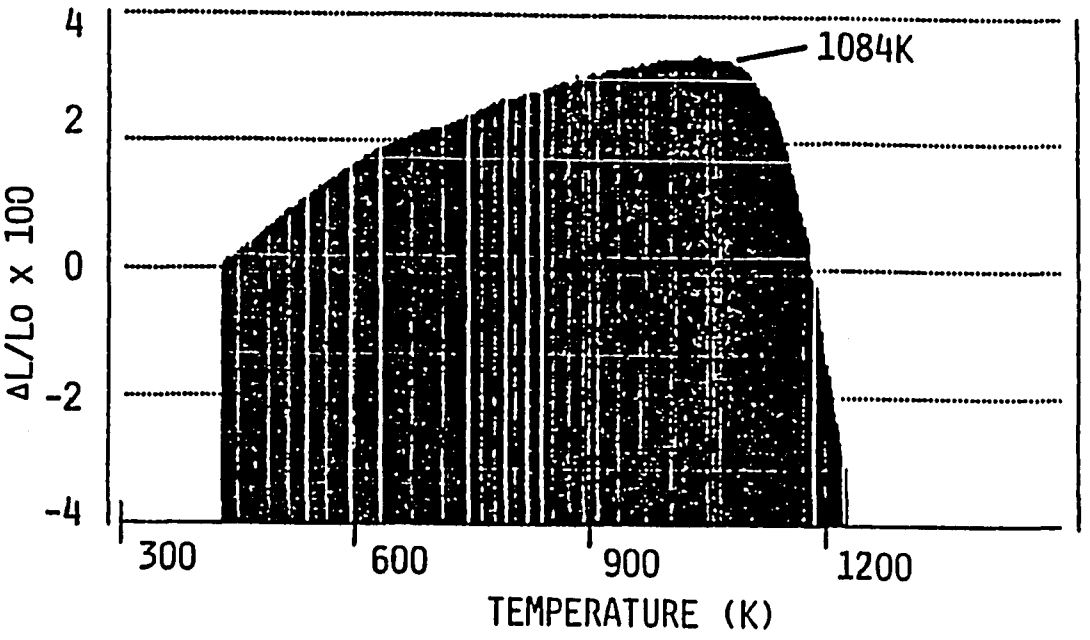

Figure 9. Elongation-Contraction for Illinois #6 Coal Ash.

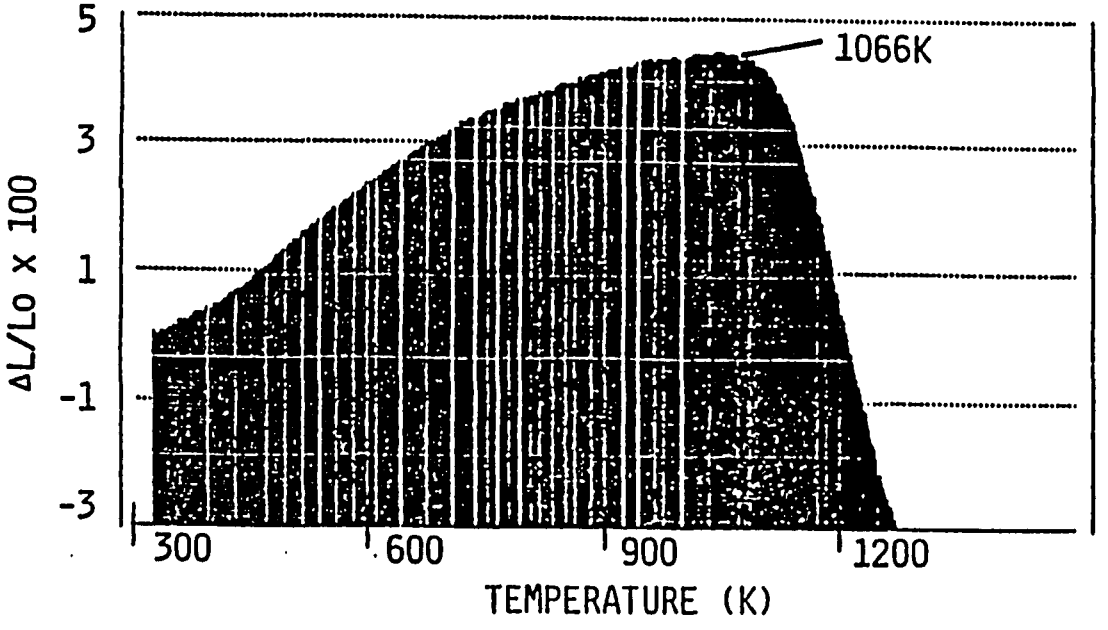

Figure 10. Elongation-Contraction for Illinois #6 HVB Coal Ash.

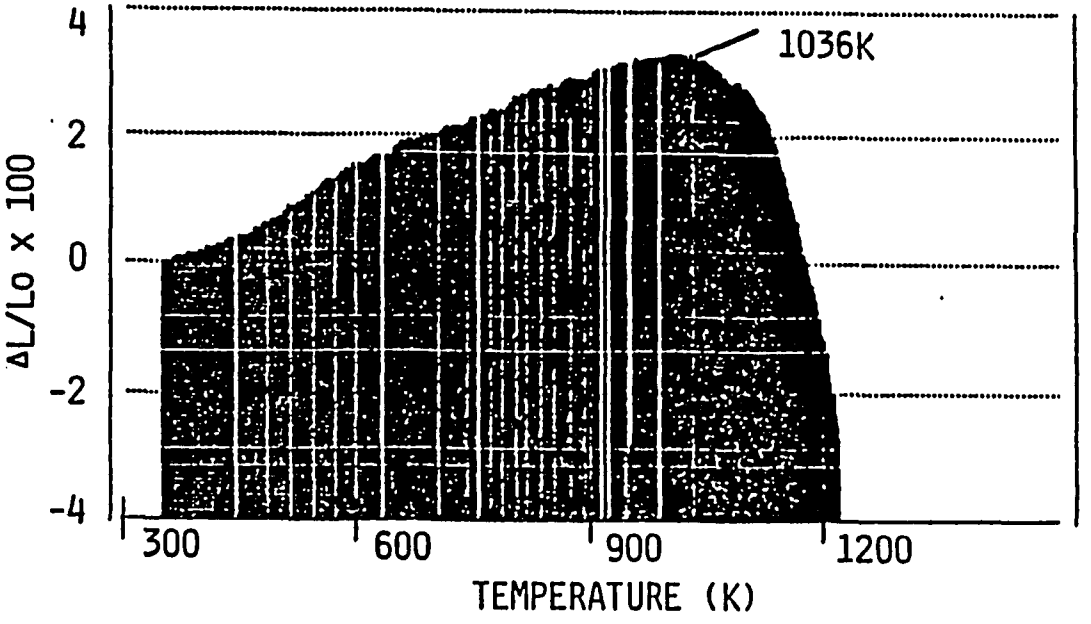

Figure 11. Elongation-Contraction For Wyoming Subbituminous B Coal Ash.

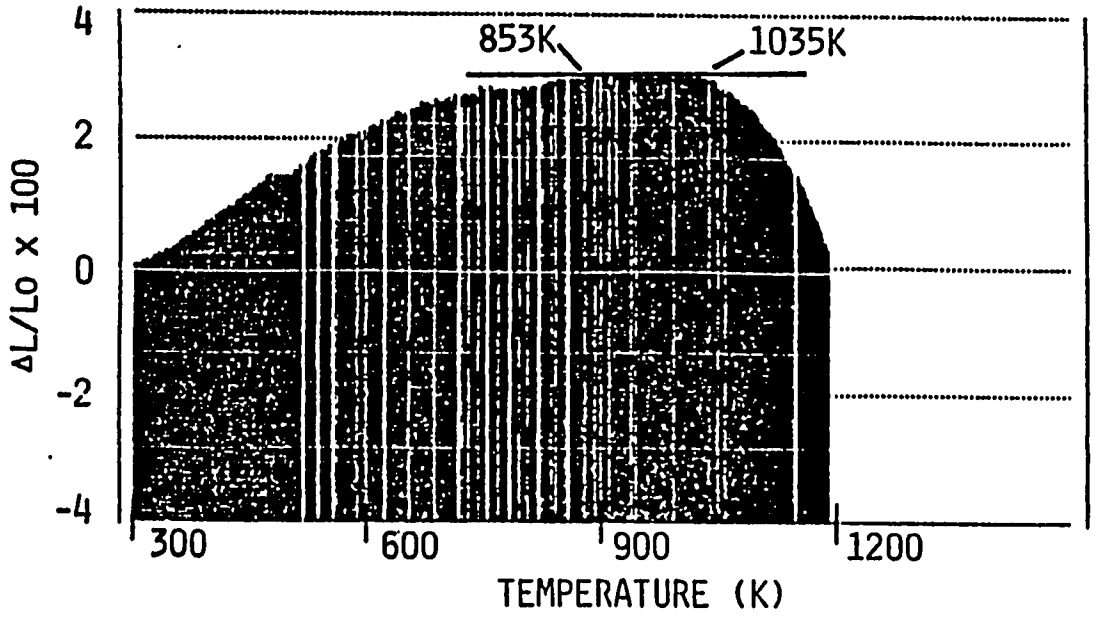

Figure 12. Elongation-Contraction for North Dakota Lignite Coal Ash.

References

1. Conn, R.E., Austin, L.G., Fuel, **63**, 1664 (1984).

2. Isaacs, L.L., Amer. Chem. Soc.,Preprint of Papers, **29** (6), 234 (1984).

3. Mraw, S.C., Nass, D.F., J. Chem. Thermodynamics, **11**, 567 (1979).

4. Compo, p., Pfeffer, R., Tardos, G.I., Powder Tech., (1987).

5. Compo, P., Mazzone, D., Tardos, G.I., Particle Characterization, **1**, 171 (1984).

6. Gomez, M., Gayle, J.B., Taylor, A.R., U.S. Bur. Mines Rep., Invest. No 6607, Pittsburgh (1965); Majundar, N.C., Stevens. T.J., J. Austral Cer. Soc., **28**, (1966); Barin, I., Knake, O., Thermochemical Properties of Inorganic Substances, New York : Heidelberg (1973); Cassis, R., OASTRA J. Research, **1**, 145 (1982).

7. Raask, E., Amer. Chem. Soc., Preprint of Papers, **27** (1), 145 (1982).

8. Siegell, J.H., PhD Thesis, City College N.Y., (1976).

9. Basu, p., Sarka, A., Fuel, **61**, 924 (1983).

10. Stallman, J.J., Neavel, R., Fuel, **59**, 584 (1980).

11. Katta, S., DOE Report No FE-19122-38, (1984).

12. Amer. Soc. Test Mat., Annual Book of ASTM Std., Phila, Designation D, 1857-68 (1978).

CHAPTER 4

Thermal Properties of Coal Ashes

4.1 Abstract

The applicability of differential thermal analysis to determine the fusibility behavior of coal ashes was investigated. The technique proved useful to obtain four specific temperatures points. These are: the minimum sintering temperature, the softening point, the point of complete fluidity and the reaction temperature which is tentatively identified as the eutectic temperature. In addition, differential scanning calorimetry was used to determine the heat capacity of ash powders between 100°K and 850°K. Ash heat capacities were correlated with ash constitution.

4.2 Introduction

There is an abundance of coal in the United States, much of which is used for power generation. It is envisioned that in the future coal will be converted to "synfuel" as a replacement for crude oil. Coal in itself is a complex mixture of organic and inorganic phases, together with large quantities of physically and/or chemically bound water. The inorganic phase, which may amount to 15 to 20% of the coal, is

a complex mixture of quartz pyrite, calcite and silicates. Trace quantities of many metals are present. In the combustion process, the inorganics are converted to ash, steam and other vapors. The ash itself is a mixture of oxides, sulfates, phosphates, and partially converted dehydrated silicates. In an industrial combustion process, a portion of the ash will be carried out along with the stack gases. This "fly ash" may differ in composition and/or structure from the remaining "bottom ash." Ash formation is a byproduct in reactions such as coal liquification. The inorganic phase itself may influence the kinetics and product distribution of various reactions and may have strong bearing in the service life of the process equipment.

The ash must be removed from the process and disposed of in a safe and economic manner. Intensive research efforts are underway to find uses for ashes of various kinds and to overcome the contamination of the environment by leaching from landfills and through the escape of fly ash into the atmosphere.

The efficient design of coal combustors, coal processing reactors, and ash removal systems mandates that the designer has information available on the thermal characteristics of the ash. The data base needed include: ash fusion characteristics, heat capacities and thermal conductivities.

The standard test to determine the fusibility behavior of coal ashes is the ASTM D-157 "Fusibility of Coal and Coke Ash" procedure. It prescribes a preparation and measurement scheme which yields four "call points" which presumably describe the fusion process. The points are empirically defined and bears tenuous relation to actual physical phenomena. For example, The first call point in the ASTM procedure is the initial deformation temperature (IDT). It is defined as the temperature where the sharp edges of the test pyramid of ash powder starts to round. It has been argued that the IDT correspond to the minimum sintering temperature for the onset of agglomeration, i.e. sintering. Other experimental techniques applied to the study of the sintering phenomena [1,2] have shown that this is not the case.

Sintering of a powder leads to the reduction of volume and surface energy. Thus, the onset of sintering, i.e. the minimum sintering or agglomeration temperature, can be determined either by dilatometry or a technique such as differential thermal analysis (DTA). DTA indicates the onset of temperature change and the direction change in the internal energy of materials due to heating. Reduction of the surface energy is an exothermic event and shows up as an increase in the DTA signal. Fusion, on the other hand, is an endothermic event and will manifest itself as a decrease in the DTA signal. Chemical reactions and Non-ideal dissolution phenomena

will show up either as increases or decreases or as slope changes in the DTA signal. In principle, besides yielding minimum sintering temperatures, DTA should provide further fusibility information on ash powders. DTA experiments were preformed together with DSC experiments on an additional set of coal ashes and are reported here.

4.3 Experimental Techniques

4.3.1 Ash Preparation

Ashes were prepared from eight coals. These were obtained from the Argonne Premium Coal Sample Bank [3]. In Table I, the rank of the original coals and their mineral contents are listed. The ashes were prepared by combustion of 100 mesh size particle at 700°C in a muffle furnace. One batch of the ashes was subdivided for DSC measurements and elemental analysis. A second batch was also subdivided. Part of it was used for DSC and part for DTA experiments. The rest was heated at 1000°C in a muffle furnace before being used for DSC and DTA experiments. Elemental analysis was performed using inductively coupled plasma technique. Results of elemental analysis are given in Table II.

4.3.2 Differential Thermal Analysis

The fusion behavior of coal ash powder was investigated with the use of DTA [4]. A Dupont 2100 Thermal Analyzer with

a high temperature (1600°C) DTA cell was employed. The samples were heated from 300°K to 1900°K at a rate of 20 C/min. in nitrogen flow. The instrument was calibrated using zinc and gold as standard materials.

4.3.3 Differential Scanning Calorimetry

Ash heat capacities were determined by differential scanning calorimetry. one series of ashes prepared at 700°C was investigated between 100°K and 700°K using a DuPont 1090 thermal analyzer system. Another batch of samples prepared at 700°C and 1000°C were investigated using a DuPont 2100 thermal analyzer system between 300°K and 900°K. samples size of 6 to 25 milligram were used. Experiments were performed at a heating rate of 10 C/min. in a nitrogen atmosphere. Heat capacities were calculated by comparing the heat flow curves for a sapphire standard with the heating flow curves for the samples.

The precision of the data for a single experimental run is estimated to be 2%. The absolute accuracy of the data for a given ash is estimated at 5%. The estimated accuracy is based on running several samples from the same ash batch in a given instrument and from running ashes prepared from a given coal at different times in different instruments.

4.4 Results and Discussion

4.4.1 Differential Thermal Analysis

The results of the DTA experiments on the ashes derived from the Pittsburgh #8 coal are shown in Figure I. The ordinate of the graph Δ represents the temperature deviation of the ash sample from a baseline which corresponds to the temperature evolution of a sample of the same type of ash not undergoing physical or chemical transformation process.

This set of results is indicative of the results obtained for other ashes with some variation in details. As was expected, several characteristic temperatures at which significant events occur may be identified. These points of interest, starting with the lowest temperature, are the:

- Onset of particle agglomeration (sintering), Ts.
- Onset of fusion (ash softening), Ti.
- Point of discontinuous change in Δ, Tr.
- Point of complete fluidity, Tf.

In Table III, we tabulate these temperatures points for all ashes. One should note that for a given origin ash there is only a relatively small variation in characteristic temperatures for the ash powders prepared at different temperatures.

4.4.2 The Minimum Sintering Temperature

We previously reported [1] the minimum sintering temperatures for a number of coal ashes spanning the same geographic spectrum as those reported here. The method of detection employed in the prior work was dilatometry. In general, the Ts value detected by dilatometry was 100°K larger than that detected by DTA. We attribute much of this discrepancy to the way the DTA method was employed in these experiments. However, it is important to note that both of these techniques yield a minimum sintering temperature substantially lower that the initial deformation temperature (IDT) of the ASTM method. Rhinehart and Attar [5] have proposed a model for the ash fusion temperatures based on the freezing point depression equation for ideal binary solutions. They used a data base of 263 ashes to perform a seven-parameter correlation analysis. Six of these parameters, Ai's, are statistically determined "pseudo" heats of fusion for the assumed ash components, and the seventh is the fusion temperature for the "average composition" ash. the calculated average ash IDT is 1411°K. Experimentally determined IDT's for the Argonne ashes range upwards from 1340°K in a reducing atmosphere and upwards 1445°K in oxidizing atmosphere [3]. It is clear that the IDT is not a measure of the onset of agglomeration.

4.4.3 The Initial Softening Temperature

The softening temperature as evaluated by Rhinehart and Attar is 1478°K for the average ash. Values for the Argonne ashes range upwards from 1365°K depending on the particular ash on the furnace atmosphere [3]. For the ash illustrated in Figure I we estimate that in an inert atmosphere the initial deformation temperature, the softening temperature, the spherical softening point and the hemispherical softening point are 1520°K, 1550°K and 1580°K respectively. From Ti values as defined, we estimate that the initial softening point for 850°K ash (ashing temperature for the ASTM test) is approximately 1375°K.

4.4.4 The Discontinuous Change Temperature

Melting is a first order phase transition phenomenon accompanied by a discontinuous increase in enthalpy for pure homogeneous compounds. For dilute solutions the freezing point depression expression may be used to determine the initial decrease in the freezing point of the solvent due to the addition of non-volatile solute. Ashes are heterogeneous mixtures and are not dilute solutions. Thus, the initial softening temperature, Ti, may be considered as the melting point of the lowest melting component in the mixture. The molten component then acts as a solvent and dissolves some of the remaining mixture. The dissolution process, unlikely to be

ideal, i.e. $H_{sol}=0$, is accompanied by an enthalpy change. Eventually a point in the process is reached where the solution composition passes a phase boundary. Such a boundary crossing may associated with a latent heat or may be athermal. It is our conjecture that the sharp change in Δ at a temperature which we call Tr indicates such an event. It is to be noted that in the vicinity of Tr we have the greatest variability in the nature of the DTA curves. Of the sixteen ashes examined, eight show only a discontinuous endothermic change in Δ, seven show exothermic behavior in Δ prior to the endothermic discontinuity, and one ash shows no discontinuity (hence no Tr)of any kind. Tr ranges from 1490°K to 1680°K. It is likely that Tr is very sensitive to both ash composition and to ashing temperature.

4.4.5 The Fluidity Temperature

The ASTM test for the fusibility of coal ash defines the fluidity temperature, Tf, as the point where the test sample height has decrease to approximately 10% of its original value. We considered it to be the temperature where there is a final change in Δ indicating the melting (or dissolution) of the last bit of solid ash. The fluidity temperature for the average ash according to Rhinehart and Attar correlation is 1581°K (1609°K for low calcium ashes). For the Pittsburgh #8 ash the measured ASTM fluidity temperature is 1600°K in a

reducing atmosphere and 1705°K in an oxidizing atmosphere. The DTA Tf point is 1720°K for this ash.

4.4.6 Calorimetry

In Figure 2, representative data obtained by differential scanning calorimetry is shown. The specific ash illustrated is that obtained from the West Virginia coal. Note that while only three sets of data are shown, each of those data sets are composites of several runs. In the region of 840°K to 860°K, there are small specific heat anomalies (peaks) in the data for the 700°C ashes. The anomalies will be discussed later. The precision of an individual data point is about 2%. However, the accuracy of the data as defined previously is no better than 5%.

The first important conclusion we can deduce from this data is that the ashing temperature is not an important variable with respect to the normal heat capacity, as long as the ash is kept from fusing. When expressing the heat capacity as a function of temperature for a given ash, the data for ashes prepared at the two ashing temperatures were combined into one set. Heat capacities were fitted to the expression:

$$C = aT^{-2} + bT^{-1} + c + dT + eT^2 + fT^3$$

using the least square procedure. The coefficients of the polynomials are given in Table IV. The use of the polynomial

fit to the experimental data reproduces the experimental curve within 5% scatter between 200°K and 700°K.

As mentioned earlier, we observed anomalies in the specific heats for the 700°C ashes, as illustrated in Figure 3. For the 1000°C ashes, only the ones obtained from the Wyoming and Utah coals have specific heats anomalies. However, the anomalies, when they occur, are always reproducible.

There are several phase transitions which may account for these anomalies. In this instance, the alpha to beta transition in quartz which occurs at 843°K and the magnetic transition of magnetite which occurs at 858°K are the causes. The contribution of the anomalies to the total specific heat of the ashes is very small. Hence fitting of data by a polynomial expression leads to their neglect when polynomial expressions are used to generate heat capacity values. This neglect is insignificant in practice.

In estimating the thermodynamic properties of minerals, it is customary to estimate their heat capacities by summing the heat capacities of their components oxides and sulfates. In Table V, the assumed ash compositions, calculated from the data given in Table II, are listed. Robinson and Haas [6] have refined this method for clay minerals by incorporating the coordinational environment of cation into heat capacity model.

In Figure 4, we compared the heat capacity curves generated by; a) the polynomial fit to the experimental data for the Lewiston-stockton ash, b) heat capacity calculated as the weighted sum of component heat capacities for the Lewiston-Stockton ash, and c) heat capacity calculated as the weighted sum of quartz and clay heat capacities [7]. Not unexpectively, the sum of the component heat capacity curves under estimates the experimental curve, while the curve generated by the weighted sum of the mineral compounds overestimates the curve. The average of the two is very close to the experimental values.

The estimation methods are quite insensitive to the exact constitution of the ashes. Hence, the present data base is insufficient to discern constitution dependent trends in heat capacity.

4.6 Conclusion

- The DTA technique to determine the fusion behavior of ashes is convenient and yield a set of physically meaningful parameters.

- An accurate model describing the fusion behavior of ashes, based on composition, ashing temperature, and physical structure might be possible once a more

extensive experimental data is collected.

- Using differential scanning calorimetry specific heat data within a few percent accuracy can be obtained.

- Within experimental accuracy the specific heat of ashes are independent of ashing temperature.

- If compositional and/or mineralogical information is available, specific heats may be calculated based on the summing of components heat capacities.

TABLE 1 - Mineral Composition of the Coals (from [3])

COAL	RANK	MINERAL MATTER wt % DRY COAL	MINERAL CONTENT (as % of mineral matter) QUARTZ	PYRITE	CALCITE	TOTAL CLAY
UF	MVB	15.53	10	22	7	61
WY	SUB	8.7	23	1	5	71
ILL	HVB	18.1	19	30	10	41
PIT	HVB	10.9	16	22	5	57
POC	LVB	5.5	5	2	31	62
UT	HVB	5.3	15	9	24	52
WV	HVB	21.6	12	1	1	86
ND	LGN	8.7	7	3	20	70

TABLE II - Elemental Composition (wt %) of the Ashes

	UF	WY	ILL	PIT	POC	UT	WV	ND
Ca	1.2	11.3	1.8	1.0	3.1	2.3	0.3	9.4
Mg	0.6	2.4	0.4	0.4	0.8	0.4	0.4	3.2
Na	0.2	1.3	0.6	0.4	1.5	2.9	0.2	5.4
Al	12.3	6.7	7.0	11.4	9.5	6.1	16.1	3.0
Fe	14.7	4.4	17.2	15.2	10.8	6.6	2.1	4.9
Si	21.9	13.9	20.0	24.1	16.7	21.9	28.0	7.9
Ti	0.6	0.7	0.4	0.7	0.8	0.5	1.2	0.2
trace	0.3	1.1	0.4	0.4	0.4	0.2	0.3	1.2
S	1.6	8.8	2.7	0.8	5.0	3.9	0.8	12.0
K	2.2	0.7	2.4	1.7	0.5	1.0	0.8	0.8

TABLE III - Fusion Temperatures (k) for the Ashes

	Onset of Aggl. (Ts)		Onset of Fusion (Ti)		Endotherm. Drop (Tr)		Fluidity (Tf)	
Ashing T	700 C	1000 C	700 C	1000 C	700 C	1000 C	700 C	1000 C
UF	900	1150	1250	1380	1675	1650	1725	1580
WY	950	950	1350	1400	1500	1490	1675	1675
ILL	950	950	1280	1440	1520	1620	1700	1540
PIT	925	950	1130	1450	1680	1660	1700	1740
POC	875	975	1350	1450	1525	1600	1650	1650
UT	975	1000	1400	1350	1620	--	1700	1650
WV	100	1100	1400	1480	1600	--	1800	1800
ND	950	1150	1325	1375	1590	1625	1650	1640

TABLE IV - Polynomial fit of Heat Capacity Vs Temperature

$C = aT + bT + dT + eT + fT$ (kJ/kg*K)

Valid Range 200 K - 800 K

ASH	ax10	bx10	c	dx10	ex10	fx10
UF	-4.1071	8.931	-5.5078	2.0149	-2.7827	1.4245
WY	-1.3538	2.5564	-2.0208	1.1534	-1.8414	1.0408
ILL	-3.2348	5.9883	-3.7819	1.4128	-1.8262	0.8868
PIT	-2.3953	5.0283	-3.9571	1.7189	-2.6440	1.4591
POC	-0.6041	0.3414	0.0232	0.4090	-0.7075	0.4544
UT	-4.3151	8.5653	-6.0570	2.3188	-3.3598	1.792
WV	-1.9383	2.9992	-1.8917	0.9601	-1.3255	0.7018
ND	2.8892	-5.5358	3.6111	0.5835	-0.4563	-0.0067

TABLE V - Assumed Ash Composition (by wt)

ASH	SiO	Al O	CaSO	Fe O	K O / Na O	MgO/MgSO4
UF	0.47	0.23	0.65	0.19	0.45 /	
WY	0.33	0.13	0.42	0.05		0.07/
ILL	0.46	0.14	0.12	0.26	0.02 /	
PIT	0.53	0.22	0.003	0.20	0.047/	
POC	0.40	0.19	0.26	0.15		
UT	0.46	0.29	0.15	0.08	/0.2	
WV	0.61	0.31	0.04	0.03	0.01 /	
ND	0.20	0.06	0.38	0.07	/0.10	/0.19

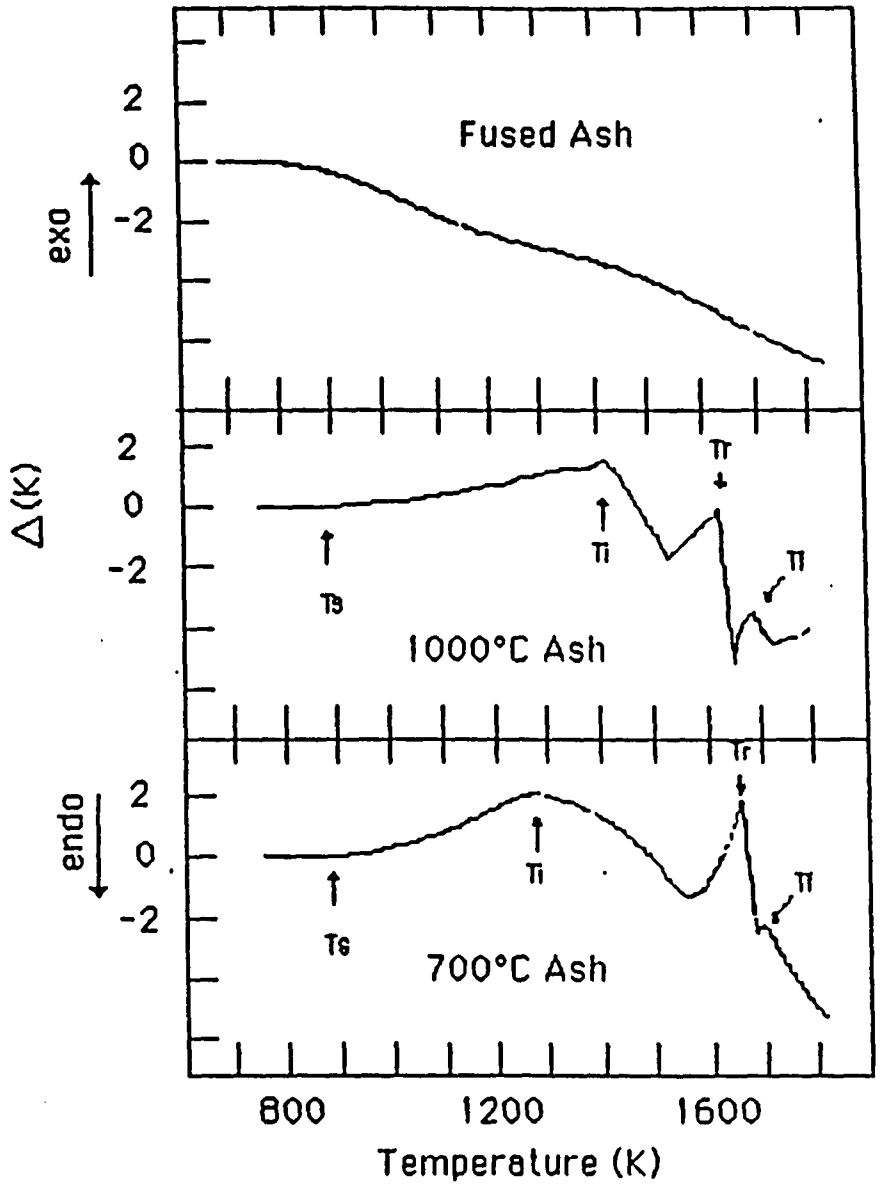

Figure 1 Differential Thermal Analysis of Pittsburgh #8 Ash

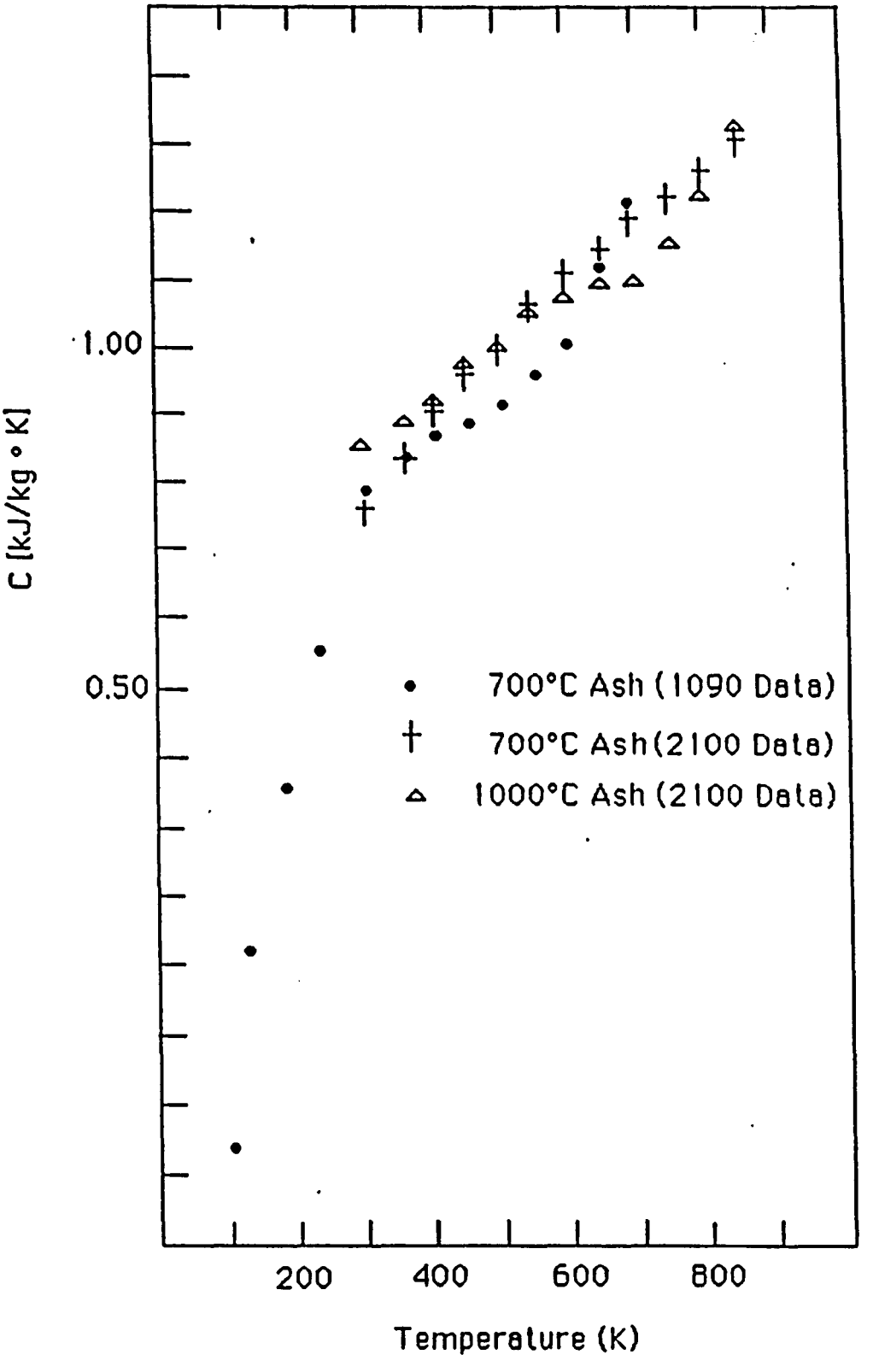

Figure 2 Heat Capacities of Lewiston-Stockton Ashes

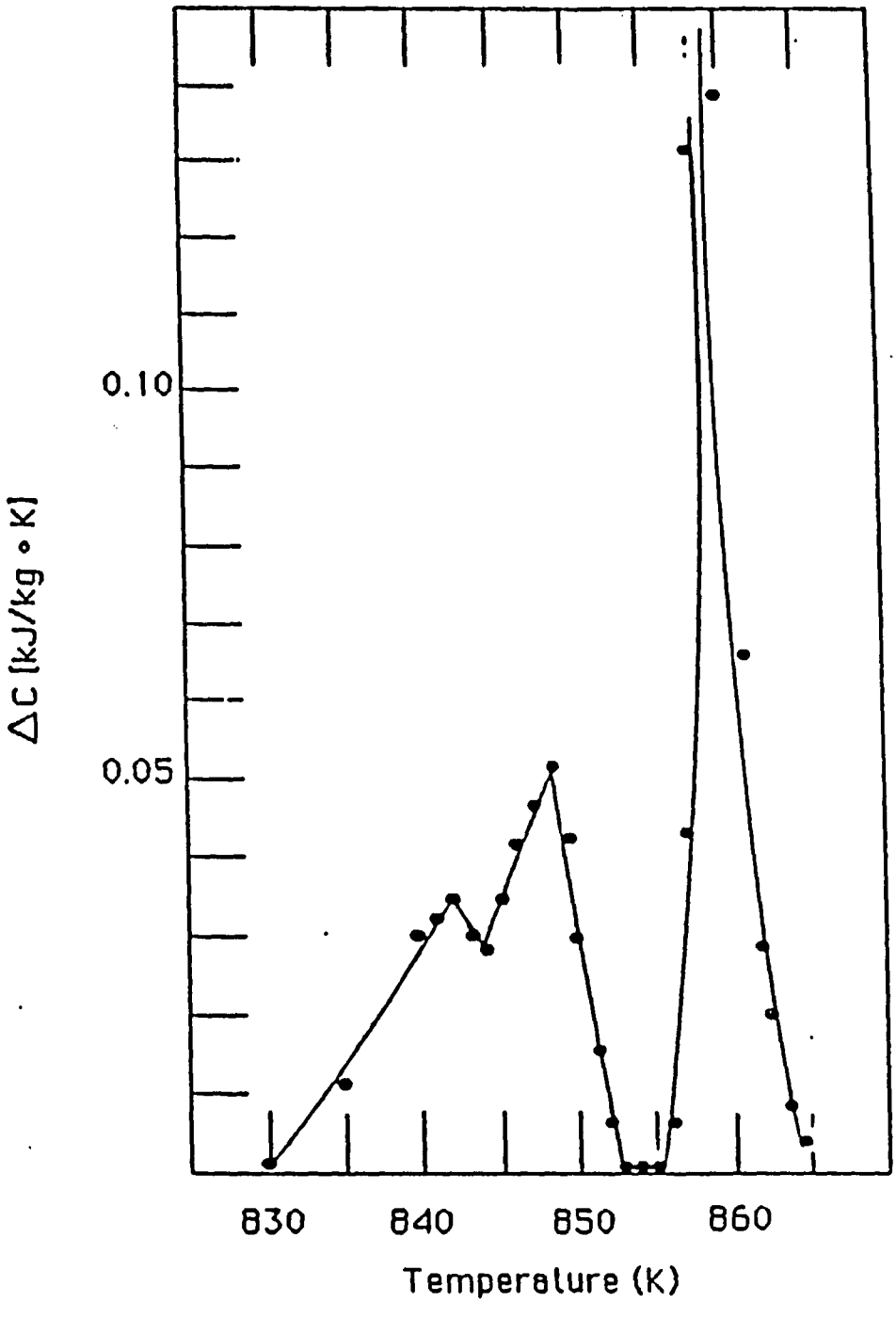

Figure 3 Heat Capcity Anomaly, 700°C UF Ash

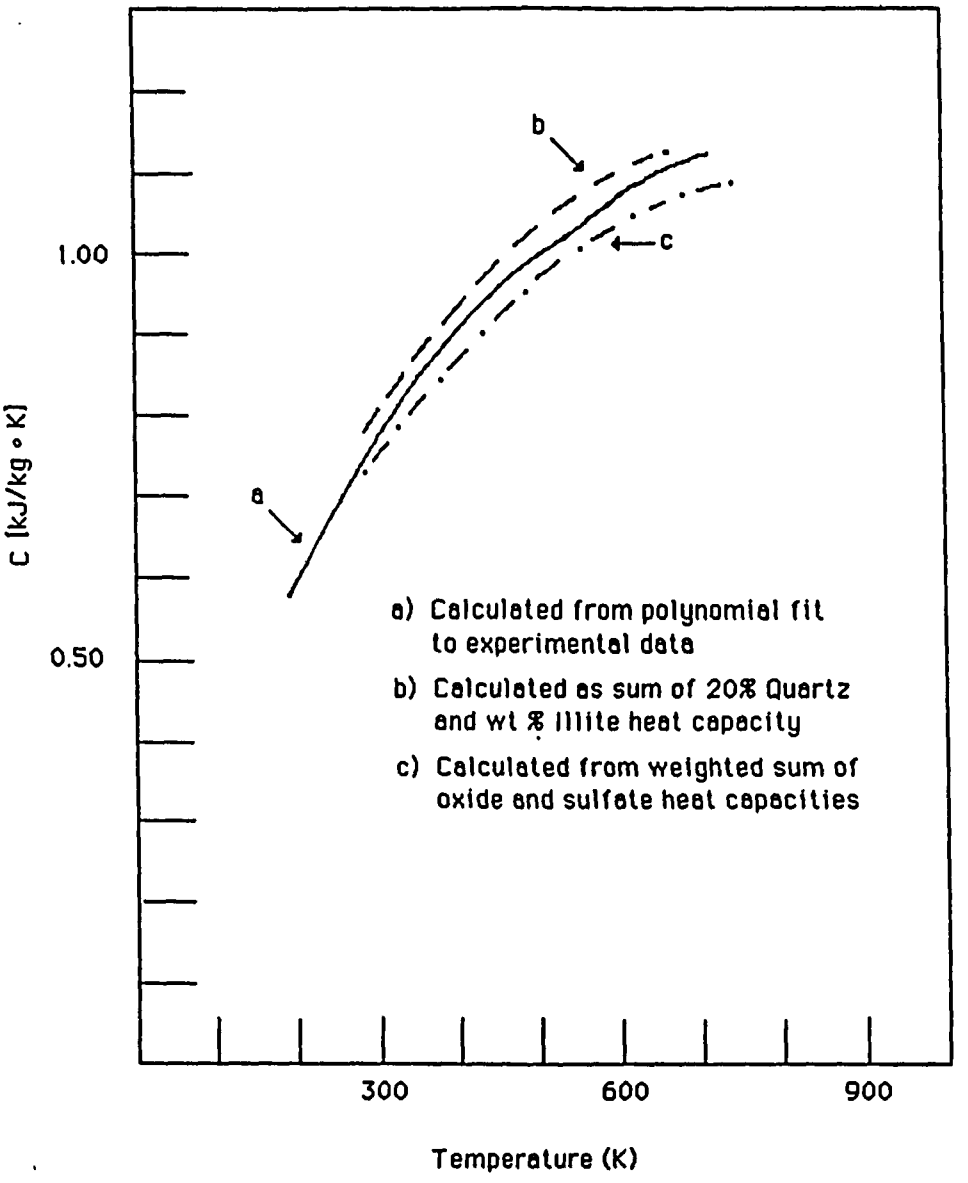

Figure 4 Calculated Heat Capacities for the LS Ash

Reference

1. Ledesma, R., Compo, P., Isaacs, L.L., Mat. Res. Soc. Proc., **86**, 127 (1987).

2. Conn, R.E., Austin, L.G., Fuel, **63**, 1664 (1984).

3. Users Handbook for Argonne Premium Coal Sample Program, ANL/PCSP - 89/1. Karl S. Vorres, ed.

4. Thermal Analysis by W.W. Wendland (3rd Ed., J. Wiley and sons) (1986).

5. Rhinehart, R.R., Attar, A.A., J. of Energy Technology, **109**, 124 (1987).

6. Robinson Jr., G.R., Haas Jr., J.L., American Minerologist, **68**, 541 (1983).

7. Skauge, A., Fuller, N., Helper, L.G., Thermochimica Acta, **61**, 139 (1983).

CHAPTER 5

Effect of Polyethylene Terephthalate (PET) on The Thermal Properties of Asphalt.

5.1 Abstract

The effect of polyethylene terephthalate (PET) additives obtained from used plastic bottles on the thermal properties of asphalt was investigated. Thermomechanical analysis (TMA) and differential scanning calorimetry (DSC) were employed to measure thermal expansion coefficients, glass transition temperatures (Tg), melting points and flow properties of asphalt, PET, and a series of asphalt-PET mixtures. The temperature ranged from 100°K to 600°K for these measurements. The results show that the two materials in the mixtures, asphalt and PET, behave as two separate entities and their original thermal properties remain almost unaffected, by the presence of the second component.

5.2 Introduction

Asphalt concretes are widely used to pave highways, parking lots, driveways, and airports. Asphalt itself is a bitumen and although it occurs naturally, it is mostly obtained as a byproduct of oil production. However, its thermoplastic characteristics cause difficulties with roads.

It has been demonstrated that the apparent glass transition temperature of asphalt is near zero degree celsius [1,2], which is in the temperature range of asphalt use. Crossing of this temperature causes the behavior of the material to change from flexible to glass like rigid behavior. Thus, asphalt concretes are susceptible to low temperature cracking that may lead to fracture. Further, in high summer temperatures asphalt undergoes flow or creep. The stability of asphalt paving surfaces requires that it does not flow or creep under heavy load. Numerous investigations are underway involving the modification of asphalt with different fillers that may improve its pavement performance [3,4,5,6,7,8]. For example, the modification of asphalt with polymers leads to bituminous materials having improved properties and allows the utilization of waste products [9].

In this investigation, the effect of polyethylene terephthalate (PET) obtained from used plastic bottles on the thermal performance of asphalt, specifically the effect on the thermal expansion coefficients, glass transition temperatures, melting points, and flow properties of asphalt, PET, and asphalt/PET mixture samples, is evaluated. Polyethylenes have been confirmed as potentially useful modifiers for increasing the low temperature fracture toughness of the asphalt and may also contribute to pavement stability at elevated temperatures by minimizing distortion due to creep [3]. The abundance of

used plastic bottles that lead to the litter problem and the resultant environmental pollution caused by conventional non-degradable plastics makes PET fillers economically attractive for improving the performance of asphalt concrete paving materials. In this chapter, the TMA and DSC results on the thermal characterization of asphalt, PET, and asphalt/PET mixture samples are reported.

5.3 Experimental Techniques

5.3.1 Sample Preparation

Asphalt of grade AC-20 certified to comply with the state of New York highway specifications was provided by Prima Asphalt Conc., Inc. Polyethylene terephthalate (PET) filling material was obtained from used plastic soda bottles that were first cut into strips about 1/4 inch in thickness and then ground using a grinder with a 20 mesh sieve.

The asphalt/PET mixtures were prepared by slowly adding a weighted amount of PET to a known quantity of asphalt maintained at 120°C while the mixture was vigorously stirred. This temperature is below the melting point of PET but above that of asphalt's. After several minutes, the mixtures were left to cool to room temperature, and stored until used for testing. Sample concentration ranged from 10 to 50% PET by weight.

Asphalt/PET mixtures were also prepared at 270°C, which is above the melting point of PET, and smooth, uniform solutions were obtained. However, it was observed that as these solutions cooled to room temperature, the PET separated from the asphalt forming a viscous layer below the asphalt. This tendency to segregate into layers made the measurements for the melt prepared mixtures irreproducible due to the segregation. Therefore, the mixtures prepared by the dispersion of the PET granules in the molten asphalt were used for the experiments. These mixtures were more uniform throughout but unlikely to be fully homogeneous.

5.3.2 TMA measurements

Thermomechanical analysis (TMA) was employed to determine the expansion coefficients, glass transition temperatures (Tg), melting points, and flow properties of asphalt, PET, and asphalt/PET mixture samples. A DuPont 2100 thermal analyzer system was used for these measurements. Zinc and indium were used as standard materials for the calibration of the instrument. The temperature range of the measurements was between 100°K and 600°K. Cylindrical samples approximately 9.5 millimeter in diameter and between 0.3 and 3.0 millimeter in thickness were heated at a rate of 5 °K/min.

Expansion coefficients were calculated from the TMA expansion profiles using aluminum expansion coefficient data

to determine the dynamic calibration constant. A 5 grams mass supplied the compressive force to the samples.

Flow properties were measured using parallel plate rheometry. Samples were compressed by a 50 gram load.

5.3.3 DSC Measurements

The glass transition temperatures (Tg) and the melting points of asphalt, PET, and asphalt/PET mixtures were also measured using differential scanning calorimetry (DSC). The samples were heated at 10 °K/min. between 100°K and 600°K. The instrument was calibrated using zinc and indium as standard materials.

5.4 Discussion and Results

5.4.1 Differential Scanning Calorimetry

A Typical DSC curve for pure asphalt is shown in Fig. 1. It features a glass transition temperature, Tg, at -42.96°C. Based on several DSC runs, the average Tg for pure asphalt was calculated to be -41.38°C. In general, the change in the heat flow curve indicating the glass transition temperature was very small and sometimes even undetectable; consequently, it was very difficult to characterize the samples using DSC technique. However, in the cases where it was detected, the DSC results were reproducible and yield Tg values within the

5% accuracy of the instrument.

The PET/asphalt mixture DSC measurements yield Tg values in the same range as those obtained for pure asphalt. There was no indication that the presence of PET fillers affected the Tg of asphalt. Fig. 2 shows the DSC results for a 50/50 PET/asphalt sample featuring a Tg for asphalt at -40.05°C which about one degree higher than the obtained average value for pure asphalt.

Values for asphalt Tg's in the literature range between -0.4°C to -53°C [10,11]. The range and average values for the Tg of asphalt determined using the DSC technique are listed in Table 1. Fig. 3 is the plot of the Tg versus PET concentration.

DSC was also used to measure the melting point, Tm, of PET. For pure PET the average melting point was determined to be 235.43°C. Fig. 4 shows a DSC curve for a PET sample with a melting point at 233.23°C. As with the asphalt Tg's, there was no indication that the melting point of PET was affected by the presence of asphalt. The average melting temperature of PET calculated using results obtained from pure PET and PET/asphalt mixtures was estimated as 234.94°C. In Table 2, the range and PET average Tm values are listed together with the compositions used. Fig. 5 is a plot of the PET average Tm values versus mixture composition. Literature gives a range

for the melting point of pure PET between 250 and 265°C. Taking into account the difference in techniques used, the accuracy of the instrumentation, and the fact that the DSC results were obtained using PET from used plastic bottles instead of pure PET, The discrepancy between the DSC findings and literature values is not unexpected.

5.4.2 Thermomechanical Analysis

As stated previously, the average Tg value for asphalt was estimated at -41.32°C. In general, the asphalt Tg obtained using the TMA technique is about 70 degrees higher than those detected by DSC. This discrepancy may be attributed to the inference that these techniques measure different phenomena. The Tg by DSC corresponds to a change in the ability of the sample to absorb heat, while the TMA detects the Tg as a change in the thermal expansion profile of the sample.

The average Tg for asphalt as determined by the TMA technique was estimated as 39.04°C; the value estimated including glass transition temperatures obtained for the PET/asphalt mixtures is 33.39°C. The asphalt Tg average and range values by the TMA method are listed in Table 3, and a plot of the average asphalt Tg values versus PET concentration is shown in Fig. 6. An example of the TMA measurement for a pure asphalt sample with a Tg of 37.50°C is shown in Fig. 7.

The melting point of PET was also measured using the TMA technique. These measurements yield 248.31°C as an average Tm for PET, and an average Tm value of 243.75°C for the asphalt/PET mixtures. These TMA results are about 10 degrees higher compared to the DSC findings and that much closer to the literature values. In Table 4, the Tm average and range values are tabulated, and in Fig 8, the average Tm values are plotted as a function of asphalt concentration. Fig. 9 is a typical TMA curve for a PET sample with a melting point at 247.92°C.

Examination of the TMA curve shows that PET exhibits a glass transition temperature at about 81°C that was not detected when the DSC technique was used. PET TMA measurements yield an average Tg of 81.75°C with values ranging from 80.36°C to 85.76°C. The PET Tg literature value [12] is 81°C. Unlike the previous findings, the glass transition temperature of PET does seem to be affected by the presence of asphalt; so much that it was not possible to detect it with certainty from examination of the TMA curves for PET/asphalt mixtures. Furthermore, when the PET samples were subjected to a heating cycle, the Tg could not be detected. Fig. 10 shows a TMA curve for a PET sample featuring a glass transition temperature at 80.36°C. Fig. 11 shows a second run for that same sample after it was cooled down to liquid nitrogen temperatures and reheated to about 150°C. Note that Fig. 11 shows no change in

the slope of the TMA curve, i.e. no Tg. This effect is permanent, and several samples were subjected to this heating treatment to confirm the findings.

The expansion coefficient was determined from TMA expansion/contraction profiles. The average initial expansion coefficient and range values are listed in Table 5. For PET samples, two distinct regions are observed: a region that ranges from liquid nitrogen temperatures to about 81°C, the glass transition temperature of PET, and second one that extends from 81°C to the final temperature. The initial expansion coefficients listed in Table 1 correspond to the first region. The average PET expansion coefficient for the second region was estimated to be 954.57 $\mu m/m^{o}C$ with values ranging from 925.6 to 982.8 $\mu m/m^{o}C$. An example of a TMA expansion/contraction profile for a PET sample is shown in Fig 12. Note that in this figure the slope of the TMA curve noticeably changes after the crossing of the glass transition temperature.

Additional information can be gained by studying the TMA derivative curve, using the parallel plate rheometer accessory [13]. The amplitude of the derivative curve will vary in intensity with the flow of the sample. Fig. 13 shows a TMA plot for one of the 50/50 PET/asphalt sample featuring the derivative curve with a peak temperature at 249.61°C. This

peak temperature is the inflection temperature (Ti) which corresponds to the point of maximum flow rate. Table 6 lists the average Ti and range values for asphalt, PET, PET/asphalt samples. In general, the inflection point for PET/asphalt samples are very similar to those of PET. The Ti values range from 248.17°C for a 10/90 PET/asphalt sample to 252.30°C for a PET sample. The inflection temperatures for pure asphalt range between 48.41°C to 58.60°C with an average Ti of 52.76°C. That is, the maximum flow rate for asphalt occurs at about this temperature.

It should be noted that for the 10/90 PET/asphalt samples the point of maximum flow rate is the same as for PET. This suggests that even at this PET concentration the overall flow of the mixture is dominated by the flow properties of PET. The PET filler acts as a binder restricting the flow of the asphalt until the filler itself starts melting.

Fig. 14 is a typical TMA plot for a 10/90 PET/asphalt sample featuring a derivative curve with two inflection points. The first one at 46.95°C corresponds to the maximum flow rate of asphalt. It is followed by a plateau due to the binding effects of the PET filler. The maximum flow rate of the mixture occurs at 251.96°C, the second inflection point. At this temperature, the PET filler is melting and flowing out of the rheometer plates together with the remaining asphalt.

TMA parallel plate rheometer (PPR) was also used for viscosity analysis. In the PPR, a sample is sandwiched between two disk-shaped stainless steel plates held in a coaxial alignment cage. By applying a known force to the upper plat, dimensional changes that occurred in the sample can be converted by suitable calculations into a measure of viscosity [14]. Fig. 15 is a plot of the viscosity versus temperature a 40/60 PET/asphalt sample. as expected, the viscosity decreases with increasing temperature. The sharp drop between 240°C and 250°C in the viscosity corresponds to the melting of the sample. After that, the melt is squeezed out from between the two plates and the viscosity essentially goes to zero. Similar plots were obtained for all other samples with some variation in detail.

As far as the exact viscosity value for each temperature point, the calculated values are so scattered that it has not been possible to obtained meaningful results. Certainly, the collected data needs to be studied more carefully, and the whole measuring procedure needs to be revised and perhaps redefined as to improve in the accuracy of the results.

5.5 Conclusions

. Thermomechanical analysis and differential scanning calorimetry are useful techniques and yield reproducible

results in obtaining melting points, glass transition temperatures, expansion coefficients, and the point of maximum flow rate (inflection temperature).

- The difference in values between the Tg of asphalt obtained using TMA and that detected by DSC may be attributed to the different ways these techniques measure the effect.

- In general, asphalt's glass transition temperature does not seem to be affected by the presence of polyethylene terephthalate fillers.

- The PET's glass transition temperature was clearly detected by the thermomechanical analysis technique even though the DSC measurements do not show a Tg for PET. The Tg of PET obtained by the TMA is reproducible and comparable to literature value.

- The overall flow of the PET/asphalt mixtures is dominated by the flow properties of the PET.

- Viscosity values obtained using TMA parallel plate rheometry (PPR) as a function of temperature are very scattered. The reason for this is not clear and further studies of the collected data need to be carried on.

However, as expected the viscosity decreases with increasing temperature as more of the sample becomes fluid.

TABLE 1

DSC Asphalt's Glass Transition
Temperature (Tg) in Degrees Celsius

	PET/Asphalt Concetrations	Tg Range (C)	Tg Average Values (C)
1	0/100	-40.56 to -42.96	-41.38
2	10/90	-42.35 to -42.59	-42.49
3	20/80	-40.23 to -41.33	-40.78
4	30/70	-40.54 to -41.01	-41.28
5	40/60	-41.33 to -41.78	-41.56
6	50/50	-39.44 to -42.39	-40.45
			Average = -41.32 C

TABLE 2

DSC PET's Melting Point (Tm)
in Degrees Celsius

	PET/Asphalt Concetrations	Tm Range (C)	Tm Average Values (C)
1	100/0	233.37 to 235.71	235.43
2	50/50	223.33 to 241.65	235.22
3	40/60	233.77 to 234.63	235.87
4	30/70	233.70 to 234.42	234.06
5	20/80	233.93 to 234.76	234.36
6	10/90	233.80 to 235.52	234.71
			Average = 234.94 C

TABLE 3

TMA Asphalt's Glass Transition
Temperature (Tg) in Degrees Celsius

	PET/Asphalt Concetrations	Tg Range (C)	Tg Average Values (C)
1	0/100	36.67 to 41.90	39.04
2	10/90	30.61 to 41.14	35.51
3	20/80	29.51 to 40.86	33.98
4	30/70	20.00 to 34.68	26.04
5	40/60	27.68 to 36.21	30.89
6	50/50	23.89 to 47.03	34.86

			Average = 33.39 C

TABLE 4

TMA PET's Melting Point (Tm)
in Degrees Celsius

	PET/Asphalt Concetrations	Tm Range (C)	Tm Average Values (C)
1	100/0	246.44 to 252.55	248.30
2	50/50	244.11 to 245.92	245.30
3	40/60	239.87 to 243.8	242.10
4	30/70	239.88 to 243.24	241.31
5	20/80	239.82 to 246.33	243.07
6	10/90	239.93 to 245.65	242.38

			Average = 243.75 C

TABLE 5

TMA Initial Expansion
Coefficient (ALPHA) in Um/m/C

	PET/Asphalt Concetrations	ALPHA Range (Um/m/C)	ALPHA Average Values (Um/m/C)
1	100/0	103.90 to 103.52	108.97
2	50/50	62.60 to 94.88	75.66
3	40/60	50.87 to 112.60	82.78
4	30/70	86.65 to 108.18	85.19
5	20/80	83.90 to 92.02	88.55
6	10/90	76.20 to 122.90	108.28
7	0/100	242.10 to 338.70	290.40

TABLE 6

Infection Temperatures (Ti)
in Degrees Celsius

	PET/Asphalt Concetrations	Ti Range (C)	Ti Average Values (C)
1	100/0	248.25 to 255.78	252.30
2	50/50	249.44 to 253.03	251.48
3	40/60	242.63 to 251.30	245.91
4	30/70	250.37 to 250.98	250.72
5	20/80	249.22 to 251.59	250.51
6	10/90	246.45 to 250.69	248.17
7	0/100	48.41 to 58.60	52.76

FIGURE 1

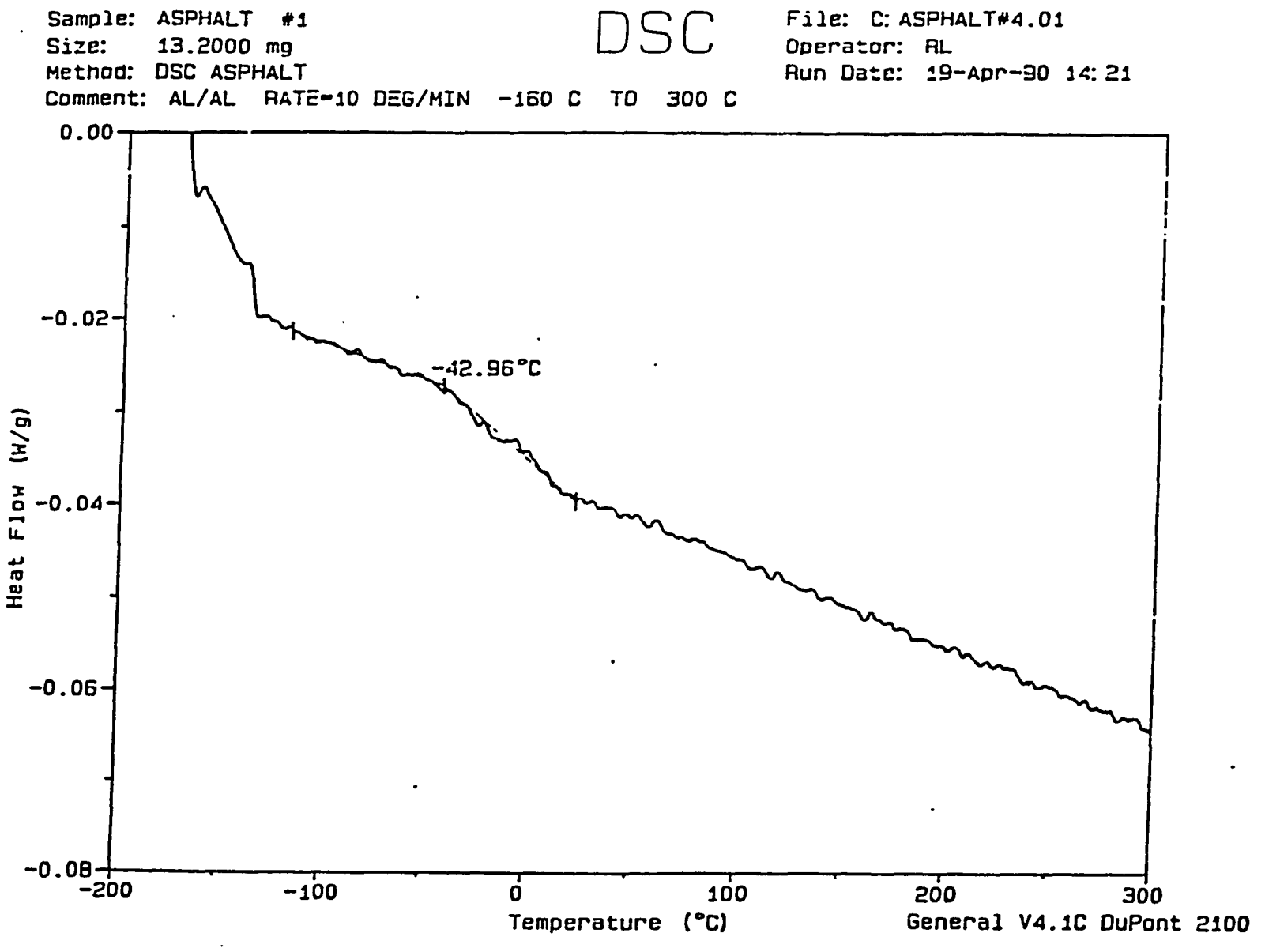
Sample: ASPHALT #1
Size: 13.2000 mg
Method: DSC ASPHALT
Comment: AL/AL RATE=10 DEG/MIN -160 C TO 300 C
DSC
File: C:ASPHALT#4.01
Operator: RL
Run Date: 19-Apr-90 14:21
0.00
-0.02
-0.04
-0.06
-0.08
Heat Flow (W/g)
-42.96°C
-200
-100
0
100
200
300
Temperature (°C)
General V4.1C DuPont 2100

FIGURE 2

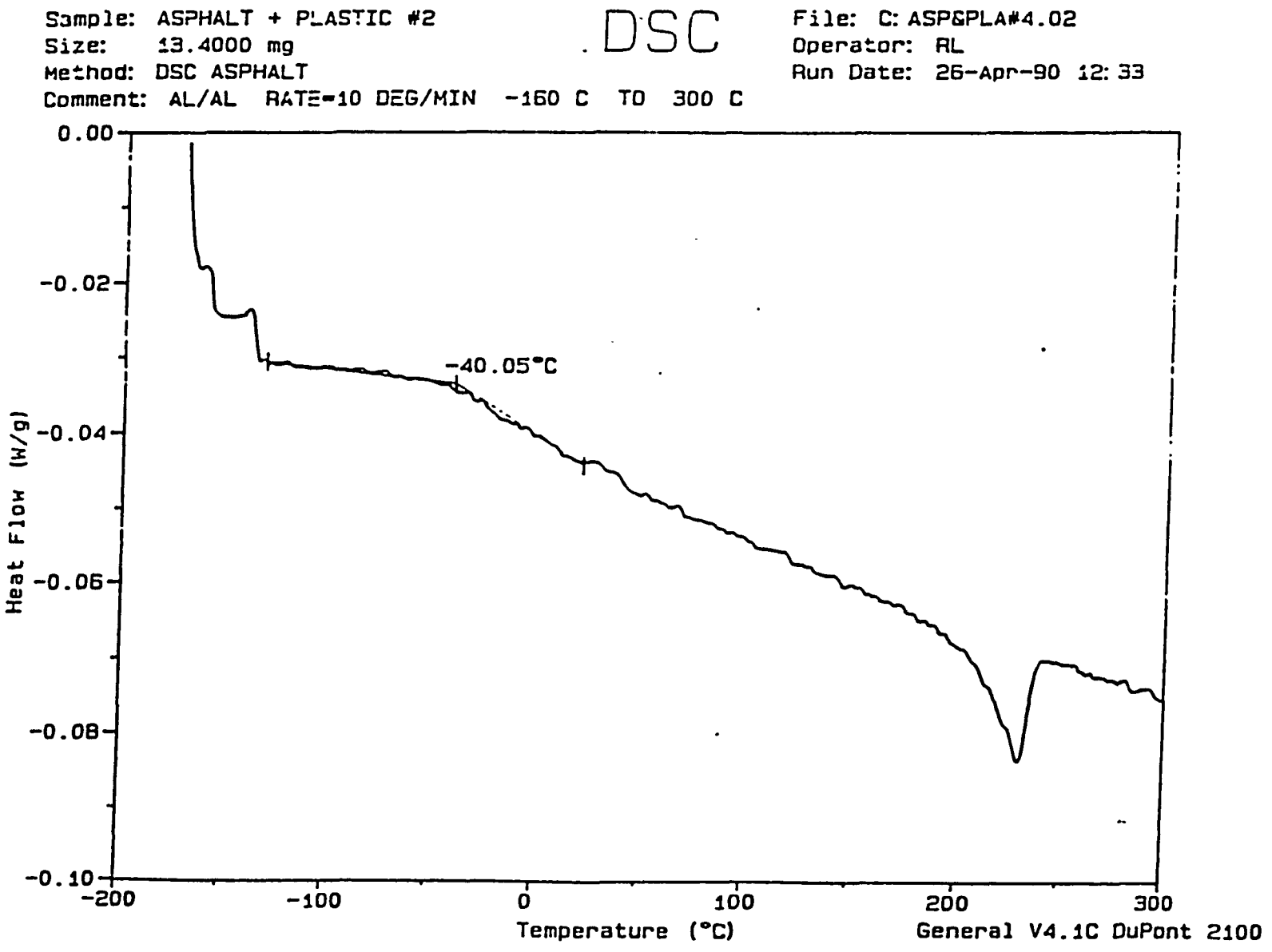
Sample: ASPHALT + PLASTIC #2
Size: 13.4000 mg
Method: DSC ASPHALT
Comment: AL/AL RATE=10 DEG/MIN -160 C TO 300 C
DSC
File: C:ASP&PLA#4.02
Operator: RL
Run Date: 26-Apr-90 12:33
0.00
-0.02
-0.04
-0.06
-0.08
-0.10
Heat Flow (W/g)
-40.05°C
-200
-100
0
100
200
300
Temperature (°C)
General V4.1C DuPont 2100

FIGURE 3

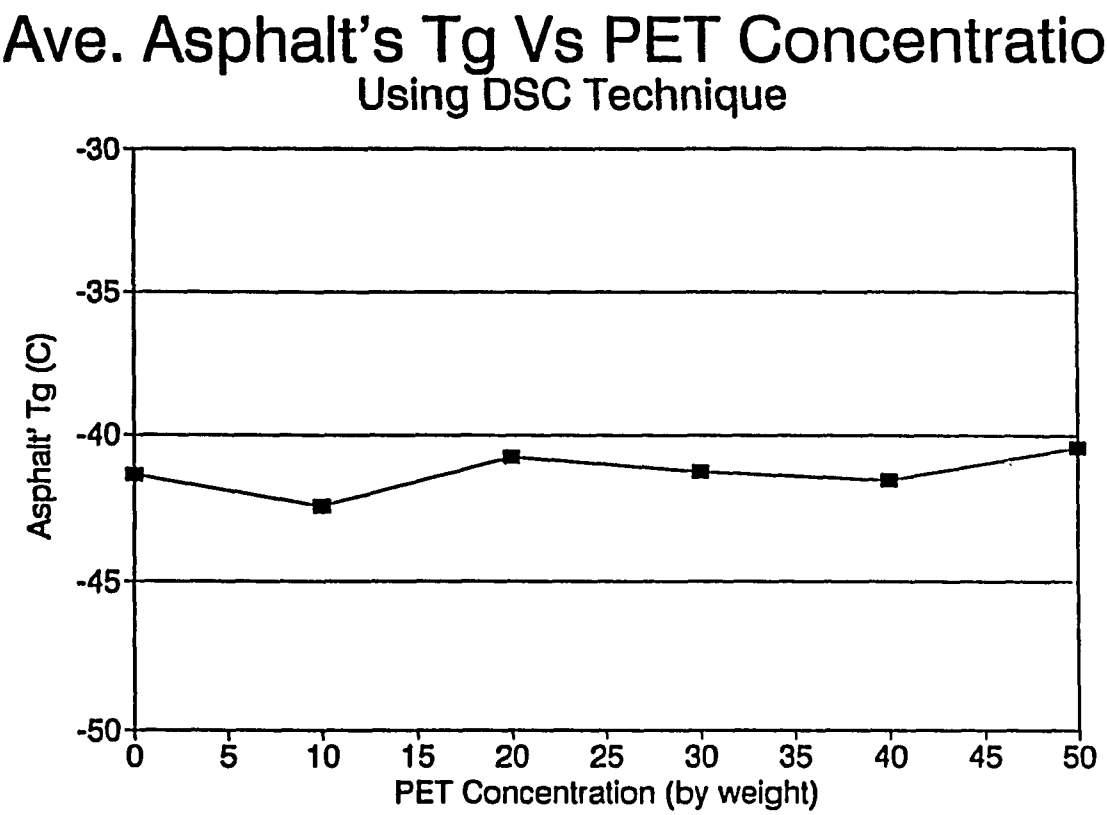
Ave. Asphalt's Tg Vs PET Concentration
Using DSC Technique
-30
-35
-40
-45
-50
Asphalt' Tg (C)
0
5
10
15
20
25
30
35
40
45
50
PET Concentration (by weight)

FIGURE 4

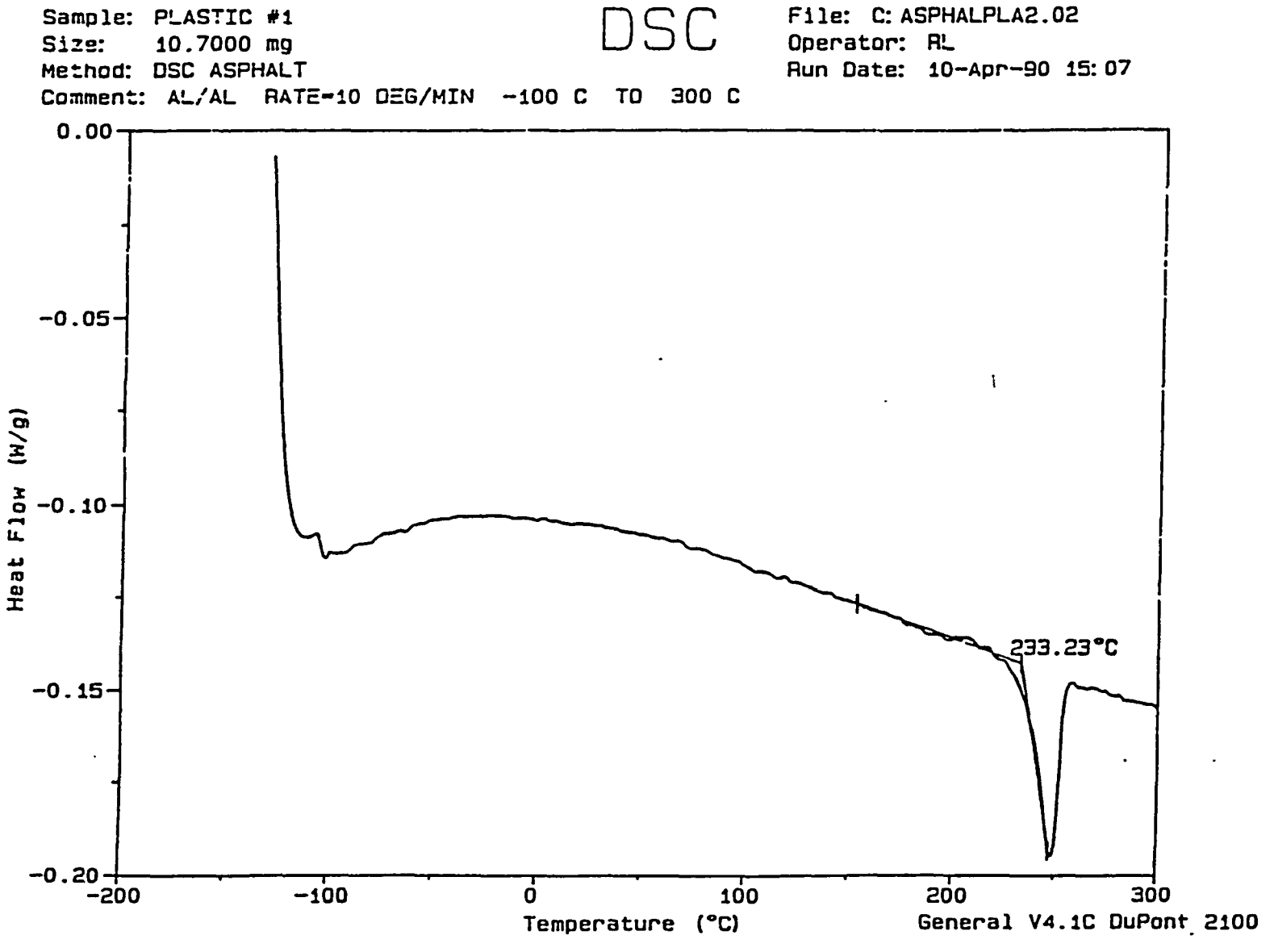
Sample: PLASTIC #1
Size: 10.7000 mg
Method: DSC ASPHALT
Comment: AL/AL RATE=10 DEG/MIN -100 C TO 300 C
DSC
File: C:ASPHALPLA2.02
Operator: RL
Run Date: 10-Apr-90 15:07
0.00
-0.05
-0.10
-0.15
-0.20
Heat Flow (W/g)
233.23°C
-200
-100
0
100
200
300
Temperature (°C)
General V4.1C DuPont 2100

FIGURE 5

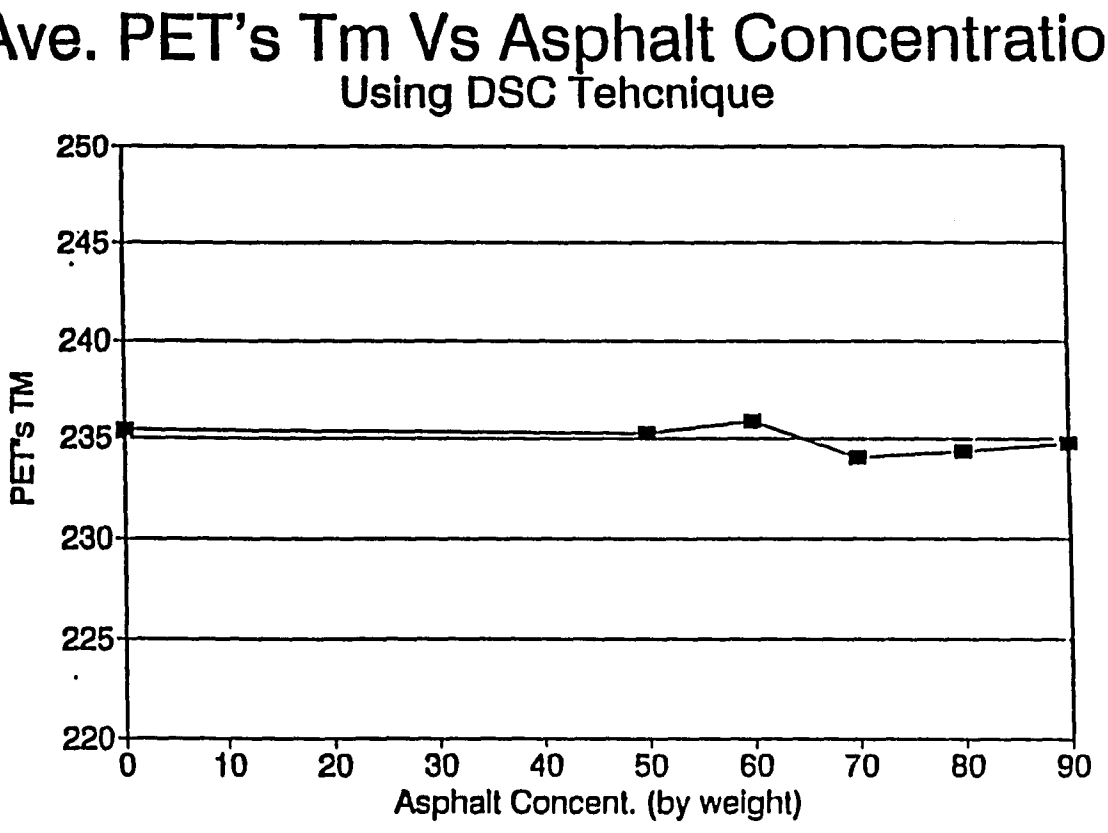
Ave. PET's Tm Vs Asphalt Concentration
Using DSC Tehcnique
PET's TM
250
245
240
235
230
225
220
0
10
20
30
40
50
60
70
80
90
Asphalt Concent. (by weight)

FIGURE 6

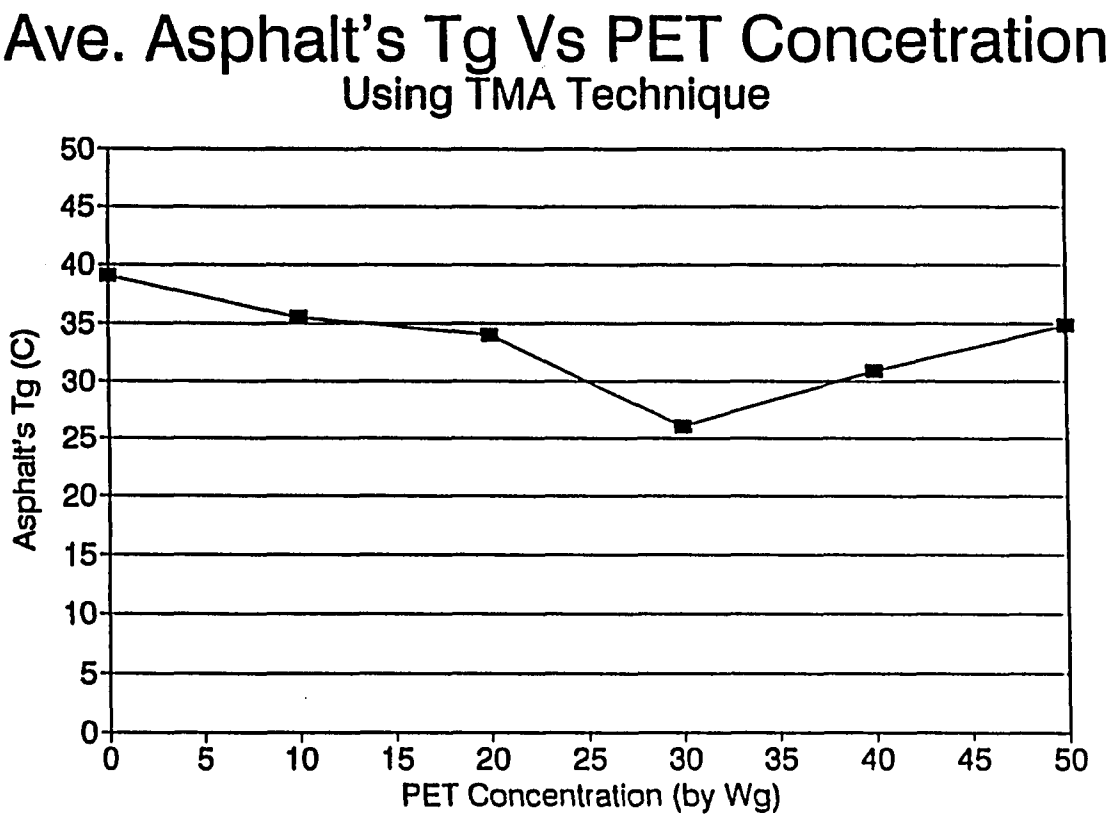
Ave. Asphalt's Tg Vs PET Concetration
Using TMA Technique
Asphalt's Tg (C)
50
45
40
35
30
25
20
15
10
5
0
0
5
10
15
20
25
30
35
40
45
50
PET Concentration (by Wg)

FIGURE 7

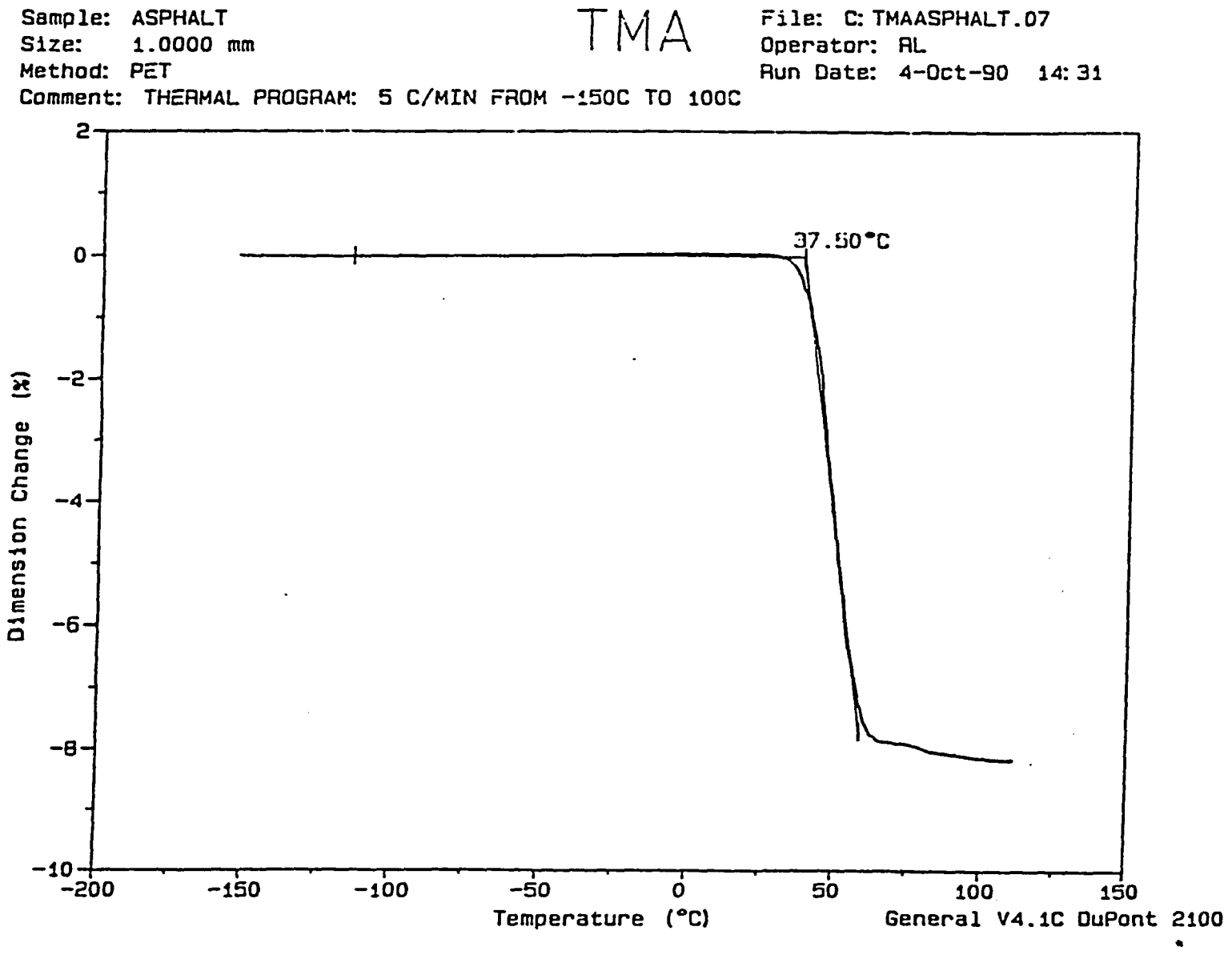
Sample: ASPHALT
Size: 1.0000 mm
Method: PET
Comment: THERMAL PROGRAM: 5 C/MIN FROM -150C TO 100C
TMA
File: C:TMAASPHALT.07
Operator: RL
Run Date: 4-Oct-90 14:31
37.50°C
Dimension Change (%)
2
0
-2
-4
-6
-8
-10
-200
-150
-100
-50
0
50
100
150
Temperature (°C)
General V4.1C DuPont 2100

FIGURE 8

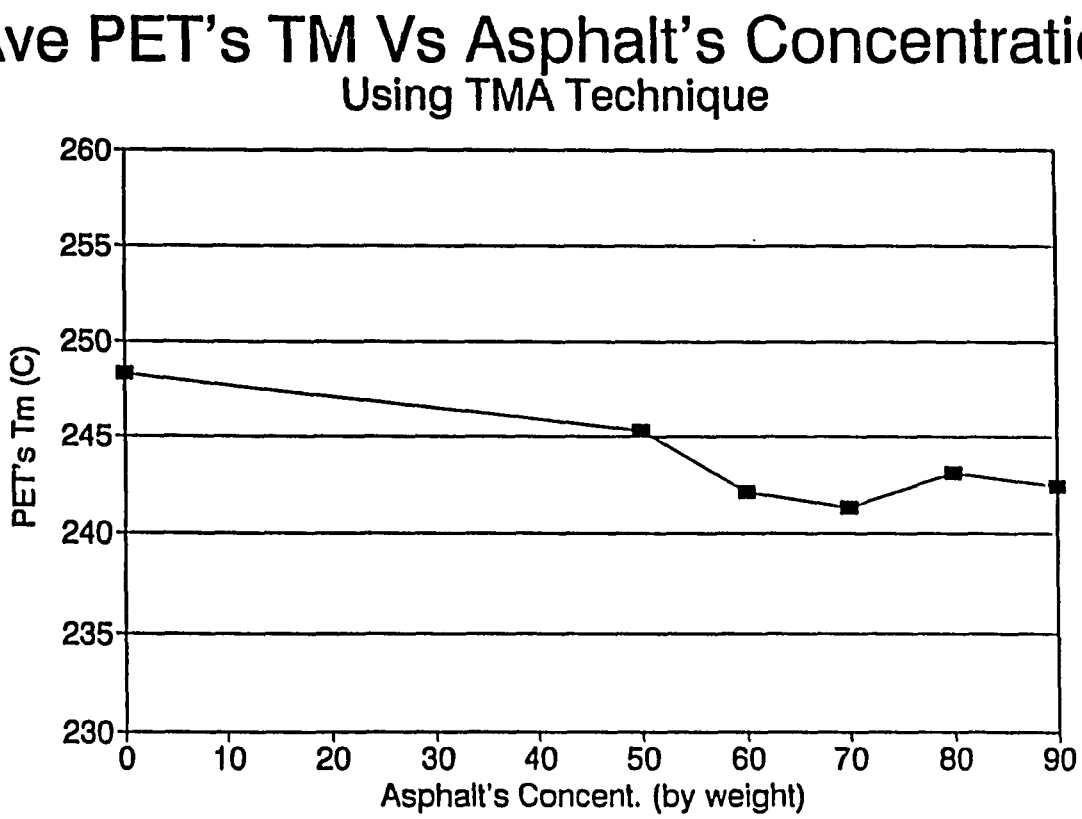
Ave PET's TM Vs Asphalt's Concentration
Using TMA Technique
PET's Tm (C)
260
255
250
245
240
235
230
0
10
20
30
40
50
60
70
80
90
Asphalt's Concent. (by weight)

FIGURE 9

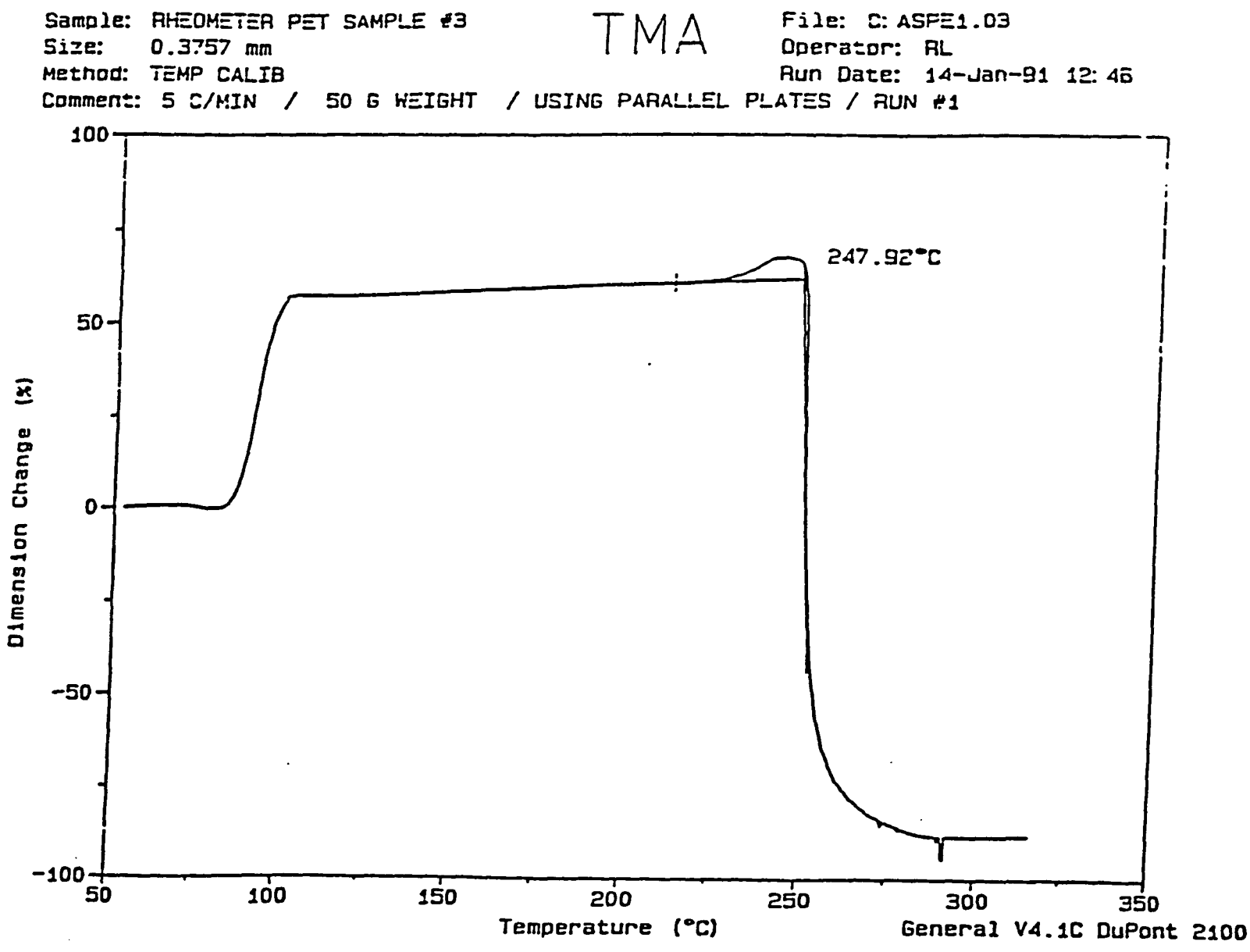
Sample: RHEOMETER PET SAMPLE #3
Size: 0.3757 mm
Method: TEMP CALIB
TMA
File: C:ASPE1.03
Operator: RL
Run Date: 14-Jan-91 12:46
Comment: 5 C/MIN / 50 G WEIGHT / USING PARALLEL PLATES / RUN #1
247.92°C
100
50
0
-50
-100
Dimension Change (%)
50
100
150
200
250
300
350
Temperature (°C)
General V4.1C DuPont 2100

FIGURE 10

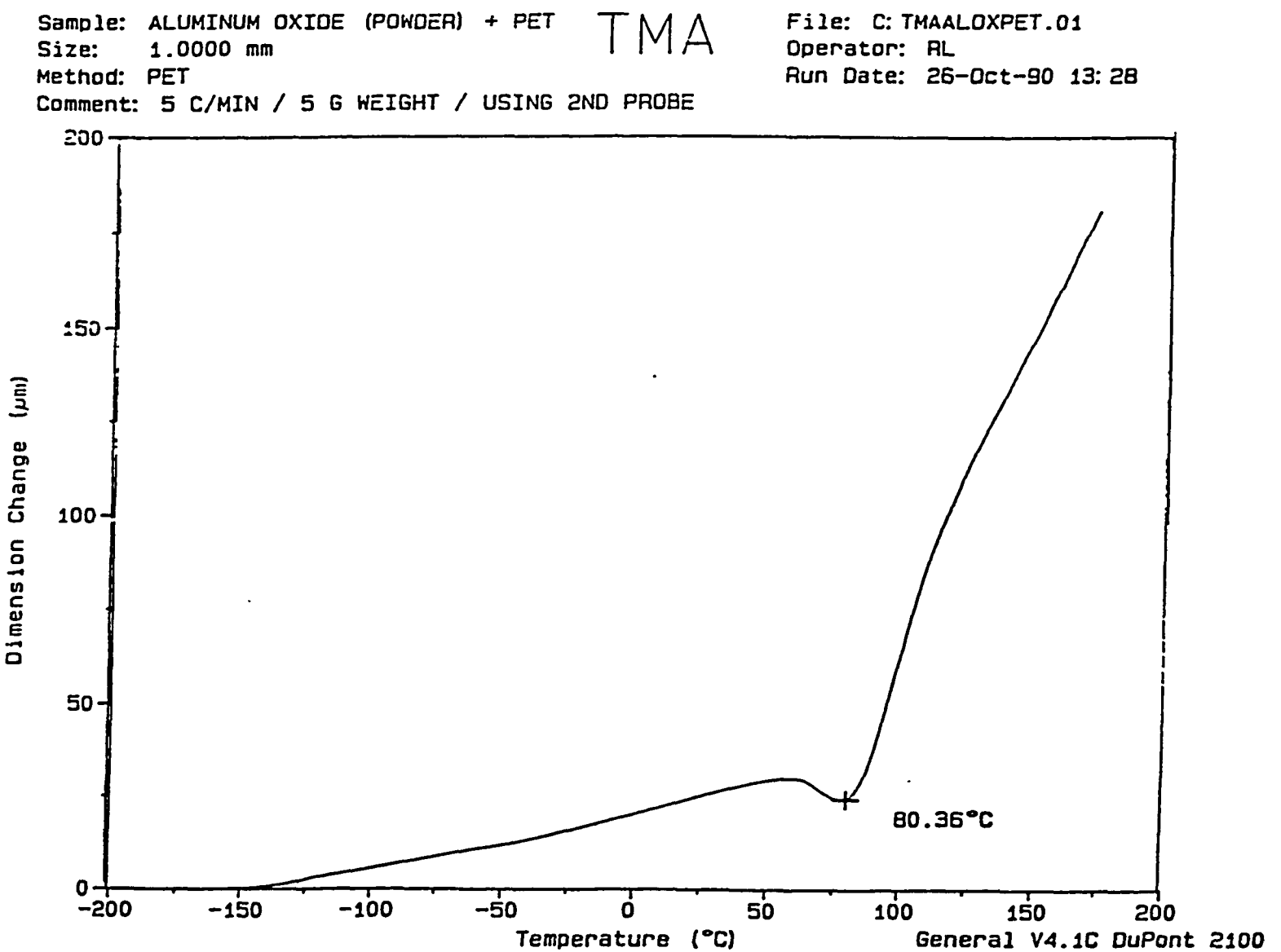
Sample: ALUMINUM OXIDE (POWDER) + PET
Size: 1.0000 mm
Method: PET
Comment: 5 C/MIN / 5 G WEIGHT / USING 2ND PROBE
TMA
File: C:TMAALOXPET.01
Operator: RL
Run Date: 26-Oct-90 13:28
200
150
100
50
0
Dimension Change (µm)
80.36°C
-200
-150
-100
-50
0
50
100
150
200
Temperature (°C)
General V4.1C DuPont 2100

FIGURE 11

Sample: ALUMINUM OXIDE (POWDER) + PET
Size: 1.0000 mm
Method: PET
Comment: 5 C/MIN / 5 G WEIGHT / USING 2ND PROBE

TMA

File: C:TMAALOXPET.02
Operator: AL
Run Date: 26-Oct-90 15:05

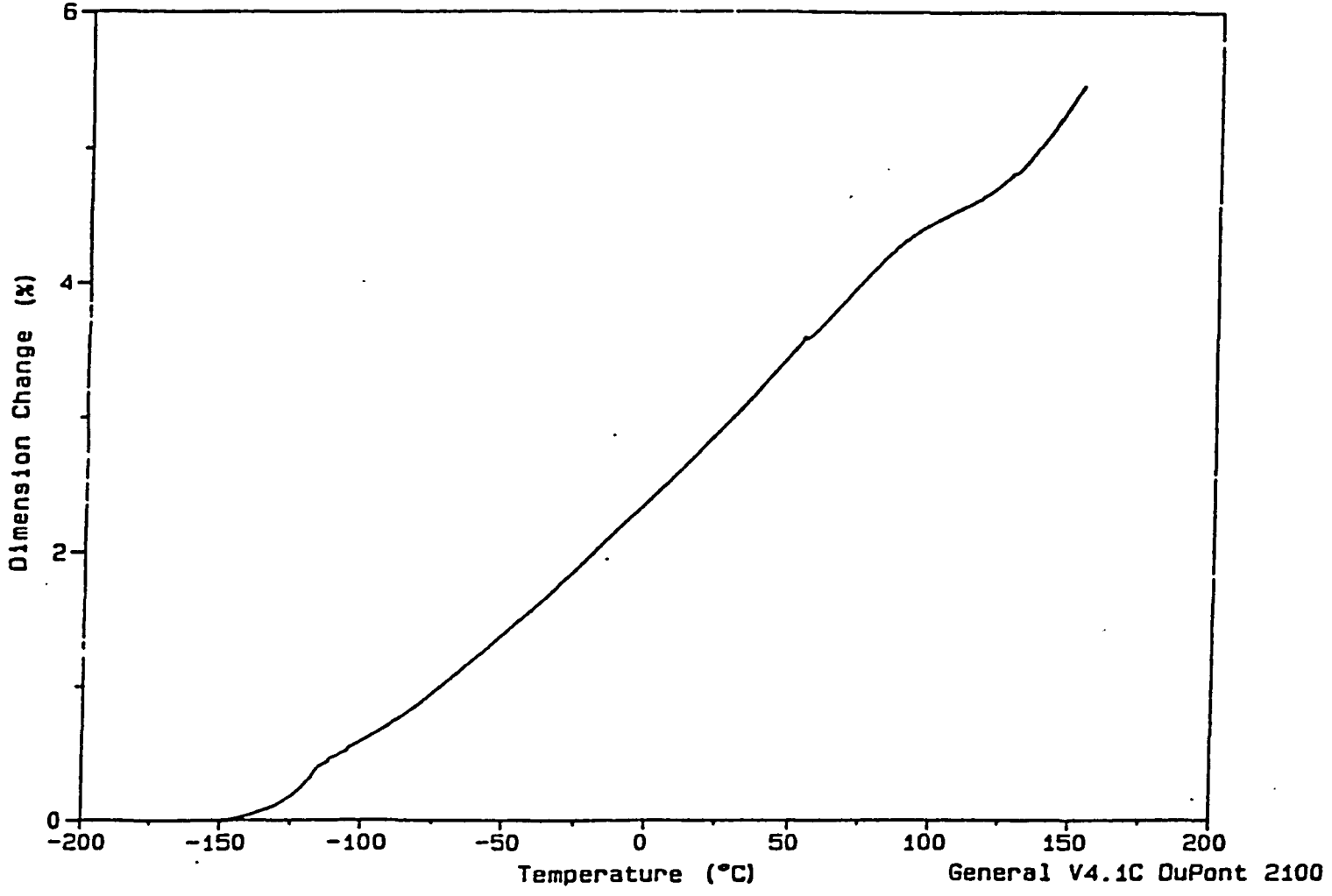

FIGURE 12

Sample: PET (POWDER) SAMPLE#4
Size: 2.2900 mm
Method: PET
Comment: 5 C/MIN / 5 G WEIGHT / USING 2ND PROBE / RUN #1

TMA

File: C:PETASP-TMA.07
Operator: RL
Run Date: 15-Nov-90 11:57

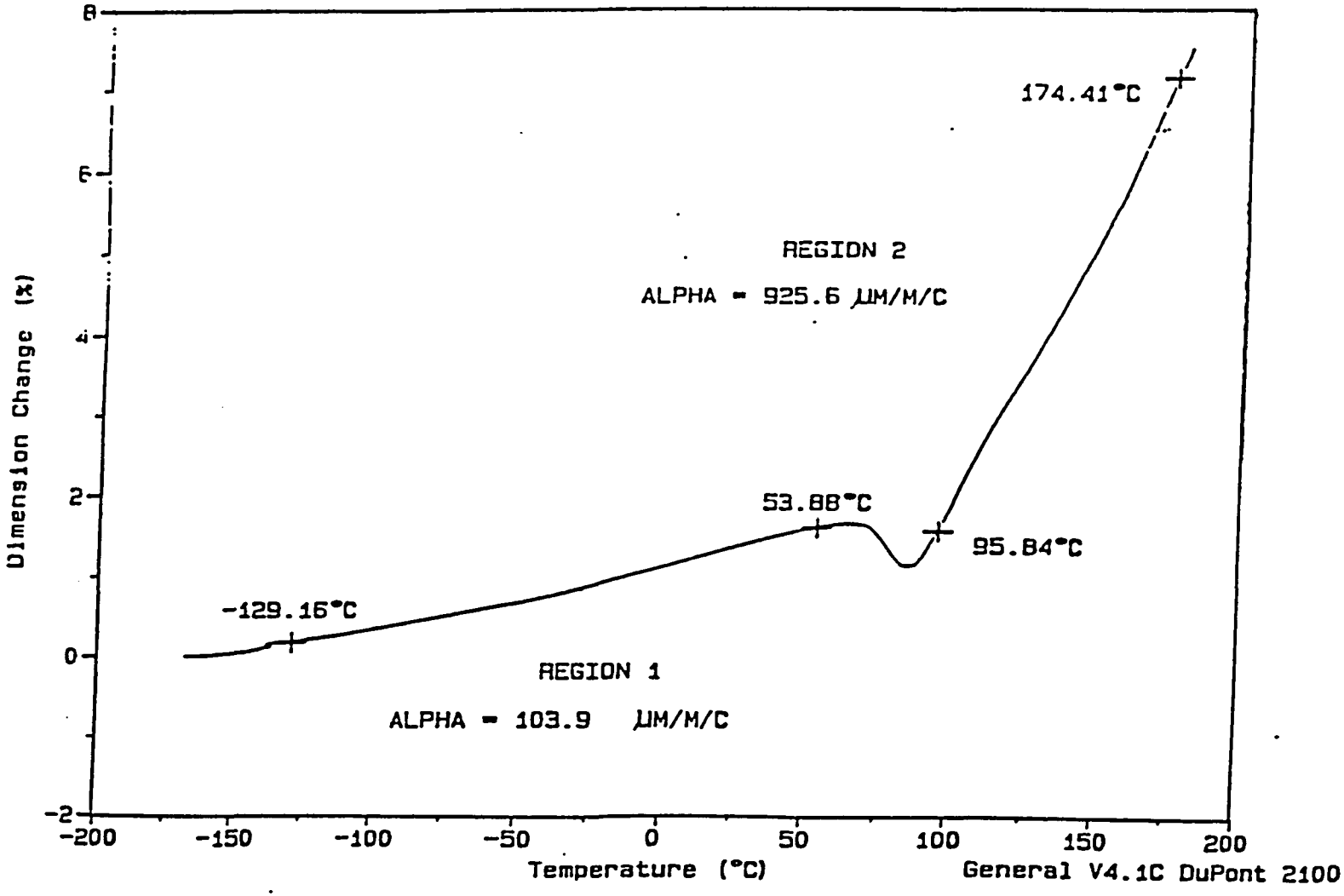

FIGURE 13

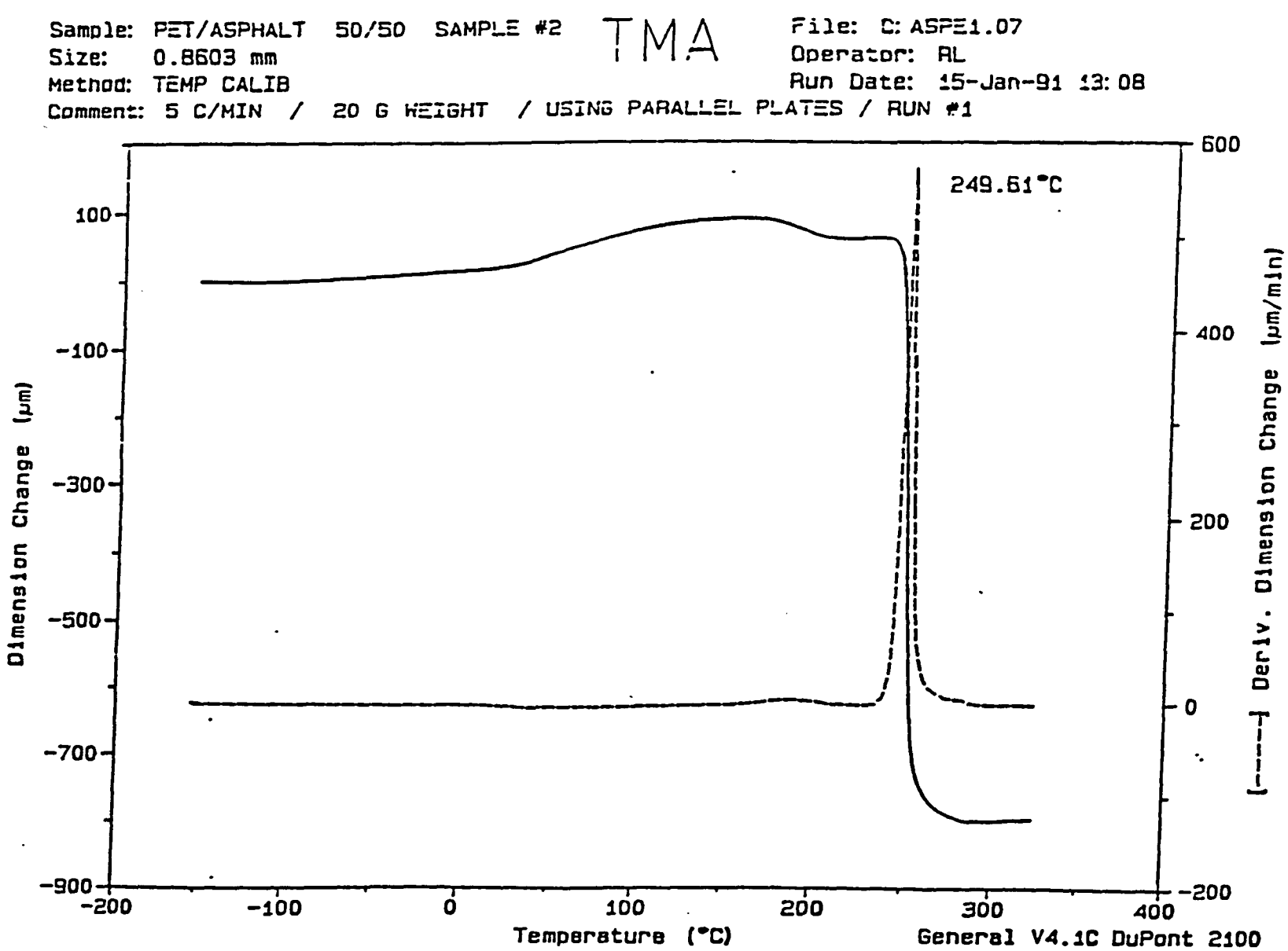
Sample: PET/ASPHALT 50/50 SAMPLE #2
Size: 0.8603 mm
Method: TEMP CALIB
Comment: 5 C/MIN / 20 G WEIGHT / USING PARALLEL PLATES / RUN #1
TMA
File: C:ASPE1.07
Operator: RL
Run Date: 15-Jan-91 13:08
249.61°C
Dimension Change (µm)
Deriv. Dimension Change (µm/min)
Temperature (°C)
General V4.1C DuPont 2100
100
-100
-300
-500
-700
-900
600
400
200
0
-200
-200
-100
0
100
200
300
400

FIGURE 14

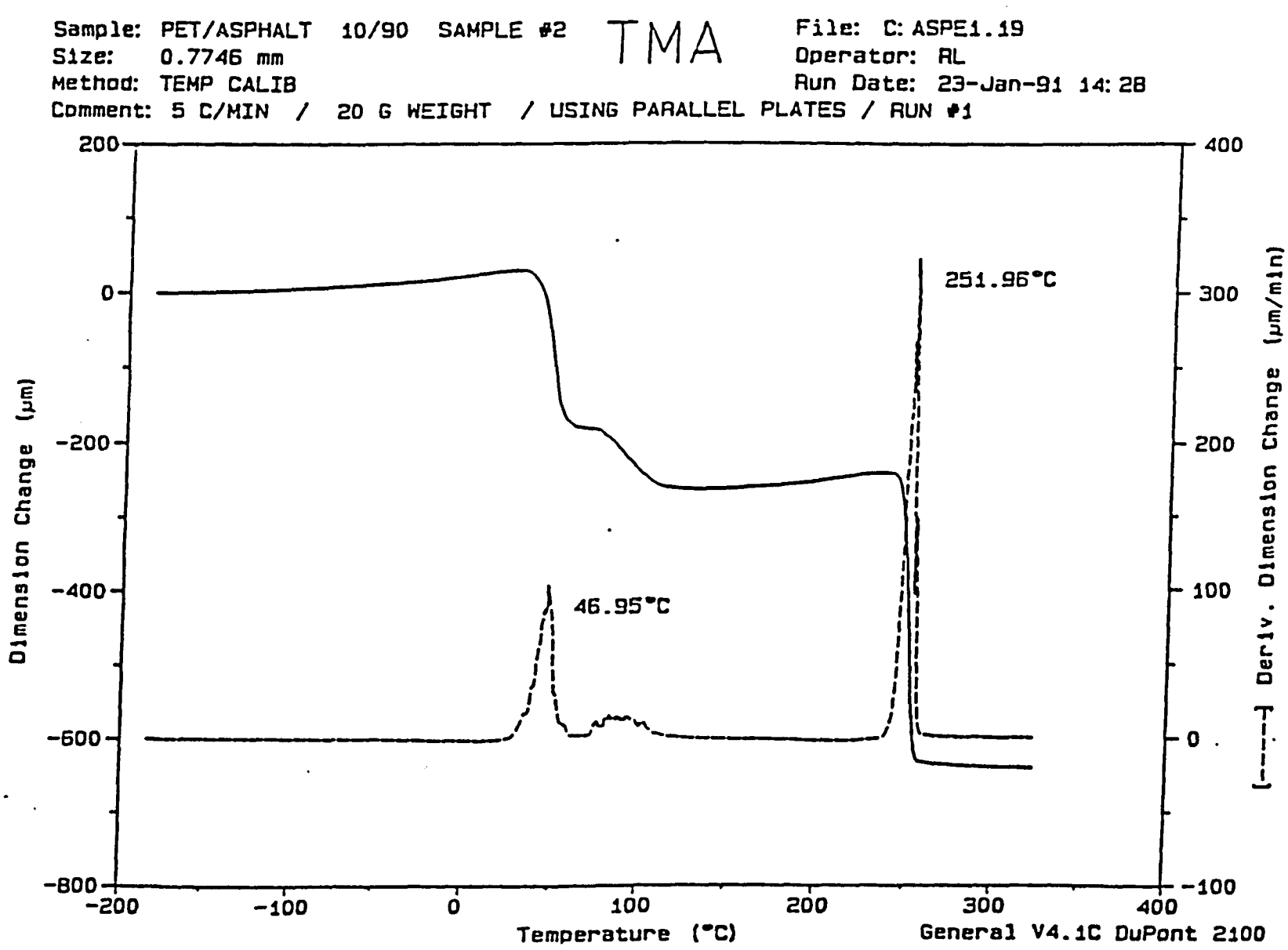
Sample: PET/ASPHALT 10/90 SAMPLE #2
Size: 0.7746 mm
Method: TEMP CALIB
Comment: 5 C/MIN / 20 G WEIGHT / USING PARALLEL PLATES / RUN #1
TMA
File: C:ASPE1.19
Operator: RL
Run Date: 23-Jan-91 14:28
251.96°C
46.95°C
Dimension Change (µm)
[----] Deriv. Dimension Change (µm/min)
Temperature (°C)
General V4.1C DuPont 2100

FIGURE 15

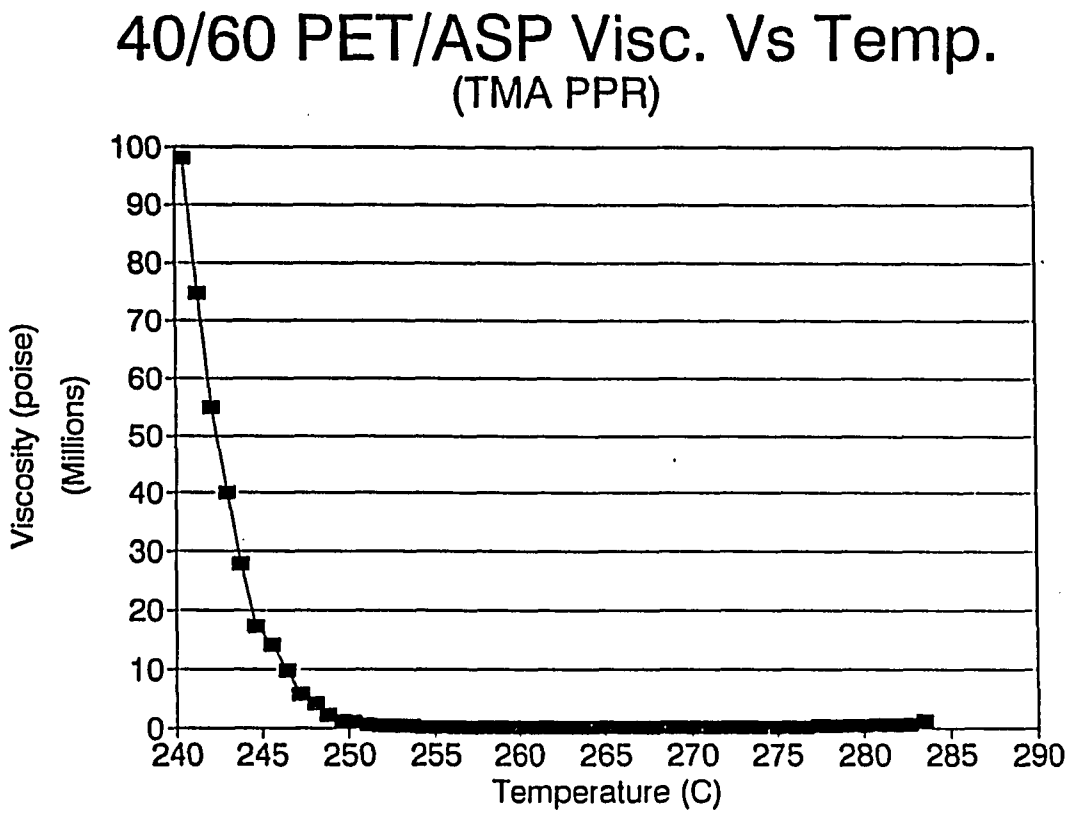
40/60 PET/ASP Visc. Vs Temp.
(TMA PPR)
Viscosity (poise)
(Millions)
100
90
80
70
60
50
40
30
20
10
0
240
245
250
255
260
265
270
275
280
285
290
Temperature (C)

References

1. Kortschot, M., Woodhams, R.T., Polymer Eng. Sci., 24 (6), 252 (1984).

2. Shim Ton, J., Kennedy, K.A., Piggot, M.R., Woodhams, R.T, Rubber Chem. Technol., 53, 88 (1980).

3. Jew, P., Woodhams, R.T., Proceedings of the Association of Asphalt Paving Technologists, 55, 541 (1987).

4. Piggot, M.R., Woodhams, R.T., "Recycling Rubber Tires in Asphalt Paving Surfaces," Enviromental Canada Contract OSU78-00103.

5. Biegenzein, G., U.S. Patent 4,314,921 (February 9, 1982).

6. Hemersam, R., U.S. Patent 4,240,946 (December 23, 1980); ibid. Canadian Patent 1.066831 (Novenber 20, 1979).

7. Denning, J.H., Carswell, J., "Assesment of NOVOPHALT as a Binder for Rolled Asphalt Wearing Course," Transportation and Road Research Laboratory Report 1101, Pavement Materials and Construction Division, Department of Transport, Crowthorne, Berkshire (1983).

8. Lisynska, B., Bukowski, A., Journal of Thermal Analysis, 29, 1009 (1984).

9. Lea,E.M., "The Chemistry of Cement and Concrete," Chemical Publ. Comp., New York, 1971.

10. Breen, J.J., Stephens, J.E., Proceedings of the Association of Asphalt Paving Technologists, 35, 19 (1966).

11. Schmith, R.J., Santucci, L.E., The Association of Asphalt Paving Technologists, 38, 706 (1969).

12. Bader, A., Harvey, D., Nagarkatti, J., Aldrich Catalog Handbook, Adrich Chemical Company, Inc., (1990).

13. Fair, P.G., Gill, P.S., Leckenby, J.N., DuPont Thermal Analysis Application Brief No. TA-90.

14. Dienes and Kelmm, J. Appl. Phys., 17, 458 (1946).

CHAPTER 6

Future Studies

The second part of this thesis deals with the fusion characteristics of coal ashes measured by dilatometry and differential scanning calorimetry (DTA). Here, the DTA technique was employed in a somewhat unconventional manner since the difference in temperature between an ash sample and a reference material was measured using an empty alumina cup as the reference. In general, when the minimum sintering temperature (Ts) obtained using the DTA method was compared to that detected by dilatometry, the dilatometry's Ts was about 100°K larger than that of the DTA's. This discrepancy may be attributed to the way the DTA technique was employed.

As part of future studies, the minimum sintering temperature (Ts) should be measured by DTA using a substance such as aluminum oxide as the reference material. This will allow more accurate measurements of the Ts which is a limiting factor in the selection of a reactor's operating temperature in processes such as coal combustion.

Another facet of the research work presented here involves the investigation of the effect of polyethylene

terephthalate (PET) on the thermal properties of asphalt. The results obtained on the glass transition temperature (Tg), the melting point, the expansion coefficient, and the flow properties of asphalt/PET mixtures show that the thermal properties of asphalt are not affected by the presence of the PET fillers. But this is only a partial picture of the whole effect. A more complete understanding of this effect should be possible once experimental data on the flexural properties of the asphalt/PET mixtures are available. These properties can be determined using a technique such as the dynamic mechanical analysis (DMA).

DMA is a measurement of the mechanical response of a material as it is deformed under periodic stress. This technique provides information necessary to predict the performance of a material under a wide range of conditions. It measures flexural modulus, loss modulus, stress relaxation, and creep as a function of time, temperature, and frequency over the temperature range between -150 and 500°C. The variety of materials that can be evaluated range from very soft, such as elastometers, to very hard, such as steel. Therefore, DMA measurements should yield the flexural properties of asphalt, PET, and asphalt/PET mixtures. A dynamic mechanical analyzer has been ordered and is expected to arrive in September of this year.

Also, as stated previously the effect of the polyethylene terephthalate on asphalt's viscosity needs further investigation. The procedure used should be reviewed and improved in order to obtain meaningful results.

Bibliography

1. Mackenzie, R. C., Thermochim. Acta, **28**, 1 (1979).

2. Mackenzie, R. C., Isr. J. Chem., **22**, 203 (1982).

3. Wendlandt, W. W., Thermal Analysis, 3rd ed., J. Wiley and Sons, 1986.

4. Gomez, M., Gayle, J. B., Taylor, A. R., U. S. Bur. Mines Rep., Invest. No 6607, Pittsburgh (1965).

5. Kirov, N. Y., Br. Coal Util. Res. Assoc. Mon. Bull., **29**(2), 33-57 (1965).

6. "Specific Heat of Coal Char, and Ash," Progress Report to ERDA, **PMa.43.1**, 145 (1976).

7. Eisermann, W., Johnson, P., Conger, W. L., Fuel Proc. Tech., **3**, 39-53 (1980).

8. Isaacs, L. L., Wang, W. Y., Chemical Eng. Thermodynamics, Ann Arbor Science (1982).

9. Mraw,S. C., Naas, D.F., J. Chem. Thermodynamics, **11**, 567-584 (1979).

10. Hemingway, B.S., American Mineralogist, **72**, 273-279 (1987).

11. Robie, R.A., Hemingway, B.S., Wilson, W. H., Jour. Research U.S. Geol. Survey, **4**, 631-644 (1976).

12. Skauge, A., Fuller, N., Hepler, L. G., Thermochemica Acta, **61**, 139-145 (1983).

13. Mackenzie, R.C., Differential Thermal Analysis, **2**, Academic Press (London and N.Y.) (1972).

14. Lyubov, v. k., Artyukhov, S., Shestakov. S. M., Bogucki, Boguslaw (Arkhangelsk For. Inst., Arkhangelsk, USRR). Energetyka, **42**(5), 192-194 (Pol) (1988).

15. Rajeshwar, K., Thermochimica Acta, **63**, 97-112 (1983).

16. "1964 Book of ASTM Standart," Published by the American Society for Testing and Materials, Part 19, 338-343 (1964).

17. O'Gorman J., Walker, P., Jr., Fuel, **52**, 71-79 (1973).

18. Conn, R.E., Austin, L. G., Fuel, **63**, 1664-1670 (1984).

19. Raask, E., personal communication, 9 July 1981.

20. Raask, E., J. Thermal. Anal., **16**, 91 (1979).

21. Basu, p., Sarka, A., Fuel, **61**, 924-926 (1983).

22. Rhinehart, R. R., Attar, A. A., J. of Energy Resources Technology, **109**, 124-128 (1987).

23. Van Vlack, L. H., Elements of Material Science and Engineering, 5th ed., Addison-Wesley Publishing Co., 584-587 (1985).

24. Thorton, P.A., Colangelo, V.J., Fundamentals of Engineering Materials, by Prentice Hall, Inc. (New Jersey), 624-625 (1985).

25. Flinn, R.A., Trojan, P.K., Engineering Materials and their Applications, by Houghton Mifflin Company (Boston), 2nd ed., 464 (1981).

26. "Ash Utilization from Suffolk County waste Water Treatment Plant Southwest District No.3," proposal to N.Y. State Energy Res. & Develop. Authority, (1989).

27. "Summary: SHRP Research Design," by the National Research Council SHRP, (1986).

28. Schmith, R.J., Santucci, L.E., The Association of Asphalt Technologists Proceedings of Technical Sessions, **35**, 61-83 (1966).

29. Williams, J.L., Landel, R.F., Ferry, J.D., J. Am. Chem. Soc., **77**, 3701 (1955).

30. Welborn, J.Y., Oglio, E.R., Zenewitz, J., Proceedings of the Association of Asphalt Paving Technologists, **35**, 19-60 (1966).

31. Breen, J.J., Stephens, J.E., Proceedings of the Association of Asphalt Paving Technologists, **38**, 706-712 (1969).

32. Puzinauskas, V.P., Proceedings of the Association of Asphalt Paving Technologists, **35**, 319 (1958).

33. Wood, L.A., Journal of Polymer Science, **28**, 319 (1958).

34. Barth, E.J., Asphalt Science and Technology, by Gordon and Breach Publishers, 1962.

35. Piggot, M.R., Woodhams, R.T., "Recycling Rubber Tires in Asphalt Paving Surfaces," Environment Canada Contract OSU78-00103 (1979).

36. Jew, P., Woodhams, R.T., Proceedings of the Association of Asphalt Paving Technologists, **55**, 541-560 (1987).

37. Emery, J., Proceedings of the 27th Annual Canadian Technical Asphalt Conference, (1982).

38. Krasavina,T.N., Onashko, I.S., Litologiya i Poleznye Iskopaemye, **3**, 160-165 (1969).

39. Razo,M. L., Asomoza, P.M., Revista del instituto Mexicano del Petroleo, **5**(4), 45-53 (1973).

40. Lisynska, B., Bukowski, A., Journal of thermal Analysis, **29**, 1009-1012 (1984).

41. Blaine, R.L., "The Case for a Generic Definition of Differantial Scanning Calorimetry", Du Pont Instruments, by DuPont Conpany.

42. Boersma, S.L., J. Amer. Ceramic Soc., **38**, 281-4 (1955).

43. Gray, A.P., Analytical Calorimetry, R.F. Porter and J.M. Johnson, eds., Plenum (New York), 209 (1968).

44. Baxter, R.A., Thermal Analysis, R.F.Schwenker, Jr., and P.D. Garn, eds., Academic Press (New York), 65 (1969).